Exploring novel methods to express cytotoxic proteins from oncolytic adenoviral vectors

George Akl

Thesis submitted to the University of Ottawa in partial fulfillment of the requirements for the degree of

Master of Science in Microbiology and Immunology

Department of Biochemistry, Microbiology and Immunology

Faculty of Medicine

University of Ottawa

Abstract

Oncolytic viruses (OVs) are promising cancer therapeutics because they can selectively infect and kill tumor cells while also stimulating anti-tumor immune responses. However, the efficacy of many OVs in solid tumors is limited by poor intratumoral spread, often resulting in incomplete tumor destruction. Conditionally replicating adenoviruses (CRAds) are a well-characterized OV platform that can be engineered to selectively replicate in tumor cells and express therapeutic transgenes. One strategy to improve OV spread and local tumor cell killing is to arm vectors with fusogenic proteins, which promote cell-cell fusion and extend cytopathic effects beyond initially infected cells. Fusion-associated small transmembrane (FAST) proteins are small, non-structural fusogenic proteins encoded by fusogenic reoviruses and represent attractive candidates for incorporation into human adenovirus (HAdV)-based vectors. However, their fusogenic activity can also complicate vector production by inducing premature syncytium formation and producer cell toxicity. Therefore, identifying an optimal FAST protein and developing strategies to regulate transgene expression during vector production are important steps toward improving FAST-armed adenoviral platforms. In this thesis, I first compared the fusogenic capacity and cytotoxic effects of three FAST proteins, p10, p14, and p15, in vitro. FAST proteins were expressed in HEK293 cells by either plasmid transfection or HAdV infection, and their effects were assessed using fluorescence microscopy, image-based fusion quantification, and metabolic activity assays. Among the FAST proteins tested, an untagged version of the p14 FAST protein induced the highest level of syncytium formation and the strongest reduction in metabolic activity, whereas p10 showed limited fusogenic activity and p15 produced an intermediate phenotype. I next evaluated two regulatory strategies to

suppress transgene expression from HAdV vectors. A miRNA-based system was tested using HAdV vectors expressing reporter genes targeted by a corresponding miRNA, while a LacI/LacO-based system was tested using LacI-expressing producer cells and HAdV vectors containing LacO sequences within the transgene expression cassette. These two systems successfully reduced transgene expression from HAdV; however, further optimization is required to minimize their effects on vector yield. Together, these studies identify untagged p14 FAST as the most fusogenic candidate among the FAST proteins tested and provide foundational data on two regulatory strategies that may be adapted to improve the production of cytotoxic transgene-armed HAdV vectors.

Acknowledgments

I would first like to thank my graduate supervisor, Dr. Robin Parks, for his incredible mentorship, guidance, and support throughout my Master's degree. Thank you for creating an environment where I felt encouraged to learn and ask questions. Working under your supervision has strengthened my passion for research and motivated me to continue pursuing a future in science and medicine. I am deeply grateful for everything I have learned from you and for the opportunity to be part of your lab.

I would also like to thank my thesis advisory committee members, Dr. Marceline Côté and Dr. Carolina Ilkow. I am grateful to have had such supportive committee members, whose feedback and perspectives helped strengthen this project.

To the past and present members of the Parks lab, I would like to thank you all for creating an environment where I felt welcomed and supported throughout my graduate studies. I have made many wonderful memories with you all that I will always cherish. A special thank you is reserved for Kathy Poulin. Thank you for welcoming me into the lab with open arms. I will miss our morning coffee runs.

Lastly, thank you to my family and friends for supporting me through my studies. To Mom and Dad, thank you for showing me what hard work looks like and for teaching me the importance of perseverance. To my friends, thank you for listening to my many rants and for being there when I needed a recharge. A special thank you to Tiana, Crystel, and Dimitri. The encouragement, love, and support you have shown me throughout this journey has meant more than I can express.

Table of Contents

List of Abbreviations

Δ24: 24 base pair deletion in E1A
A549: human lung adenocarcinoma epithelial cells
Ad: adenovirus
ANOVA: analysis of variance
BGHpA: bovine growth hormone polyadenylation sequence
CAR: Coxsackie-adenovirus receptor
Cas9: CRISPR-associated protein 9
CMV: cytomegalovirus
CRAd: conditionally replicating adenovirus
CRISPR: Clustered Interspaced Short Palindromic Repeats
DMEM: Dulbecco's Modified Eagle Medium
DNA: deoxyribonucleic acid
dpi: days post infection
E1: early region 1
E2: early region 2
E3: early region 3
E4: early region 4
ER: endoplasmic reticulum
eYFP: enhanced yellow fluorescent protein
FAST: fusion-associated small transmembrane protein
FBS: fetal bovine serum
Fluc: firefly luciferase
GALV: Gibbon-ape leukemia virus
GM-CSF: granulocyte-macrophage colony-stimulating factor
h: hours
HA: hemagglutinin
HAdV: human adenovirus (serotype 5 unless otherwise noted)
HAdV-C5: human adenovirus species C, serotype 5
HEK293: human embryonic kidney 293 cells
HIV: human immunodeficiency virus
hpi: hours post infection
HSV: herpes simplex virus
HSV-1: herpes simplex virus type 1
hTERT: human telomerase reverse transcriptase
IL: interleukin
IL-6: interleukin-6

IL-10: interleukin-10
IPTG: isopropyl β-D-1-thiogalactopyranoside
IRES: internal ribosome entry site
ITR: inverted terminal repeat
kDa: kilodalton
LacI: lac repressor
LacO: lac operator
mCherry: monomeric cherry fluorescent protein
MEM: Minimum Essential Media
miRNA: micro ribonucleic acid
MLP: major late promoter
MLTU: major late transcription unit
MOI: multiplicity of infection
mRNA: messenger ribonucleic acid
MTS: 3-(4,5-dimethylthiazol-2-yl)-5-(3-carboxymethoxyphenyl)-2-(4-sulfophenyl)-2H-Tetrazolium
Nluc: NanoLuc luciferase
OV: oncolytic virus
PBS: phosphate buffered saline
PBST: phosphate-buffered saline containing 0.1% Tween 20
PFA: paraformaldehyde
PFU: plaque forming units
PVDF: polyvinylidene fluoride
Rb: retinoblastoma protein
RLU: relative light units
RSV: respiratory syncytial virus
RT-PCR: reverse transcription polymerase chain reaction
SA: splice-acceptor
SD: standard deviation
SDS-PAGE: sodium dodecyl sulfate polyacrylamide gel electrophoresis
TGF-β: transforming growth factor beta
TNF-α: tumor necrosis factor alpha
T-Vec: talimogene laherparepvec
UTR: untranslated region
VA: viral associated
VEGF: vascular endothelial growth factor
VSV: vesicular stomatitis virus

List of Figures

Chapter 1: Introduction

1.1 Cancer Burden and Current Therapeutic Strategies

Cancer remains one of the most significant global health challenges. Worldwide, cancer accounted for approximately 20 million new cases and 9.7 million deaths in 2022, and the global cancer burden is projected to continue increasing in the coming decades[1]. In Canada, cancer represents a major public health burden, with hundreds of thousands of new cases diagnosed each year and an estimated 42% of people expected to receive a cancer diagnosis during their lifetime[2]. For 2026, approximately 254,100 new cancer cases and 87,900 cancer deaths are projected nationally[3].

Cancer is not a single disease, but rather a broad group of disorders characterized by the acquisition of biological capabilities that enable malignant cells to proliferate, survive, invade surrounding tissues, and adapt to selective pressures[4]. The Hallmarks of Cancer framework describes cancer through nine acquired functional capabilities: sustained proliferative signaling, inactivation of growth suppressors, resistance to programmed cell death, replicative immortality, induction or access to vasculature, invasion and metastasis, deregulated cellular metabolism, immune evasion, and phenotypic plasticity[4]. However, these capabilities are not driven by malignant cells alone. They are also influenced by interactions with non-malignant cells within the tumor microenvironment, including cancer-associated fibroblasts, endothelial cells, immune cells, and other stromal components[4,5]. Overall, these interactions can support tumor growth, promote immune evasion, and contribute to therapeutic resistance[4,5]. The biological complexity of cancer is reflected by the existence of hundreds of distinct cancer types and subtypes, each with unique genetic, molecular and cellular features[4,6]. Many of

the most common adult cancers arise as solid tumors, including cancers of the lung, breast, colorectum, prostate, stomach, and liver[1]. This is particularly relevant because solid tumors present several therapeutic challenges, including heterogeneous cell populations, abnormal vasculature, poor therapeutic penetration, and complex tumor microenvironments[5-7]. As a result, treatment responses can vary widely depending on the tissue of origin, tumor location, stage of disease, and extent of dissemination. These challenges highlight the need for therapeutic strategies capable of improving tumor cell targeting and treatment distribution within solid tumor masses.

Current cancer treatments commonly include surgery, radiation therapy, chemotherapy, targeted therapy, and combinations of these modalities[8]. Surgery and radiation therapy can be effective for localized tumors, but their use may be limited by tumor location, invasiveness, and the potential for damage to surrounding healthy tissue[9,10]. Chemotherapy remains an important systemic treatment option, particularly for disseminated cancers, but its lack of specificity can result in substantial toxicity to rapidly dividing healthy cells[11]. Targeted therapies have improved outcomes for cancers driven by specific molecular alterations, but their efficacy can be limited by tumor heterogeneity, resistance mechanisms, and the absence of actionable targets in some patients[12]. In recent years, immunotherapy has emerged as a promising treatment strategy by harnessing the patient's immune system to recognize and eliminate malignant cells[13,14]. Immune checkpoint inhibitors, adoptive cell therapies and cancer vaccines have produced durable responses in many patients and have reshaped the therapeutic landscape for several cancer types[14]. However, the clinical benefit of immunotherapy remains limited in some patients due to primary or acquired resistance, immune-related toxicities and variability in tumor

immunogenicity[15]. These challenges have encouraged continued investigation into alternative or complementary strategies capable of directly killing tumor cells while also promoting anti-tumor immune responses.

1.2 Oncolytic Virotherapy as an Anti-Cancer Therapeutic Strategy

Oncolytic virotherapy is a cancer treatment strategy that uses viruses that selectively replicate in tumor cells, ultimately leading to tumor cell death[16]. Oncolytic viruses (OVs) are of particular interest because they combine direct tumor cell killing with the capacity to stimulate anti-tumor immune responses and alter the tumor microenvironment[17]. As such, they represent a promising platform for the development of novel cancer therapeutics. In oncolytic virotherapy, viral vectors can be engineered to deliver genes encoding therapeutic anti-cancer proteins, selectively replicate in cancer cells and induce tumor cell lysis[18]. More specifically, the anti-tumor effects of OVs can occur through several mechanisms. Direct virus-mediated cell lysis involves the replication of oncolytic viruses in tumor cells, eventually leading to the rupture of the cell membrane[18,19]. OVs can also trigger innate and adaptive immune-mediated destruction by promoting the release of tumor-associated antigens, enhancing the visibility of the tumor to the immune system[20]. Some OVs can also disrupt the tumor vasculature, limiting the supply of oxygen and nutrients required for tumor growth[21]. Furthermore, OVs can be engineered to deliver various therapeutic transgenes to tumor cells, inducing diverse effects that enhance their overall therapeutic potential[18,22].

The potential of viruses for cancer treatment has been recognized since the mid-1800s, where tumor regression was observed coinciding with natural virus infection[23,24]. The first clinical trials investigating viruses as anti-cancer therapeutics began in the 1950s,

with early studies using wild-type or attenuated viruses, including hepatitis B virus, West Nile virus, adenovirus, and mumps virus[24,25]. However, these early viral agents were often rapidly eliminated by the immune system and produced limited therapeutic benefit[24]. In addition, concerns regarding safety and the inability to reliably restrict viral replication to cancer cells raised questions about the clinical potential of oncolytic virotherapy[24]. As a result, despite substantial activity in the 1950s and 1960s, interest in oncolytic virotherapy declined during the 1970s and 1980s[24]. The field was later revitalized in the 1990s by advances in molecular biology and reverse genetics, which enabled the development of genetically engineered oncolytic viruses with improved tumor specificity and oncolytic potency[24,25]. Currently, a wide range of oncolytic viruses have shown significant potential in both pre-clinical and clinical studies, including herpesvirus, reovirus, vaccinia virus, adenovirus and others[26,27]. The first oncolytic virus to receive approval by a regulatory agency was Oncorine (H101), approved in 2005 by the Chinese State Food and Drug Administration[28,29]. Oncorine is a recombinant human adenovirus type 5 approved for the treatment of head and neck cancer[28]. In 2015, the U.S. Food and Drug Administration approved talimogene laherparepvec (T-VEC), a modified herpes simplex virus type 1 (HSV-1), for the treatment of advanced melanoma[30,31]. Due to its demonstrated clinical benefit, T-VEC has since received approval in a number of other regions, including Europe and Australia[31]. More recently, Delytact, also known as teserpaturev or G47Δ, became the first oncolytic virus approved in Japan for the treatment of malignant glioma[32]. Delytact is a genetically engineered HSV-1-based oncolytic virus and received conditional approval from the Japanese Ministry of Health, Labour and Welfare in 2021[32].

A major consideration in the development of OVs is ensuring that viral replication and cytotoxicity are preferentially restricted to tumor cells. In some cases, tumor selectivity can occur naturally because cancer cells often contain defects in antiviral signaling pathways, making them more permissive to viral infection and replication[33]. However, tumor selectivity can also be enhanced through genetic engineering. For example, viral replication can be restricted by placing essential viral genes under the control of tumor-specific promoters, deleting or modifying viral genes that are required for replication in normal cells but dispensable in cancer cells, or modifying viral tropism to enhance entry into tumor cells[18,34]. These strategies have contributed to the development of safer and more selective OVs with improved therapeutic potential.

Although OVs have demonstrated clinical promise, their efficacy as monotherapies can be limited by several factors, including inefficient delivery to tumor sites, antiviral immune clearance, poor intratumoral spread, and the immunosuppressive tumor microenvironment[18,35,36]. As a result, considerable effort has focused on developing "armed" OVs that express therapeutic transgenes to enhance anti-tumor activity[37-39]. The therapeutic transgenes incorporated into armed OVs can vary widely depending on the intended mechanism of action. These transgenes may encode cytokines, chemokines, immune checkpoint inhibitors, prodrug-converting enzymes, or pro-apoptotic proteins[22,40]. In this way, armed OVs can be designed to enhance viral growth, improve intratumoral spread, stimulate anti-tumor immunity, or directly increase tumor cell killing. By combining tumor-selective replication with local therapeutic transgene expression, armed OVs provide a versatile platform to increase tumor cell killing while limiting systemic

toxicity. This strategy is particularly relevant for solid tumors, where limited therapeutic distribution within the tumor mass remains a major barrier to treatment efficacy[41-43].

1.3 Adenovirus Biology and Applications

Among the various oncolytic viruses explored, human adenovirus (HAdV) vectors have emerged as a particularly versatile and promising platform. Adenoviruses (Ads) are non-enveloped, double-stranded DNA viruses with well-characterized biology and a genome that can be readily manipulated to alter viral replication, tropism and transgene expression[44]. These properties have made HAdV vectors widely used in gene therapy, vaccination and cancer therapeutics[28,45-47]. In the context of oncolytic virotherapy, Ads are especially attractive because they can be engineered to selectively replicate in tumor cells while also serving as delivery vehicles for therapeutic transgenes[34]. Despite these advantages, the clinical efficacy of oncolytic HAdV remains limited in some solid tumors, in part due to inefficient intratumoral spread and restricted therapeutic distribution following local administration[48,49]. Therefore, understanding the biology, engineering strategies, clinical applications and limitations of HAdV-based vectors is essential for developing improved oncolytic Ad platforms.

The following sections will first provide an overview of Ad biology and genome organization, followed by a discussion of their use as gene delivery platforms, their development as oncolytic agents and the current barriers limiting their therapeutic efficacy in solid tumors.

1.3.1 Adenovirus Biology and Genome

Ads are non-enveloped icosahedral viruses containing a linear double stranded DNA, belonging to the *Mastadenovirus* genus within the *Adenoviridae* family[50]. They were

first isolated from human adenoid tissue in the 1950s and are now recognized as common human pathogens[51,52]. In most healthy individuals, Ad infections are mild and self-limiting; however, more severe disease can occur in young children, older adults and immunocompromised individuals[53-55]. Depending on the viral type and site of infection, Ads can cause a range of clinical manifestations, including respiratory disease, conjunctivitis and gastroenteritis[56,57].

The Ad virion consists of an icosahedral capsid shell approximately 70-100 nm in diameter that encloses a linear double-stranded DNA genome of approximately 30-40 kb[58,59]. The capsid is primarily composed of three major structural proteins: hexon, penton base, and fiber[59,60]. Hexon proteins form the majority of the capsid surface, whereas penton base and fiber proteins are located at the vertices of the capsid and are important for viral attachment and entry[61]. The capsid also possesses five minor polypeptides, IIIa, IVa2, VI, VIII, and IX which contribute to capsid stability[59,61]. Within the capsid, the viral genome is packaged with core-associated proteins, including proteins V, VII, and Mu (μ), which help organize and condense the viral DNA[59,62-64].

Human adenovirus type 5 (HAdV-C5), a member of species C, is one of the most extensively characterized Ads and has served as a major platform for vector development[59]. The HAdV-C5 genome is approximately 36 kb in size which encodes approximately 40 proteins expressed in two main phases: early and late (Figure 1.1)[64-66]. The early transcriptional regions, including E1A, E1B, E2, E3 and E4, are expressed prior to viral DNA replication and encode proteins involved in creating a cellular environment that supports viral replication. The E1A proteins play a central role by promoting cell cycle progression into S phase and activating the expression of other viral genes, thereby

initiating the viral replication program[65,67]. The E1B proteins primarily function to support productive viral replication, in part through regulation of p53 and host antiviral responses[68]. The E2 proteins mediate viral DNA replication, whereas E3 and E4 proteins contribute to modulation of host immune responses, cell signaling and other processes that support productive infection[69,70]. Together, these early gene products promote viral gene expression, drive viral DNA synthesis and counteract host antiviral defenses. Following the onset of viral DNA replication (~8 hpi), Ad late gene expression becomes strongly activated[71,72]. Late gene expression is primarily driven by the major late promoter (MLP), which regulates transcription of the major late transcription unit (MLTU)[72]. Through alternative splicing, this transcription unit gives rise to five groups of late mRNAs, designated L1 to L5[73]. These late regions encode many of the structural proteins required for capsid assembly, genome packaging and production of infectious virions[74]. In addition, four small products are expressed at intermediate or intermediate-late times of infection, after early gene expression but before full activation of late gene expression[75]. These include protein IX (pIX) and IVa2, which contribute to capsid assembly and viral genome packaging[75]. Ads also express virus-associated RNAs, VA RNA I and VA RNA II, which are non-coding RNAs involved in modulating host antiviral responses and cellular RNA-processing pathways[76,77]. Finally, the Ad genome is flanked by inverted terminal repeats (ITRs), which function as origins of viral DNA replication, and contains a packaging sequence near the left end of the genome that is required for packaging viral DNA into newly assembled virions[59].

The Ad life cycle begins with attachment of the viral fiber protein to a primary cellular receptor, such as the coxsackievirus and adenovirus receptor (CAR) for many

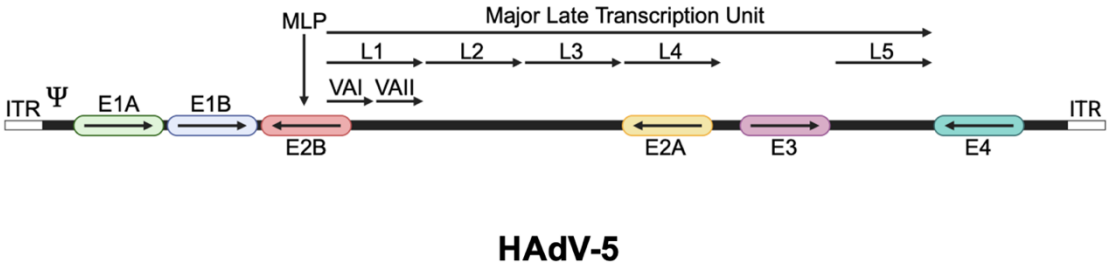

Figure 1.1 Genome of the human adenovirus C serotype 5. Early transcription regions include E1-E4. L1–L5 are late transcription regions within the major late transcription unit (MLTU), which is expressed from the major late promoter (MLP). The inverted terminal repeats (ITRs) are located at both ends of the genome. The packaging element is denoted by the symbol Ψ. Elements of the genome are not shown to scale. Schematic created with BioRender.com.

species C Ads[78]. Internalisation of the virion is then initiated by interactions between the penton base proteins and cellular integrins[79]. These interactions trigger clathrin-mediated endocytosis, allowing the virion to enter the cell[79,80]. Following internalization, partial capsid disassembly exposes the viral protein VI, which functions as a membrane-lytic protein that disrupts the endosomal membrane and facilitates the release of the partially disassembled capsid into the cytoplasm[81]. Once in the cytoplasm, the capsid recruits cytoplasmic dynein through interactions with hexon and is transported along microtubules toward the nuclear pore complex[82,83]. Docking at the nuclear pore complex promotes further capsid disassembly and the import of the viral genome into the nucleus, where viral transcription, DNA replication, and virion assembly occur[84,85]. At late stages of infection, newly assembled virions are released following virus-induced cell lysis, allowing spread to neighboring cells[86]. The Ad replication cycle is completed within approximately 24-36 h[59,60].

1.3.2 HAdV as Therapeutic Vector Platforms

For several decades, HAdV vectors have been extensively used in biomedical research and therapeutic development due to their ability to efficiently deliver transgenes and drive high-level gene expression in mammalian cells[45]. In the most recent published update of the Gene Therapy Clinical Trials Worldwide database, which included trials up to March 2023, Ad vectors represented the most commonly used viral vector system in human gene therapy clinical trials, accounting for 14.7% of all vectors used (n = 574)[87]. This widespread use is largely due to several advantageous features of HAdVs as vector platforms. HAdVs have been extensively characterized and their molecular biology,

genome organization, and structural components are well understood[44]. They are also capable of efficiently transducing a broad range of cell types, including both dividing and non-dividing cells, making them suitable for diverse therapeutic applications[88,89]. In addition, their large double-stranded DNA genome provides a relatively high cloning capacity, allowing the insertion of therapeutic transgenes or regulatory elements through recombinant DNA engineering[59,90]. These features make HAdV vectors highly adaptable platforms for gene delivery, vaccination, and cancer therapy.

The most commonly used HAdV gene therapy vectors are first-generation replication-defective vectors, in which the E1 region is deleted[45,91]. As described above, the E1 region encodes proteins required to initiate the viral replication program, including activation of viral gene expression and induction of a cellular environment that supports viral DNA replication[65,67]. Therefore, deletion of E1 prevents productive viral replication in most cell types, while still allowing the vector to deliver its DNA cargo to transduced cells. The E3 region is also frequently deleted because it is not essential for vector production or vector-mediated gene delivery, and its removal increases the available cloning capacity for foreign expression cassettes[45,90]. Together, deletion of the E1 and E3 regions allows E1/E3-deleted vectors to accommodate approximately 8 kb of foreign DNA[90]. Since E1 is required for productive viral replication, E1-deleted vectors are propagated in E1-complementing producer cell lines, such as the widely used HEK293 cell line[92].

Several HAdV-based vectors have advanced into clinical use, highlighting the versatility of this platform. For example, Gendicine is a replication-defective HAdV vector encoding the tumor suppressor p53 and was approved in China for the treatment of head

and neck squamous cell carcinoma[93]. Similarly, Adstiladrin is a non-replicating HAdV vector designed to deliver the human interferon α-2b gene to the bladder epithelium for the treatment of high-risk non-muscle-invasive bladder cancer[94]. Beyond cancer gene therapy, Ad vectors have also been widely developed as vaccine platforms, including vectors used to deliver antigen-encoding transgenes for infectious disease vaccination[95-97]. These examples illustrate the broad utility of Ad vectors across therapeutic areas, from gene replacement and cancer therapy to vaccination. While these approaches often use replication-defective vectors, Ads can also be designed for replication-competent strategies, forming the foundation for oncolytic HAdV vectors.

1.3.3 Oncolytic Adenoviral Vectors for Cancer Treatment

Ad vectors are among the most widely used viral platforms in oncolytic virotherapy clinical trials[98]. In contrast to replication-defective Ad vectors used primarily for gene delivery, oncolytic Ad vectors are designed to retain replicative capacity while restricting productive replication preferentially to cancer cells[34]. These vectors, also referred to as conditionally replicating adenoviruses (CRAds), exploit molecular differences between normal and malignant cells to achieve tumor-selective replication and cancer cell lysis[34,99].

Tumor-selective replication can be achieved through several genetic engineering strategies. One method involves placing essential Ad genes, most commonly E1A, under the control of tumor or tissue specific promoters[100-102]. Since E1A is required to initiate the viral replication program, restricting its expression to cells in which the selected promoter is active can limit viral replication to specific tumor types. Examples of promoters used for this purpose include prostate-specific antigen regulatory elements for prostate cancer, α-fetoprotein regulatory elements for hepatocellular carcinoma, and human telomerase

reverse transcriptase regulatory elements[100-102]. A second strategy involves deleting or modifying viral genes that are required for efficient replication in normal cells but become dispensable in cancer cells due to oncogenic pathway alterations. One example is the E1AΔ24 mutation, which consists of a 24-bp deletion in conserved region 2 of E1A[103]. During wild-type Ad infection, E1A binds to retinoblastoma (Rb) proteins, disrupting Rb-mediated repression of E2F-dependent transcription[104,105]. This promotes the expression of genes required for S-phase entry and viral DNA replication[104,105]. The E1AΔ24 mutation impairs the ability of E1A to bind Rb proteins[106,107]. Therefore, in normal cells with an intact Rb pathway, E1AΔ24 limits the ability of the virus to drive S-phase entry, thereby restricting efficient viral replication[106,107]. In contrast, many cancer cells have defects in the Rb pathway, resulting in deregulated E2F activity[108]. As a result, E1AΔ24-containing Ads can preferentially replicate in malignant cells where E2F-dependent transcription and cell cycle progression are already dysregulated[107,108]. Similarly, deletion of E1B-55K was used in early oncolytic Ads such as ONYX-015, which was originally designed to replicate selectively in p53-deficient tumor cells[109], although the actual mechanism of action for this virus may be more complex[110,111].

Several oncolytic Ad vectors have been developed using these design principles. ONYX-015 was one of the earliest and most extensively studied CRAd and contains a deletion in the E1B-55K region[109]. H101, also known as Oncorine, is a related oncolytic HAdV vector that was approved in China for the treatment of head and neck cancer in combination with chemotherapy[28]. Similar to ONYX-015, H101 contains a deletion in the E1B-55K region, which was intended to restrict viral replication to tumor cells with defective p53-mediated antiviral responses[28]. Although these early vectors demonstrated

clinical safety, their anti-tumor efficacy as monotherapies was generally limited, highlighting the need for further vector optimization[112,113].

OBP-301, also known as Telomelysin, is an example of a promoter-regulated CRAd. In this vector, the human telomerase reverse transcriptase (hTERT) promoter regulates expression of E1A and E1B, thereby linking viral replication to hTERT promoter activity, which is elevated in many tumors but limited in most normal differentiated adult cells[114]. In a multicenter phase II study, OBP-301 was evaluated in combination with pembrolizumab in patients with advanced gastroesophageal adenocarcinoma[115]. Patients received direct intratumoral injections of OBP-301 together with pembrolizumab, and treatment was reported to be well tolerated. Among 16 enrolled patients, two patients achieved a partial response and one patient achieved a complete response. OBP-301 remains under clinical and regulatory development, including evaluation for potential approval in Japan.

DNX-2401, also known as Delta-24-RGD or tasadenoturev, is an E1AΔ24-based CRAd with enhanced tumor cell infectivity[116]. In addition to the E1AΔ24 mutation, DNX-2401 contains an RGD-4C motif in the fiber H-loop, which promotes viral entry through αvβ3 and αvβ5 integrins. In a phase I trial in recurrent malignant glioma, DNX-2401 was administered by direct intratumoral injection and was well tolerated, with no dose-limiting toxicities observed[117]. Evidence of viral replication was detected in post-treatment tumor specimens, and three patients showed ≥95% reduction in tumor volume, supporting both direct oncolytic and immune-mediated anti-tumor activity.

ICOVIR-7 is another E1AΔ24-based CRAd designed to improve both tumor selectivity and infectivity. In this vector, tumor-selective replication is mediated by the

E1AΔ24 mutation together with a modified E2F promoter controlling E1A expression, while an RGD-4C modification in the fiber HI-loop enhances entry into tumor cells[118,119]. In a clinical study of 21 patients with advanced and refractory solid tumors, ICOVIR-7 treatment was generally well tolerated, with mainly mild to moderate adverse symptoms[119]. Objective evidence of anti-tumor activity was observed in 9 of 17 evaluable patients, including one partial response, two minor responses, and two cases of stable disease by radiological assessment.

Collectively, these clinical studies show that oncolytic Ad vectors are a feasible therapeutic platform for several cancer types, with generally acceptable safety profiles and evidence of anti-tumor activity. However, the clinical benefit observed with unarmed CRAds has often been limited, particularly when used as monotherapies[18,113]. This suggests that replication-mediated oncolysis alone may be insufficient to fully eliminate tumors, especially in the context of advanced or solid malignancies. As a result, continued development of oncolytic Ads has focused on improving viral potency, enhancing intratumoral spread, and incorporating therapeutic transgenes to augment anti-tumor efficacy[120,121].

1.3.4 Limitations of CRAd Therapy and Strategies to Improve Efficacy

Although CRAds have shown promise as cancer therapeutics, several biological and physical barriers continue to limit their clinical efficacy. One major challenge is the complexity of the tumor. Solid tumors often contain dense stromal tissue, abundant extracellular matrix components, abnormal vasculature, and elevated interstitial pressure[43,122]. These features can act as physical barriers that prevent viral particles from distributing evenly throughout the tumor mass[123]. In addition, regions of poor perfusion

and hypoxia may further limit productive Ad replication[124,125]. As a result, following local administration, viral infection can remain concentrated near the injection site, leaving distant regions of the tumor insufficiently infected[49]. Consistent with this, a phase I trial evaluating intratumoral administration of an Ad-p53 vector in recurrent glioma found that transduced cells were located within only ~5 mm of the injection site, highlighting the limited distribution of HAdV vectors following local delivery[126]. This limited intratumoral dissemination reduces the ability of CRAds to amplify throughout the tumor and can contribute to incomplete tumor destruction[126].

The tumor microenvironment can also suppress anti-tumor immune responses that would otherwise contribute to CRAd efficacy. Tumor cells and stromal cells can produce factors such as TGF-β, IL-10, IL-6, VEGF, GM-CSF and other inflammatory mediators that promote the recruitment and activity of immunosuppressive cell populations[127,128]. These include myeloid-derived suppressor cells (MDSCs), M2 macrophages, and regulatory T cells, which can inhibit dendritic cell maturation and suppress cytotoxic T lymphocyte activity[127,128]. As a result, although CRAds can directly lyse infected cancer cells and promote immunogenic cell death, the development of a durable anti-tumor immune response may be weakened by the suppressive conditions present within many solid tumors[129].

To overcome these limitations, several strategies have been explored to improve CRAd potency, spread, and immune activation. One major strategy involves arming CRAds with therapeutic transgenes[38,130,131]. Rather than relying solely on viral replication and direct oncolysis, armed CRAds are engineered to express therapeutic transgenes that can increase tumor cell killing, promote viral release, remodel the tumor

microenvironment, and/or stimulate anti-tumor immune responses[38,130,131]. These transgenes may encode cytotoxic or pro-apoptotic proteins, prodrug-converting enzymes, extracellular matrix-modifying proteins, cytokines, immune co-stimulatory molecules, or other immunomodulatory factors[40]. Several armed CRAds have been developed to express defined therapeutic transgenes. For example, CG0070 is an HAdV-C5 based CRAd regulated by an E2F-responsive promoter and armed with GM-CSF, which is intended to enhance anti-tumor immune activation[132]. TILT-123 is a CRAd vector expressing TNF-α and IL-2, and is being evaluated in clinical trials for multiple solid tumors[133]. Other examples include LOAd703, which encodes CD40L and 4-1BBL to promote immune co-stimulation, and VCN-01, which expresses hyaluronidase to degrade extracellular matrix components and improve viral penetration through solid tumors[38,134]. Together, these examples illustrate how therapeutic transgenes can be selected to enhance distinct aspects of CRAd activity, including immune activation, direct tumor cell killing, and intratumoral spread. When designing armed replication-competent Ad, the size of the transgene, its insertion site, and the timing of expression must be carefully considered to avoid impairing viral replication and/or genome packaging[59].

The E3 region is frequently used as a site for transgene insertion because it contains genes that are not essential for viral replication and can provide additional cloning capacity[38,69]. Transgene expression can be regulated either by exogenous promoters inserted into the viral genome or by endogenous Ad regulatory elements[131]. In CRAd vectors, late transgene expression is often desirable because it links transgene production to productive viral replication. The Ad major late promoter is weakly active during early infection but becomes strongly activated after the onset of viral DNA replication[72].

Therefore, transgenes placed under MLP control are expected to be expressed primarily at late stages of infection and mainly in cells that support Ad replication[135]. This provides an additional level of tumor selectivity by coupling therapeutic transgene expression to the same cellular context in which the CRAd replication program is active. Late transgene expression can be achieved by incorporating a splice acceptor sequence upstream of the transgene, allowing the transgene to be expressed as part of the major late transcription unit[135,136]. This design is particularly relevant for therapeutic proteins that may be cytotoxic or otherwise harmful if expressed too early or in non-target cells.

As previously mentioned, poor intratumoral spread remains a major limitation of CRAd therapy, as with other oncolytic viruses[49,126]. To address this limitation, several armed vectors have been designed to modify the extracellular matrix, enhance intratumoral spread, and/or increase local tumor cell killing. For example, relaxin-expressing oncolytic Ads have been shown to decrease tumor collagen content, improve viral distribution, and enhance anti-tumor efficacy in vivo[137,138]. Similarly, hyaluronidase-expressing Ads, such as ICOVIR17, degrade hyaluronan within the extracellular matrix, resulting in improved viral spread and increased tumor regression[139]. Decorin-expressing Ads have also been shown to remodel extracellular matrix components, improve tumor penetration, and enhance the therapeutic efficacy of replicating Ads[140].

In addition to extracellular matrix-remodeling strategies, fusogenic proteins represent another method to enhance intratumoral spread and/or local tumor cell killing[141]. This strategy will be discussed in the following section.

1.4 Fusogenic Proteins as Anti-Cancer Therapeutics

1.4.1 Fusogenic Proteins as Therapeutic Transgenes in Oncolytic Vectors

Fusogenic proteins have emerged as promising therapeutic transgenes for improving the anti-tumor activity of oncolytic viruses[142]. Many enveloped viruses use viral fusion proteins to mediate fusion between the viral envelope and the host cell membrane during entry[143]. However, some viral fusion proteins can also mediate cell-cell fusion when expressed on the surface of infected cells[142]. In this context, the fusion protein is transported to the plasma membrane of an infected cell, where it interacts with receptors on neighboring cells and induces membrane fusion[142]. This results in the formation of large, multinucleated cells known as syncytia, thereby improving the spread of the virus and extending cytopathic effects beyond the initially infected cell[144-146].

This mechanism may provide several advantages over non-fusogenic OVs. By promoting direct cell-to-cell spread, fusogenic proteins can enhance local tumor cell killing without relying exclusively on the release and extracellular diffusion of mature virions[142]. This is particularly relevant in solid tumors, where extracellular matrix barriers, high interstitial pressure, and heterogeneous viral distribution can limit the spread of OVs[123]. OVs encoding fusogenic proteins can therefore increase the area of tumor destruction initiated by a relatively small number of infected cells[147]. In addition, syncytium formation may enhance anti-tumor immune activation. Fusion-mediated cell death can promote the release of tumor antigens, viral products, and damage-associated signals that support antigen uptake and presentation by dendritic cells[144,148]. Syncytia can also release exosome-like particles, termed syncytiosomes, which have been shown to promote dendritic cell activation and cross-presentation of tumor antigens to cytotoxic T cells[144,148]. Therefore, fusogenic proteins may enhance oncolytic vector efficacy by increasing direct fusion-

mediated tumor cell killing while also promoting immune-mediated anti-tumor responses[142,144,148].

Several viral platforms have been engineered to express fusogenic proteins in preclinical cancer models, including herpes simplex virus, vesicular stomatitis virus, vaccinia virus, paramyxovirus-based vectors, and Ad vectors[142]. Oncolytic herpes simplex virus (HSV) vectors expressing the gibbon ape leukemia virus (GALV) fusogenic glycoprotein showed enhanced tumor cell killing and improved anti-tumor activity compared with a non-fusogenic control HSV vector in preclinical tumor models[149]. Similarly, vesicular stomatitis virus (VSV) vectors expressing modified fusion proteins from Newcastle disease virus or measles virus exhibited increased syncytium formation, enhanced cytotoxicity, and improved therapeutic activity compared with non-fusogenic controls[150,151].

1.4.2 Adenovirus Vectors Armed with Fusogenic Proteins

Several studies have evaluated the use of fusogenic proteins to improve the anti-tumor activity of HAdV vectors[141]. Dewar et al. generated an E3-deleted replication-competent HAdV vector expressing the HIV-1 envelope glycoprotein, known as Ad5env[152]. Subsequent work showed that syncytium formation induced by the HIV-1 envelope glycoprotein enhanced viral release and promoted dispersion of viral particles through tumor cell cultures[146]. These findings provided proof-of-concept that expression of a fusogenic protein from a replication-competent HAdV vector could enhance aspects of viral spread and cytotoxicity.

A more direct example is the development of GALV-armed Ad vectors. Guedan et al. generated AdwtRGD-GALV, a replication-competent HAdV vector expressing a

hyperfusogenic GALV envelope glycoprotein under control of the Ad major late promoter[153]. This design was intended to delay expression of the cytotoxic fusogenic protein until later stages of infection, thereby limiting premature syncytium formation during early viral replication. AdwtRGD-GALV formed large, fused cell structures and showed increased cytotoxicity compared with the non-fusogenic parental virus[153].

Fusogenic proteins have also been evaluated in replication-defective Ad vectors. For example, Hoffmann et al. generated an E1/E3-deleted Ad vector expressing the respiratory syncytial virus fusion protein, Ad.RSV-F, and tested it in syngeneic colorectal cancer mouse models[145]. Intratumoral administration of Ad.RSV-F reduced tumor growth and also promoted regression of contralateral, untreated tumors, suggesting the induction of systemic anti-tumor immunity[145].

Despite these promising results, incorporating fusogenic proteins into replication-competent Ads presents important design challenges. Fusogenic proteins derived from enveloped viruses are relatively large and their incorporation can complicate vector construction within Ad genome packaging constraints[59,90].

1.4.3 Arming Adenovirus Vectors with Fusion Associated Small Transmembrane (FAST) Proteins

Fusion-associated small transmembrane proteins (FAST) are a group of small viral non-structural (i.e. not part of the mature virion) proteins first identified by the laboratory of Dr. Roy Duncan (Dalhousie University, NS, CAN)[154,155]. Unlike enveloped viral fusogenic membrane glycoproteins, FAST proteins are not involved in virus-cell fusion during viral entry. Instead, they are expressed in infected cells and promote cell-cell fusion, leading to the formation of multinucleated syncytia[155,156]. FAST proteins were originally

characterized in fusogenic reoviruses, including members of the Orthoreovirus and Aquareovirus genera[156]. The best-characterized FAST proteins are those encoded by fusogenic reoviruses and include p10, p13, p14, p15, p16, and p22[156]. However, more recently, FAST or FAST-like proteins have been identified in a broader range of viruses. NSP1-1 proteins encoded by rotavirus species B, G, and I have been shown to function as FAST proteins, with fusion activity that can vary depending on cell type[157]. In addition, putative FAST proteins have been described in the Pistolviridae virus family, including CLuTLV p10 and SBTLV p11[158]. The PMCV, GSTLV-1, and CCTLV-1 viruses of the Pistolviridae family have shown predicted FAST-like regions within the C-terminal portions of their ORF3-encoded proteins[158]. FAST-like proteins have also been reported in avian deltacoronaviruses[159].

Although reovirus FAST proteins, including p10, p13, p14, p15, p16, and p22, have limited sequence similarity, they share several general structural features[156]. These proteins are small, single-pass membrane proteins that typically contain an N-terminal ectodomain, a transmembrane domain, and a C-terminal cytoplasmic endodomain[156]. All three regions contribute to the fusion process, although the specific fusion mechanisms and functional motifs differ between FAST proteins[156].

Within the reovirus FAST protein family, p10, p14, and p15 are among the most extensively characterized. The p10 FAST protein is encoded by avian reovirus and is approximately 10 kDa[160]. Its small ectodomain contains a hydrophobic patch that has membrane-destabilizing properties and is thought to function in a manner similar to fusion peptides found in enveloped viral fusion proteins[160]. The p14 FAST protein, encoded by reptilian reovirus, is approximately 14 kDa and contains a myristoylated N-terminal

ectodomain with a hydrophobic patch that contributes to membrane fusion activity[161]. The p15 FAST protein, encoded by baboon reovirus, is approximately 15 kDa and contains a highly compact N-terminal ectodomain in which both myristoylation and a polyproline type II helix are required for membrane fusion[162].

Reovirus FAST proteins are synthesized within infected cells and traffic through the endoplasmic reticulum (ER)–Golgi pathway, where they gradually accumulate before being transported to the plasma membrane[155]. During the pre-fusion stage, FAST proteins accumulate at the cell surface and help bring adjacent cellular membranes into close proximity. The fusion stage then involves membrane merger, beginning with hemifusion, in which the outer leaflets of the two membranes mix, followed by fusion pore formation[155]. Finally, during the post-fusion stage, the fusion pore expands, allowing the cytoplasms of adjacent cells to merge and form mature multinucleated syncytia[155].

Previous studies have explored p14 FAST as a fusogenic transgene in VSV-based platforms. Brown et al. expressed p14 FAST from a recombinant VSV backbone to determine whether FAST-mediated syncytium formation could enhance viral dissemination[163]. In cell culture, VSV/FAST induced large syncytia without impairing viral replication compared with a VSV/GFP control[163]. However, in vivo, VSV/FAST showed increased dissemination and neuropathogenesis in BALB/c mice, including higher viral titers in the brain and increased clinical signs following intranasal infection[163]. The therapeutic potential of p14 FAST was later evaluated in an interferon-sensitive oncolytic VSVΔM51 platform. Le Boeuf et al. generated VSV-p14 and showed that it enhanced viral dissemination, increased oncolytic activity in breast cancer spheroids, reduced 4T1 breast tumor growth, and prolonged survival in primary and metastatic tumor models compared

with a VSV-GFP control[164]. VSV-p14 also increased activation of CD4 and CD8 T cells, NK cells, and NKT cells, suggesting that p14 FAST can enhance oncolytic virotherapy through both increased cytolytic activity and immune stimulation[164].

Our laboratory has also evaluated p14 FAST expression in HAdV-based vectors. Wong et al. first generated AdFAST, a non-replicating E1/E3-deleted HAdV expressing p14 FAST from the CMV promoter[165]. AdFAST induced extensive syncytium formation in vitro, reduced metabolic activity, increased membrane permeability, and induced caspase-3 cleavage in A549 cells[165]. However, AdFAST did not significantly reduce tumor burden or improve survival in an A549 xenograft model in immunodeficient mice, suggesting that p14 FAST expression from a non-replicating HAdV vector was insufficient for therapeutic efficacy in vivo[165]. In a subsequent study, Wong et al. evaluated AdFAST in an immunocompetent 4T1 mammary carcinoma model to determine whether FAST-mediated effects could promote anti-tumor activity in the presence of an intact immune system[166]. In vitro, AdFAST produced only modest effects in 4T1 cells, including limited fusion and reduced metabolic activity. However, these effects did not translate in vivo, as AdFAST did not reduce tumor growth, improve survival, or induce detectable tumor cell fusion[166]. These studies suggest that p14 FAST expression from a replication-defective HAdV vector is insufficient to provide therapeutic benefit in both immunodeficient and immunocompetent tumor models. To address this limitation, Del Papa et al. later developed CRAdFAST, a conditionally replicating oncolytic HAdV expressing p14 FAST from the E3 region through a splice acceptor linked to the Ad major late transcription unit[167]. Compared with the control CRAd vector, CRAdFAST enhanced syncytium formation and cancer cell killing in vitro[167]. In an immunodeficient A549 xenograft model, CRAdFAST

induced tumor cell fusion, generated large acellular regions within tumors, and reduced the rate of tumor growth[167]. However, despite this improvement, substantial viable tumor tissue remained, indicating that further optimization is required to enhance the therapeutic effect of FAST-armed CRAds.

1.5 Production Challenges and Regulatory Strategies for Cytotoxic Transgene-Armed Viral Vectors

1.5.1 Production Challenges Associated with Cytotoxic Transgene-Armed Viral Vectors

The development of armed viral vectors requires balancing therapeutic potency with efficient vector production. Although cytotoxic transgenes can improve anti-tumor activity, their expression during vector amplification can be detrimental to producer cells[142]. Transgenes that induce apoptosis, membrane disruption, immune activation, or cell-cell fusion may reduce producer cell viability, interfere with viral replication, and decrease final vector yield[153]. This issue is particularly relevant for fusogenic proteins, since premature expression during production could induce syncytium formation and cell death before sufficient viral titers are generated[153]. For example, Guedan et al. reported that previous attempts to generate Ad vectors encoding the GALV fusogenic glycoprotein were difficult, likely because premature cell fusion interfered with virus replication[153]. Even when GALV expression was delayed by placing it under the control of the Ad major late promoter, syncytium formation still reduced total virus production under low-MOI conditions, despite increasing cytotoxicity[153]. This issue is also relevant to FAST-armed vectors, as our lab has observed that viruses encoding FAST proteins can be difficult to propagate, likely due to premature fusion and producer cell toxicity.

1.5.2 Strategies to Improve the Production of Cytotoxic Transgene-Armed Viral Vectors

Several regulatory strategies have been developed to limit unwanted transgene expression during viral vector production or to restrict transgene activity to target cells. One strategy is the use of tissue or tumour specific promoters, which place transgene expression under the control of regulatory elements that are preferentially active in specific cell types. In cancer gene therapy, promoters such as prostate-specific antigen (PSA), human telomerase reverse transcriptase, or other tumour-associated promoters have been used to restrict viral gene expression or therapeutic transgene expression to malignant cells[101,168,169].

An alternative strategy involves the use of inducible promoters, which allow the expression of transgenes to be activated only under specific conditions or in the presence of an inducer. Massie et al. developed a Tet-Off Ad expression system in which transgene expression was driven by the tetracycline-controlled transactivator (tTA) and repressed in the presence of tetracycline[170]. Using this system, they generated an HAdV vector expressing a toxic truncated HSV-2 ribonucleotide reductase protein that could otherwise not be rescued using constitutive expression systems[170]. Similar regulatory concepts have also been applied to fusogenic transgenes. Brade et al. used a modified human HSP70b heat-inducible promoter to regulate expression of the GALV fusogenic membrane glycoprotein[171]. This promoter had low basal activity at 37°C but was strongly induced following mild hyperthermia, allowing GALV-mediated syncytium formation to be selectively activated after heat treatment[171].

In addition to promoter-based regulation, transgene expression can be controlled following transcription. miRNA-based regulation can suppress transgene expression by

placing miRNA target sequences within the viral transcript[172]. In cells expressing the miRNA, the transcript is recognized by the miRNA-silencing machinery and is degraded and/or translationally repressed[172]. Transcription can also be inhibited through steric interference. In the LacI/LacO system, LacI binds to LacO sequences inserted within the transgene expression cassette[173,174]. When positioned near the promoter or within the transcribed region, bound LacI can act as a physical barrier to RNA polymerase, reducing transgene transcription during vector production in LacI-expressing producer cells[173,174].

The following sections will expand on miRNA and LacI/LacO systems as methods for silencing cytotoxic transgenes during viral vector production.

1.5.3 miRNA-Based Strategies to Suppress Cytotoxic Transgene Expression During Vector Production

miRNAs are part of a broader group of RNA-silencing pathways that use small RNA molecules to regulate gene expression in a sequence-specific manner. This broader category, known as RNA interference, includes small interfering RNAs (siRNAs), short hairpin RNAs (shRNAs), and microRNAs (miRNAs)[175]. These three RNA-silencing systems differ in their origin, structure, and processing, but they all function to reduce gene expression[175]. The following paragraphs focus specifically on the use of miRNA-based regulation to suppress cytotoxic transgene expression during viral vector production.

miRNAs are endogenous, short non-coding RNAs that naturally regulate gene expression in eukaryotic cells. In the canonical pathway, miRNAs are typically transcribed as longer primary miRNA transcripts, which are processed by Drosha-DGCR8 and Dicer to generate mature miRNA duplexes[176]. One strand of the duplex is loaded into an Argonaute-containing silencing complex and guides the complex to complementary

sequences in target mRNAs[176]. The complementary sequences are most commonly within the 3' untranslated region (UTR) of the target mRNA[176]. This leads to reduced protein expression through translational repression and/or mRNA destabilization[176]. This pathway can be adapted for viral vector regulation by inserting artificial miRNA target sites into the transgene transcript, allowing expression to be reduced in cells that express the corresponding miRNA[172].

miRNA-based regulation has been applied to Ad vectors to restrict viral gene expression or replication in specific cellular contexts. For example, Ylösmäki et al. inserted six complementary target sites for miR-122, a liver-specific miRNA, into the 3′ UTR of the Ad E1A gene[177]. This modification strongly suppressed Ad replication in normal human liver tissue where miR-122 is typically highly enriched. However, in tumour cells with low or absent miR-122 expression, E1A is not targeted for miRNA-mediated repression, allowing viral replication to proceed. A similar strategy was applied by Palmer et al. during the production of CRISPR/Cas9-expressing helper-dependent Ad vectors[178]. In this system, miRNA target sequences were inserted into the Cas9 3′ UTR to reduce Cas9 mRNA during vector production and limit unwanted vector self-cleavage.

1.5.4 LacI/LacO-Based Strategies to Regulate Cytotoxic Transgene Expression During Vector Production

The lactose repressor (LacI) is a bacterial DNA-binding protein encoded by the *lacI* gene of the *Escherichia coli* (E. *coli)* lactose operon[179]. In its natural context, LacI regulates lactose metabolism by binding to lac operator (LacO) sequences located near the lac promoter, where it acts as a physical barrier to RNA polymerase and prevents transcription of the downstream genes required for lactose metabolism[179,180]. When lactose

or an inducer such as isopropyl β-D-1-thiogalactopyranoside (IPTG) is present, LacI undergoes a conformational change that reduces its affinity for LacO, allowing transcription to proceed[180]. This inducible and reversible DNA-binding system has been adapted from bacteria for use in mammalian gene regulation, including viral vector production[173,174]. By incorporating LacO sequences into an expression cassette and using producer cells that express LacI, transgene expression can be repressed during vector amplification. This strategy is particularly useful for vectors encoding cytotoxic or difficult-to-produce transgenes, where reducing expression in producer cells may improve vector rescue, propagation, and final yield.

This bacterial regulatory system has therefore been adapted for vector silencing methods. Matthews et al. developed a 293-derived LacI-expressing cell line, termed 293LAP13, to produce Ad vectors encoding rabies virus glycoprotein, which had been difficult to rescue in standard 293 cells[173]. In this system, a single LacO sequence was inserted immediately downstream of the transcription start site, allowing LacI to repress transgene expression during vector production by physically blocking passage of the RNA polymerase[173]. This improved vector rescue, plaque formation, and viral titers in LacI-expressing producer cells[173]. Edholm et al. used a related strategy to reduce leaky expression from an inducible Ad vector[174]. They inserted three LacO sequences into the β-globin intron of the expression cassette and used LacI-expressing 293 cells to block transcriptional elongation[174]. Combining inducible promoter control with LacI/LacO-mediated repression reduced basal transgene expression, supporting this system as a method to improve production of Ad vectors encoding toxic or growth-inhibitory proteins[174].

1.6 Rationale, Hypothesis, and Objectives

Although CRAds are promising cancer therapeutics, their efficacy in solid tumors is limited in part by poor intratumoral spread and incomplete tumor destruction[49,126]. Arming CRAds with fusogenic proteins may help overcome this limitation by promoting cell-cell fusion, thereby extending cytopathic effects beyond initially infected cells and enhancing local tumor cell killing. FAST proteins are attractive fusogenic transgenes because they are small, non-structural proteins that induce cell-cell fusion[155,156]. Previous work from our lab showed that p14 FAST can enhance syncytium formation and improve tumor cell destruction in vivo[167]. Despite this, substantial viable tumor tissue remained following CRAdFAST treatment, suggesting that further optimization is required[167]. Since FAST proteins differ in their structural features and mechanisms of membrane fusion, comparing p10, p14, and p15 may identify a more suitable candidate for future HAdV-based vector development[156,160-162]. A second challenge is that FAST-mediated fusion may complicate vector production. Premature expression of fusogenic transgenes during viral amplification can induce syncytium formation and producer cell death, reducing viral yield[153]. Therefore, regulatory systems that suppress transgene expression during production may improve the feasibility of generating FAST-armed CRAds[170,173,174,178]. I hypothesize that p10, p14, and p15 FAST proteins differ in their fusogenic activity and cytotoxic effects, with one FAST protein demonstrating greater potential for incorporation into HAdV-based vectors. I further hypothesize that miRNA-mediated silencing and LacI/LacO-mediated repression can reduce HAdV-encoded transgene expression, supporting their potential use as regulatory systems for the production of cytotoxic transgene-armed CRAds. My objectives include:

1. Evaluate the relative fusogenic capacity and cytotoxic effects of p10, p14 and p15 FAST proteins in vitro.
2. Investigate the efficacy of a miRNA-based system in silencing the expression of proteins expressed from HAdV.
3. Investigate the efficacy of a Lac repressor-based system in silencing the expression of proteins expressed from HAdV.

Chapter 2: Materials and Methods

2.1 Cell culture

Human embryonic kidney 293 cells (HEK-293)[92], 293 suspension cells (293N3S)[181] and adenocarcinomic human alveolar basal epithelial cells (A549)[182] were maintained in Minimum Essential Medium (MEM) (Sigma Aldrich, Oakville, ON, Canada) supplemented with 10% (v/v) Fetal Bovine Serum (FBS) (Corning, Corning, NY), 2 mM GlutaMAX (Gibco, Grand Island, NY) and 1X Antibiotic-Antimycotic (Gibco). Cells were incubated at 37°C with 5% CO_2. Two additional cell lines were engineered from HEK-293 cells. 293:eYFP-miFluc was generated by transfecting a plasmid expressing a micro-RNA targeting firefly luciferase (Fluc) located within the 3' untranslated region (UTR) of an eYFP reporter gene. This cassette was a kind gift from Dr. Maxime Rousseau (University of Ottawa, ON, CAN). 293:mCherry-LacI was similarly generated by transfecting a plasmid expressing a fusion protein of the Lac repressor and the mCherry reporter, which was obtained from Dr. Joan L. Betz (Regis University, Denver, CO). Plasmids contained a hygromycin resistance gene linked to the reporter cassette through an internal ribosome entry site (IRES) and cells were selected for the highest reporter signal at 200 μg/mL of hygromycin B (Invitrogen, Waltham, MA). Cells were maintained at the same conditions as regular HEK-293 but kept under selection with 200 μg/mL of hygromycin B (Invitrogen) to ensure stable expression of the transgene. 293 and 293 N3S cells were a kind gift from Dr. Frank Graham (McMaster University, ON, CAN). A549 cells were obtained from the American Type Culture Collection (ATCC) (CCL-185, ATCC, Manassas, VA).

2.2 Adenoviral constructs and adenovirus purification

Schematic representations of HAdV used are in Figure 3.3, 4.2 and 5.2. Viruses are based on adenovirus serotype 5 (HAdV-C5) and generated through traditional and RecA-mediated cloning[183]. AdFAST-HA (AdCW103) is a non-replicating HAdV deleted of the E1 and E3 regions and possesses the p14 FAST HA-tagged gene under regulation by the human cytomegalovirus (CMV) immediate early enhancer/promoter as well as the bovine growth hormone polyadenylation sequence (BGHpA) replacing the E1 region. This virus has been previously described in Wong et al.[165]. A similar virus, AdFAST (AdRP2872), contains the same genetic elements as AdFAST-HA but lacks the HA tag, and has been previously described[165]. AdEmpty (AdRP2014) is a HAdV lacking any transgenes and is deleted of the E1 and E3 regions and has been previously described[165].

AdNlucFluc (AdRP3285) is a replication incompetent HAdV which expresses NanoLuc luciferase (Nluc) in the E1 region and Fluc in the E3 region. Expression of both transgenes is driven by the CMV immediate-early enhancer/promoter, providing constitutive protein expression. AdNlucSAFluc (AdGA102) is similar in structure to AdNlucFluc but instead possesses a splice acceptor (SA) site-Fluc expression cassette in the E3 region, which places the Fluc gene under regulation by the viral major late promoter (MLP). The MLP is greatly activated following the onset of viral DNA replication (~8 hpi)[71,72], linking expression of the Fluc gene to viral replication and ensuring that the protein is expressed only in cells permissive to viral replication. This construct more closely resembles the architecture of an oncolytic HAdV as described in Del Papa et al.[167]. AdNluc (AdRP3279) possesses a CMV-Nluc expression in the E1 region and is devoid of any transgenes in the E3 region.

AdLacONlucFluc (AdRP3510) is a E1/E3 deleted HAdV-based vector with a similar structure to AdNlucFluc but with the addition of 16 tandem repeats of a synthetic Lac operator (LacO) sequence (5'-AATTCCACATGTGGAATTGTGAGCGGATAACA ATTTGTGG-3')[184] positioned between the CMV promoter and the Nluc gene in the E1 region. This synthetic LacO sequence was obtained from Dr. Joan L. Betz (Regis University, Denver, CO) and is based on the natural LacO sequence from the *E. coli* lac operon, with additional EcoRI-compatible flanking sequences to facilitate cloning of tandem LacO repeats[184]. In *E. coli*, LacO is located within the lac operon and serves as the binding site for the Lac repressor (LacI), which represses transcription of downstream genes responsible for the metabolism of lactose[179]. In our viral construct, the LacO sequence repeats should enable LacI-mediated steric repression of Nluc transcription in cells where the LacI is present. AdNlucLacOFluc (AdRP3511) possesses the same genetic elements but in this configuration, the 16 tandem repeats of the LacO sequence are inserted between the Nluc gene and the bovine growth hormone polyadenylation sequence (BGHpA) in the E1 region. AdFlucSANlucLacO (AdGA130) contains a CMV-Fluc expression cassette in the E1 region and a SA-Nluc cassette followed by 16 repeats of the LacO site positioned downstream of the Nluc gene in the E3 region. AdFlucSANluc (AdGA133) shares the same overall design but does not contain the LacO repeats. Viruses were grown on 293 and 293N3S cells, then purified and titered as previously described in Ross et al.[185].

2.3 Viral infection

Cells were infected at varying multiplicities of infection (MOIs) with a volume of 200 µL or mock infected with phosphate buffered saline (PBS; Sigma Aldrich, Oakville,

ON, Canada) for 1 h at 37°C, with gentle rocking every 15 mins to redistribute the virus evenly across the bottom of the well. Fresh media was then added to each well. For burst size titer assays, wells were washed once with PBS to remove unbound virus prior to the addition of fresh medium.

2.4 Luciferase assay

293 cells were seeded in 6-wells plates at density of 6 x 10^5 cells per well or in 12-well plates at a density of 3 x 10^5 cells per well. Twenty-four hours after seeding, cells were infected with corresponding virus at an MOI of 1. Cells were subsequently harvested at 8 hours post-infection (hpi) or 24 hpi with 200 µL (6-well plates) or 150 µL (12-well plates) of 1x passive lysis buffer (PLB; diluted from 5x Passive Lysis Buffer, E1941, Promega, Madison, WI) and stored at −20°C. Luciferase assays were conducted using the Nano-Glo Dual Luciferase Reporter Assay kit (N1630, Promega, Madison, WI) according the manufacturer's protocol. Luciferase activity was recorded using a 20/20 luminometer (Turner Biosystems, Sunnyvale, CA).

2.5 Immunoblot

Cells in 35 mm dished were lysed with 200 µL of 2x Laemmli buffer (LB, 0.125M Tris HCl pH 6.8, 20% glycerol, 4% SDS, 0.004% Bromophenol Blue, 5% 2-mercaptoethanol) and stored at −20°C. Luciferase assay samples in 1x passive lysis buffer were mixed at a 1:1 ratio with 2x LB. All samples were boiled at 100°C for 10 mins prior to protein separation by sodium dodecyl sulphate-polyacrylamide gel electrophoresis (SDS-PAGE). Proteins were transferred to an Immobilon-P polyvinylidene difluoride (PVDF) membrane (Millipore, Burlington, MA). Membranes were blocked for 1 h at room temperature (RT) or overnight with Intercept (PBS) Blocking Buffer (927-70001, LI-COR

Biosciences, Nebraska). Membranes were then probed with the following primary antibodies diluted in blocking buffer supplemented with 0.2% Tween 20: α-Tubulin (1:10000 for 1 h at RT, 05-829, Millipore, Burlington, MA), β-Tubulin (1:10000 for 1 h at RT, ab6046, Abcam, Cambridge, UK), FLAG (1:5000 overnight at 4°C, F1804, Sigma), RFP (1:3000 overnight at 4°C, ab62341, Abcam), GFP (1:5000 for 1 h at RT, A11122, Invitrogen), Nluc (N700A, Promega, Madison, WI), Fluc (1:1000 overnight at 4°C, L0159, Sigma), Adenovirus Type 5 (1:1000 overnight at 4°C, ab6982, Abcam). Subsequent to primary antibody incubation, membranes were washed three times with PBS containing 0.1% Tween 20 (PBST) and probed with the following fluorescently labelled secondary antibodies diluted in blocking buffer supplemented with 0.2% Tween 20 and 0.01% SDS: IRDye goat anti-mouse 680 (926-68070, LI-COR), IRDye goat anti-mouse 800 (925-32210, LI-COR), IRDye goat anti-rabbit 680 (925-68071, LI-COR), and IRDye goat anti-rabbit 800 (926-32211, LI-COR). Membranes were developed using the Odyssey CLx infrared fluorescence detection system (LI-COR Biosciences, Nebraska) and visualized with the LI-COR Image Studio 4.0 software.

2.6 Fluorescence microscopy and image quantification

293 cells were seeded in 6-well plates with coverslips at a density of 6 x 10^5 cells per well. The following day, cells were transfected with plasmids encoding the indicated FAST proteins, each co-expressing an mCherry reporter: p10, p10-HA, p14, p14-HA, p15, and p15-HA. An empty plasmid expressing mCherry alone was included as a control. To allow quantification of the fusion events, plasmids were diluted 1:10 with empty pcDNA3 vector prior to transfection. Therefore, each transfection contained 0.2 µg of corresponding plasmid and 1.8 µg of empty pcDNA3, for a total of 2 µg of plasmid DNA. This dilution

was used to reduce the extent of fusion and prevent widespread fusion of the entire cell monolayer, which would make image-based quantification difficult. Transfections were performed in plain MEM using 4 µL of Lipofectamine 2000 (Invitrogen, Waltham, MA) per 2 µg of plasmid DNA or mock transfected with PBS. Twenty-four hours post transfection (hpt), media was removed and cells were rinsed 3 times with PBS and fixed with 4% paraformaldehyde (PFA) in PBS for 10 min at RT. Cells were subsequently washed 3 times with PBS and stained with Hoechst 33342 at a concentration of 1 µg/mL (H3570, Invitrogen, Waltham, MA) in PBS for 5 mins. Coverslips were then mounted onto slides with Dako Fluorescence Mounting Medium (S3023, Agilent, Santa Clara, CA) and imaged with a Zeiss Axio Imager upright microscope using the ZEN imaging software. Images were processed using FIJI Image J. Quantification of fluorescence signal was conducted using CellProfiler (version 4.2.8).

2.7 MTS metabolic activity assays

293 cells were seeded in 96-well plates at a density of 3×10^4 cells per well. The following day, cells were transfected with plasmids expressing the indicated FAST proteins, including p10, p10-HA, p14, p14-HA, p15, and p15-HA, or with an empty pcDNA3 plasmid. Transfections were performed using 4 µL of Lipofectamine 2000 per 2 µg of plasmid DNA or mock transfected with PBS. For metabolic activity assays involving AdFAST and AdFAST-HA, 293 or A549 cells were seeded at densities of 3×10^4 cells per well and 4×10^4 cells per well respectively. The following day, 293 cells were infected at an MOI of 10, whereas A549 cells were infected at varying MOIs (1, 10, 50, and 100). Cellular metabolic activity was measured at various time points using the CellTiter 96 AQueous Non-Radioactive Cell Proliferation Assay (G5430, Promega, Madison, WI).

Cells were incubated with 15 µL of MTS reagent [3-(4,5-dimethylthiazol-2-yl)-5-(3-carboxymethoxyphenyl)-2-(4-sulfophenyl)-2H- tetrazolium] added directly to the culture medium for 1 h at 37°C. Absorbance values were measured at 490nm measured using a SpectraMax 190 plate spectrophotometer (Molecular Devices, San Jose, CA).

2.8 Assessment of HAdV Growth Kinetics

Growth kinetics assays were performed to assess whether the indicated regulatory cell lines affected HAdV amplification over time. In this context, growth kinetics refers to the relative amount of virus produced following infection of different producer cell lines with the same input virus dose and harvesting at defined time points post-infection.

Parental 293 cells and the corresponding regulatory cell line were seeded at a density of 6×10^5 cells per well in 35 mm dishes. For the miRNA-based system, 293 cells and 293:eYFP-miFluc cells were infected with AdNluc at an MOI of 1 and AdNlucSAFluc at an MOI of 0.1. For the LacI/LacO-based system, 293 cells and 293:mCherry-LacI cells were infected with the at an MOI of 3. Infections were performed for 1 h at 37°C, with rocking every 15 min. Following infection, cells were rinsed with PBS and fresh medium was added. At 4, 24, or 48 hpi, cells were harvested directly into the culture medium, supplemented with 4% sucrose, and stored at −80°C. Samples were then subjected to two rounds of freeze-thaw to release progeny virions.

For the miRNA-based system, relative virus growth was assessed using a NanoLuc luciferase-based readout. Harvested virus-containing lysates from 293 and 293:eYFP-miFluc cells were used to infect parental 293 cells. At 24 hpi, NanoLuc luciferase activity was measured as a surrogate readout of viral amplification. For the LacI/LacO-based system, viral growth was assessed by plaque assay. Harvested virus-containing lysates from

293 and 293:mCherry-LacI cells were serially diluted and used to infect parental 293 cells. Viral titers were determined by plaque counting 10 days post infection (dpi)[185].

2.9 Statistical analysis

All statistical analyses were performed using GraphPad Prism version 10.5.0. The specific type of test performed is indicated within the figure legends. One asterisk (*) represents $p<0.05$, two asterisks (**) represent $p<0.01$, three asterisks (***) represent $p<0.001$, and four asterisks (****) represent $p<0.0001$.

Chapter 3: Evaluating the fusogenic capacity and cytotoxic effects of p10, p14, and p15 FAST proteins *in vitro*

3.1 Introduction

Previous work from our lab has demonstrated the effectiveness of an HA-tagged version of the p14 FAST protein at inducing cell fusion and apoptosis in vitro[165]. However, when a replication-defective HAdV expressing p14-HA was delivered in a xenograft mouse model harbouring subcutaneous A549 tumors, its therapeutic potential was limited, inducing minimal fusion and no reduction in tumor size[165]. More recent work from our lab showed that a conditionally replicating HAdV expressing p14-HA FAST induced syncytium formation in A549 tumors in vivo and showed evidence of nuclear fragmentation, an early marker of apoptosis[167]. Despite these findings, the virus had limited impact on tumour size reduction. These observations suggest that while p14-HA FAST retains fusogenic activity, its efficacy in vivo may be suboptimal. The HA tag was originally included to facilitate detection of FAST protein expression, as antibodies against native FAST proteins are not commercially available. Although epitope tags are widely used and often assumed to have minimal impact on protein function, some studies have shown that they can affect protein folding, localization, and activity[186,187]. This may be particularly relevant for FAST proteins, as they are small membrane fusogens whose activity depends on interactions between their ectodomain, transmembrane domain, and cytoplasmic endodomain[156]. Given the limitations observed with the p14-HA FAST expressing vectors, I evaluated the potential of other FAST proteins (p10 and p15 FAST) at inducing fusion and apoptosis. In addition, I examined whether the addition of the HA tag to the protein reduces fusion capacity.

3.2 Results

3.2.1 Untagged p14 FAST induces the highest level of fusion in HEK293 cells

Our lab previously attempted to generate HAdV vectors expressing p10 and p15, however, this proved difficult and achieving high titers of the virus was unsuccessful. Thus, we hypothesized that these proteins may exhibit greater cytotoxicity than p14 FAST and induce increased fusion. We first evaluated their fusogenic capacity following plasmid transfection in HEK293 cells. To initially examine the fusogenic capacities of p10, p14, and p15 FAST proteins, as well as their HA-tagged counterparts, we generated six plasmids: one for each untagged FAST protein and one for each corresponding HA-tagged version. Each plasmid also co-expresses an mCherry reporter. The plasmids were then transfected at a 1:10 dilution with an empty pcDNA3 plasmid into 35mm dishes of HEK293 cells. This dilution was used to reduce the extent of fusion and prevent complete fusion of the cell monolayer, allowing fusion events to be more accurately quantified by image analysis. For controls, an mCherry plasmid lacking any FAST expression cassette was also transfected along with a mock (PBS) treatment. At 24 hours post-transfection (hpt), cells were fixed, stained with Hoechst and mounted to slides. Fluorescence microscopy showed that cells transfected with untagged p14 FAST exhibited the highest level of fusogenic activity compared with the other FAST proteins tested (Figure 3.1A). To gain a better understanding of the amount of fusion induced by the different FAST proteins, we quantified the microscopy images with the use of the CellProfiler software. To achieve this, the experiment was repeated once more resulting in two biological replicates overall. Each transfection in each of the biological replicates was done twice for a total technical replicate count of four. To obtain a more robust assessment of fusion, six images were

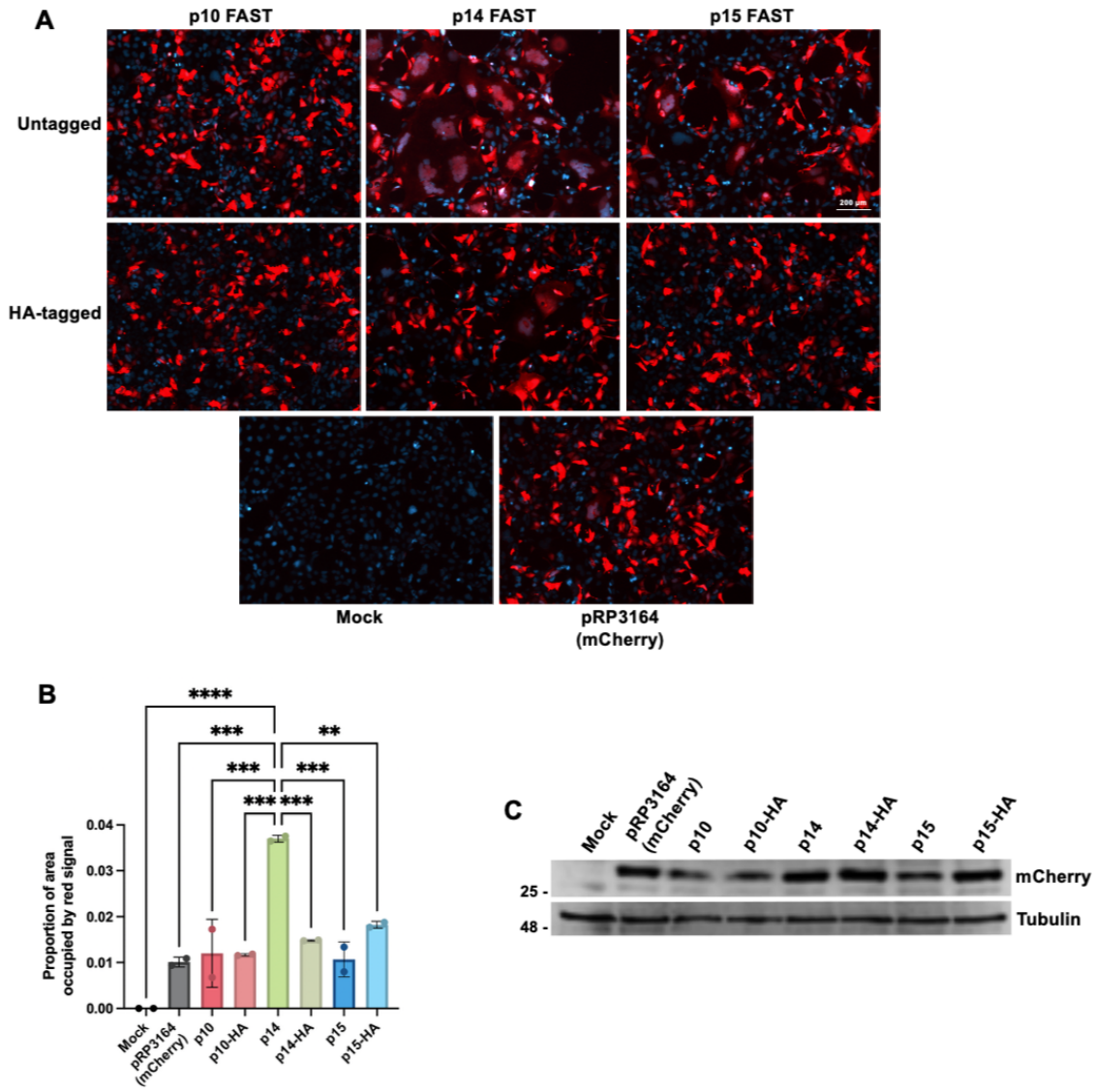

Figure 3.1 Untagged p14 FAST induces the highest level of fusion in HEK293 cells. Cells were transfected with plasmids encoding the indicated FAST proteins, each co-expressing an mCherry reporter, diluted 1:10 with an empty pcDNA3 vector in plain MEM. Mock-transfected cells (PBS) and cells transfected with a simple mCherry plasmid (pRP3164) served as controls. Cells were fixed and stained with Hoechst 24 hpt. A) Images were captured by fluorescence microscopy. Scale bar represents 200 µm. B) Quantified red signal from the images captured in panel A. Data is representative of two biological replicates (n=2), each biological replicate included two technical replicates, and six images were collected for each technical replicate. Statistical significance was assessed by one-way ANOVA followed by Sidak's multiple comparisons test. Two asterisks (**) indicate $p<0.01$, three asterisks (***) indicate $p<0.001$ and four asterisks (****) indicate $p<0.0001$. C) Immunoblot performed in parallel, cells were lysed and harvested with 2x Laemmli buffer.

captured from distinct fields of each coverslip, resulting in a total of 12 images per treatment group per biological replicate. As previously mentioned, each plasmid co-expresses an mCherry reporter. Therefore, cells expressing the FAST protein also express mCherry. This construct allowed us to quantify fusion by measuring the total red fluorescent area in each image. Data was then averaged per biological replicate for each treatment group and plotted as the percentage of area occupied by the red signal (Figure 3.1B). Untagged p14 FAST produced the highest level of red fluorescent area, occupying an average of 3.7% (± 0.07% SD) of the field of view (Figure 3.1B). This was significantly higher than the mock-transfected control, where no red signal was detected. In contrast, p10 and p15 FAST occupied average red fluorescent areas of 1.2% (± 0.7% SD) and 1.07% (± 0.4% SD), respectively, both of which were significantly lower than p14 FAST ($p = 0.0002$ for both comparisons). p10 and p15 were also similar to the mCherry control (1.01% (± 0.1% SD)), indicating that they induced limited detectable fusion under these conditions. Furthermore, the addition of an HA tag substantially reduced the fusogenic activity of p14 FAST. Cells transfected with p14-HA occupied an average red fluorescent area of 1.4% (± 0.01% SD), compared with 3.7% (± 0.07% SD) for untagged p14 FAST ($p = 0.0005$) (Figure 3.1B). In contrast, HA tagging did not markedly affect p10 or p15 FAST, as p10-HA and p15-HA occupied average red fluorescent areas of 1.2% (± 0.02% SD) and 1.8% (± 0.08% SD) respectively. Together, these findings suggest that p14 FAST exhibits superior fusogenic activity relative to p10 and p15, and that addition of an HA tag specifically interferes with p14 FAST-mediated fusion.

To confirm comparable transfection efficiency across all treatment groups, we performed an immunoblot in parallel. Since antibodies were not available for all FAST

proteins and only the HA-tagged constructs could be directly detected, mCherry expression was used as a surrogate marker of plasmid uptake and transgene expression. Each FAST expression plasmid co-expresses mCherry; therefore, similar mCherry levels across treatment groups would suggest comparable transfection efficiency. Qualitative analysis indicated that mCherry protein levels were consistent across all transfection groups, with tubulin serving as a stable control (Figure 3.1C). This result suggests that the observed differences in fusion were not due to differences in plasmid uptake, but rather the result of differences in the fusogenic activity between the FAST proteins. However, because FAST protein levels were not directly measured for all constructs, this interpretation assumes that FAST protein expression generally followed the same pattern as mCherry expression from the corresponding plasmids.

3.2.2 Untagged p14 FAST induces the most pronounced decrease in metabolic activity in HEK293 cells

Syncytium formation caused by FAST proteins can activate apoptotic signaling pathways, resulting in decreased membrane integrity and cell viability[188]. Based on these findings, we evaluated the metabolic activity of cells expressing p10, p14 and p15 FAST and their HA-tagged counterparts. Through this analysis, we sought to confirm our previous findings that p14 FAST induces the highest level of fusion and that the addition of the HA tag impairs this activity, as reflected by changes in metabolic activity. Using the same plasmids described above, HEK293 cells were transfected and metabolic activity was measured at 24 and 48 h post-transfection (hpt) using an MTS-based assay. At 24 hpt, metabolic activity remained relatively variable across treatment groups (Figure 3.2A). Although p10 FAST and p14 FAST showed average relative metabolic activity values of

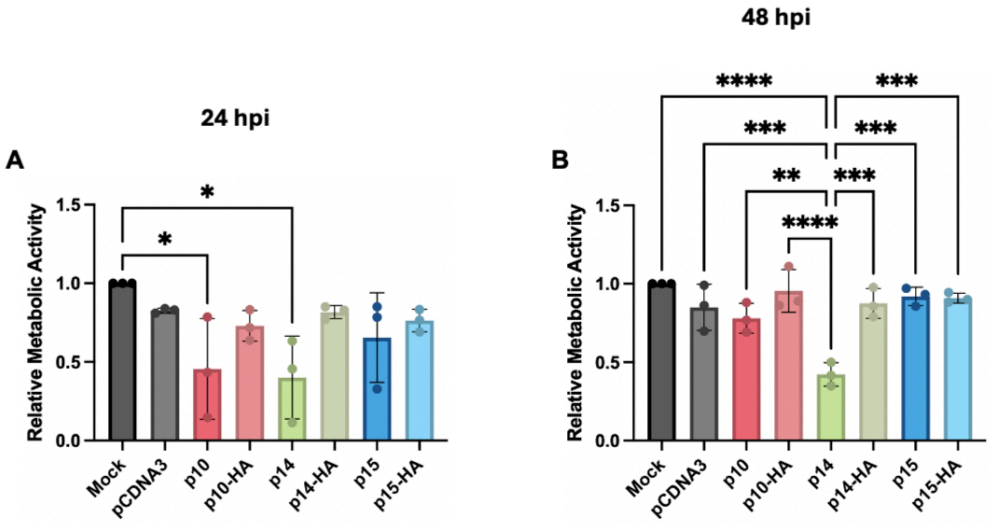

Figure 3.2 Untagged p14 FAST induces a pronounced decrease in metabolic activity in HEK293 cells. Cells were transfected with plasmids encoding the indicated FAST proteins in plain MEM. Metabolic activity was measured 24 hpt (panel A) and 48 hpt (panel B) by MTS assay. Values were normalized to mock transfected cells. Data is representative of three biological replicates (n=3) with three technical replicates per transfection. Statistical significance was assessed by one-way ANOVA followed by Tukey's multiple comparisons test. One asterisk (*) indicates $p<0.05$, two asterisks (**) indicate $p<0.01$, three asterisks (***) indicate $p<0.001$ and four asterisks (****) indicate $p<0.0001$.

46% (± 26% SD) and 40% (± 21% SD) respectively, neither condition was significantly different from the pcDNA3 control. Therefore, FAST-specific effects on metabolic activity appeared limited at this early time point. By 48 hpt, the cytotoxic effect of untagged p14 FAST became more pronounced (Figure 3.2B). Cells expressing untagged p14 FAST had a relative metabolic activity of 42% (± 6% SD) to that of mock transfected cells. This was lower than the pcDNA3 control (85% (± 12% SD)) and all the other FAST-expressing conditions. In contrast, the metabolic activity of cells expressing p10, p15, or the HA-tagged FAST proteins was not significantly different from pcDNA3-treated cells. These results indicate that untagged p14 FAST was associated with the strongest reduction in metabolic activity in HEK293 cells at 48 hpt. This delayed reduction in metabolic activity likely reflects the time required for syncytium formation to progress, consistent with the greater fusogenic activity of p14 FAST relative to p10, p15, and the HA-tagged versions. Taken together, these findings indicate that untagged p14 FAST not only drives the strongest fusion activity but is also associated with a larger decrease in metabolic activity relative to the other FAST proteins tested and their HA-tagged counterparts, consistent with a stronger cytotoxic phenotype.

3.2.3 E1/E3-deleted HAdV expressing untagged p14 FAST induces a more pronounced decrease in metabolic activity than the HA-tagged version in HEK293 cells

The results presented above demonstrate that untagged p14 FAST induces the highest level of fusion in HEK293 cells. Consistent with this observation, syncytium formation was associated with a significant reduction in metabolic activity relative to its HA-tagged counterpart and the other FAST proteins evaluated. The experiments described above were performed using plasmid-based expression systems. Although this

experimental design enabled direct comparison of fusion among the different FAST proteins, it does not fully reflect the context of viral delivery. Having established that p14 was the most fusogenic FAST protein in the plasmid-based system, subsequent experiments were conducted using HAdV vectors expressing either p14 or p14-HA to determine whether the HA tag similarly reduced p14 FAST activity following viral delivery. Although the vectors used in these experiments were replication-defective E1/E3-deleted HAdVs, HEK293 cells provide E1 in trans and therefore support their replication[92]. This experiment therefore provided a replication-permissive context to assess p14 FAST-mediated fusion and potential challenges associated with vector amplification. Schematics of viruses which were used can be found in Figure 3.3. AdFAST is a replication defective HAdV, deleted of the E1 and E3 regions, possessing a CMV-p14 FAST expression cassette in E1. AdFAST-HA is identical to AdFAST with the addition of the HA tag to the p14 FAST protein. As a control, we used replication defective HAdV devoid of any transgenes in the E1 and E3 region (AdEmpty). Including AdEmpty as a control allowed us to attribute any observed reductions in metabolic activity to the fusion activity of the FAST proteins rather than to viral replication. HEK293 cells were seeded into 96-well plates and then infected with either AdEmpty, AdFAST or AdFAST-HA at an MOI of 10. A mock infection using PBS was included as an additional control. Metabolic activity was then assessed at 24, 48 and 72 hours post infection (hpi) using an MTS-based assay.

At 24 hpi, there was no observed decrease in metabolic activity (Figure 3.4A). Interestingly, cells infected with AdEmpty or AdFAST-HA showed a modest increase in metabolic activity relative to the mock control, although these differences were not statistically significant (Figure 3.4A). At 48 hpi, cells infected with AdFAST showed a

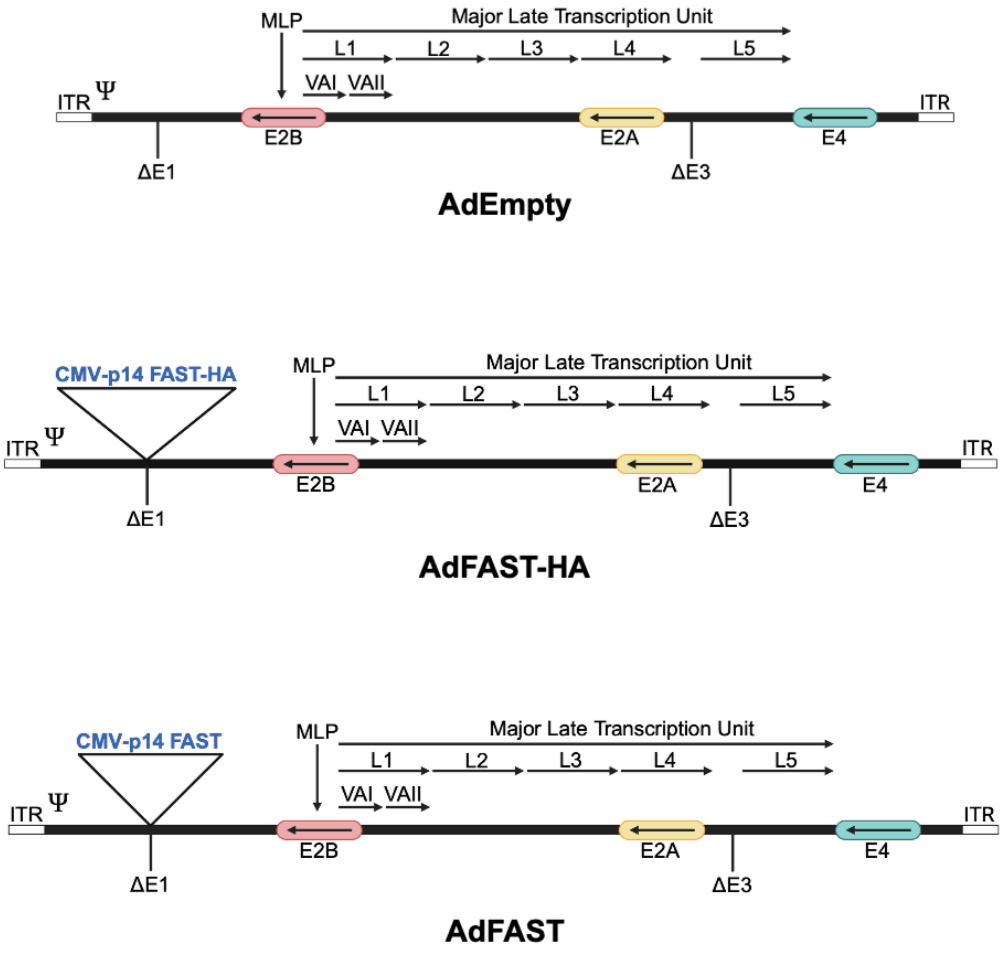

Figure 3.3 Schematic representation of viruses used to compare p14 FAST and HA-tagged p14 FAST. AdEmpty is a replication-incompetent HAdV devoid of the E1 and E3 region with no additional transgenes. AdFAST-HA is a E1 and E3 deleted vector expressing HA-tagged p14 FAST from the cytomegalovirus (CMV) immediate early enhancer/promoter in the E1 region. AdFAST is identical to AdFAST-HA with the removal of the HA tag from p14 FAST. Schematics created with BioRender.com.

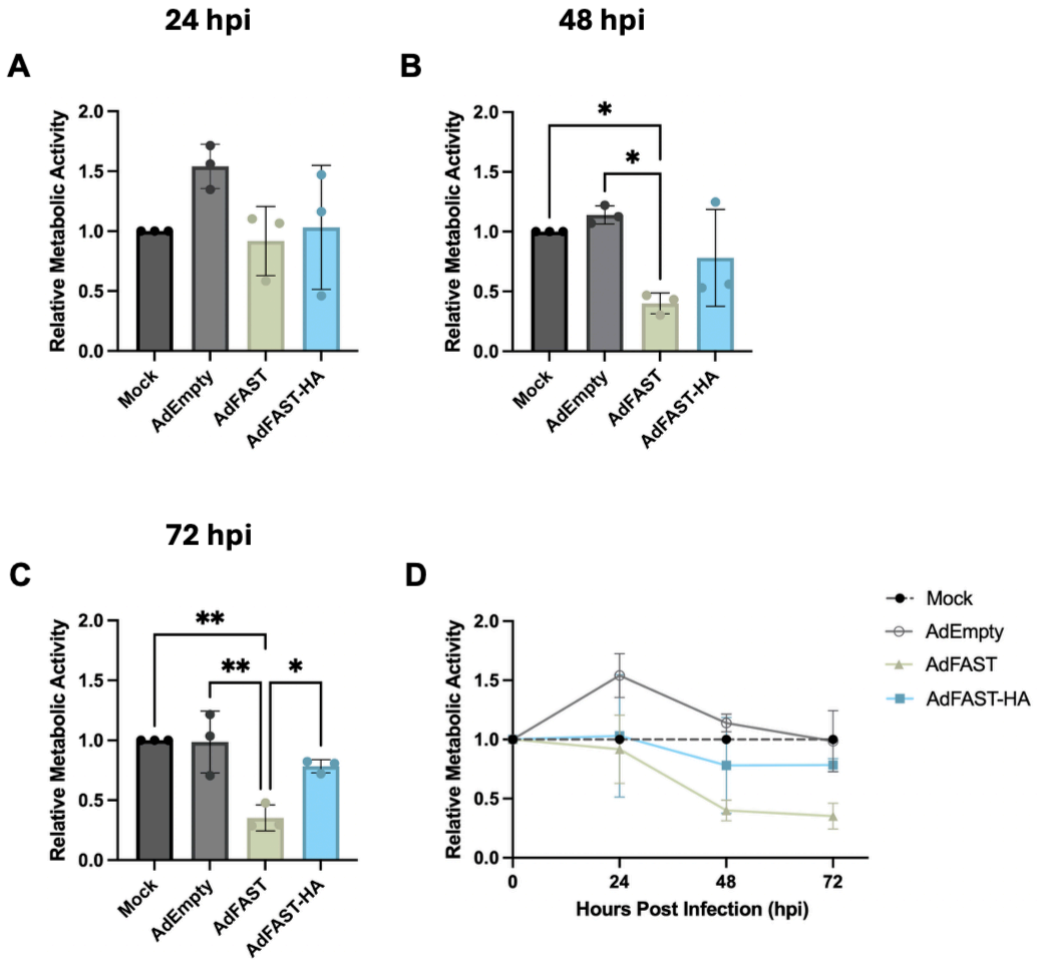

Figure 3.4 Untagged p14 FAST expressed from E1/E3-deleted HAdV induces a more pronounced decrease in metabolic activity than HA-tagged p14 FAST in HEK293 cells. Cells were infected at MOI of 10 with either AdEmpty, AdFAST (untagged p14 FAST) or AdFAST-HA (HA-tagged p14 FAST), with PBS used as mock control. Metabolic activity was measured 24 hpi (panel A), 48 hpi (panel B) and 72 hpi (panel C) by MTS assay. Statistical significance assessed by one-way ANOVA. Values were normalized to mock transfected cells. Data is representative of three biological replicates (n=3) with three technical replicates per infection. Panel D shows metabolic activity as a function of time. One asterisk (*) indicates $p<0.05$ and two asterisks (**) indicate $p<0.01$.

significant decrease in metabolic activity, with activity reduced to 40% (± 9% SD) of mock levels (Figure 3.4B). This was significantly lower than both mock-infected cells ($p = 0.03$) and AdEmpty-infected cells (114% (± 8% SD), $p = 0.01$). In contrast, AdFAST-HA did not significantly reduce metabolic activity, with levels remaining at 78% (± 40% SD) of mock levels. Similar trends were observed at 72 hpi, where AdFAST-infected cells showed a further decrease in metabolic activity to 35% (± 11% SD) of mock levels (Figure 3.4C). This was significantly lower than mock-infected cells ($p = 0.002$) and AdEmpty-infected cells (99% (± 25% SD), $p = 0.003$). Metabolic activity in AdFAST-HA-infected cells remained closer to control levels at 78% (± 5% SD) of mock levels and was significantly higher than AdFAST-infected cells ($p = 0.025$). When metabolic activity was plotted over time, AdFAST-infected cells showed a progressive decrease in metabolic activity from 24 to 72 hpi, whereas mock, AdEmpty, and AdFAST-HA infected cells remained closer to baseline levels (Figure 3.4D). Together, these results indicate that untagged p14 FAST retains strong activity when expressed from an HAdV vector, whereas HA tagging limits p14 FAST-associated reductions in metabolic activity.

3.2.4 E1/E3-deleted HAdV expressing untagged p14 FAST induces a more pronounced decrease in metabolic activity than the HA-tagged version in A549 cells

The results described above characterize the fusion efficiency and potential cytotoxic effects of the untagged p14 FAST protein in HEK293 cells. While it is important to assess these effects in HEK293 cells, as this provides a relevant context for HAdV vector production, it is also necessary to determine whether similar cytopathic effects are observed in a cancer cell line model to better reflect the intended therapeutic context. Previous work from our lab showed that in vitro infection of A549 cells with an E1/E3-deleted HAdV

expressing untagged p14 FAST significantly reduced metabolic activity[165]. However, previous in vivo studies using mice bearing A549 xenograft tumors evaluated the HA-tagged version of p14 FAST expressed from a conditionally replicating HAdV[167]. Building on these findings, we performed a comparative analysis in A549 cells to determine whether HA tagging alters the ability of p14 FAST to reduce metabolic activity. Cells were seeded into 96-well plates and then infected with either AdEmpty, AdFAST or AdFAST-HA (schematics in Figure 3.3). Unlike HEK293 cells, A549 cells do not express the E1A protein required for Ad replication and therefore do not support replication of E1/E3-deleted HAdV vectors. Although the ultimate goal is to incorporate FAST proteins into CRAd vectors, the use of replication-defective HAdV allowed us to directly compare untagged p14 FAST and p14-HA in a cancer cell line without the added influence of viral amplification. In this context, differences in metabolic activity are expected to primarily reflect differences in transgene delivery and FAST protein activity rather than differences in viral replication. Therefore, this experiment served as an intermediate model to determine whether HA tagging alters p14 FAST-associated effects following Ad delivery. Since A549 cells do not support replication of these vectors, higher multiplicities of infection (MOIs) are typically required to increase transgene delivery and produce detectable FAST-associated effects on metabolic activity. Therefore, cells were infected at MOIs of 1, 10, 50, and 100 to ensure that differences between untagged p14 FAST and p14-HA could be detected across a range of viral inputs. Metabolic activity was assessed at 24, 48 and 72 hpi using an MTS-based assay.

At 24 h post-infection, no decrease in metabolic activity was observed for any of the viruses at any MOI. Interestingly, metabolic activity was increased in virus-infected

cells relative to PBS-treated controls (Figure 3.5A). At 48 hpi, cells infected with AdFAST at an MOI of 50 showed the most pronounced reduction in metabolic activity, decreasing to approximately 53% (± 10% SD) of mock-treated cells (Figure 3.5B). Notably, at an MOI of 50, AdFAST-HA infection did not decrease metabolic activity relative to mock-treated cells, with levels remaining similar to those observed in AdEmpty-infected cells. At this same time point, cells infected with AdFAST at an MOI of 100 showed a similar reduction in metabolic activity to those infected at an MOI of 50, decreasing to approximately 54% (± 21% SD) of mock-treated cells (Figure 3.5B). In contrast, AdFAST-HA infection at an MOI of 100 resulted in only a modest, non-significant decrease in metabolic activity at 48 hpi, with levels decreasing to approximately 70% (± 35% SD) of mock-treated cells (Figure 3.5B). At 72 hpi, cells infected with AdFAST at an MOI of 50 showed a marked reduction in metabolic activity, decreasing to approximately 22% (± 11% SD) of mock-treated cells (Figure 3.5C). At the same MOI and time point, AdFAST-HA decreased metabolic activity to approximately 58% ± [SD]% of mock-treated cells, although this reduction was not significant. At 72 hpi and an MOI of 100, both AdFAST and AdFAST-HA significantly decreased metabolic activity, with levels reduced to approximately 17% (± 10% SD) of mock-treated cells for AdFAST ($p < 0.0001$) and 29% (± 16% SD) for AdFAST-HA ($p = 0.0002$) (Figure 3.5C). Notably, infection at MOIs of 1 and 10 did not result in any change in metabolic activity for any of the treatment groups relative to mock-infected cells, likely reflecting insufficient Ad genome copy numbers within the cells. Collectively, these results demonstrate that untagged p14 FAST decreases metabolic activity more effectively than the HA-tagged version, with this decrease becoming more pronounced at higher MOIs, likely due to increased FAST protein expression with greater viral input.

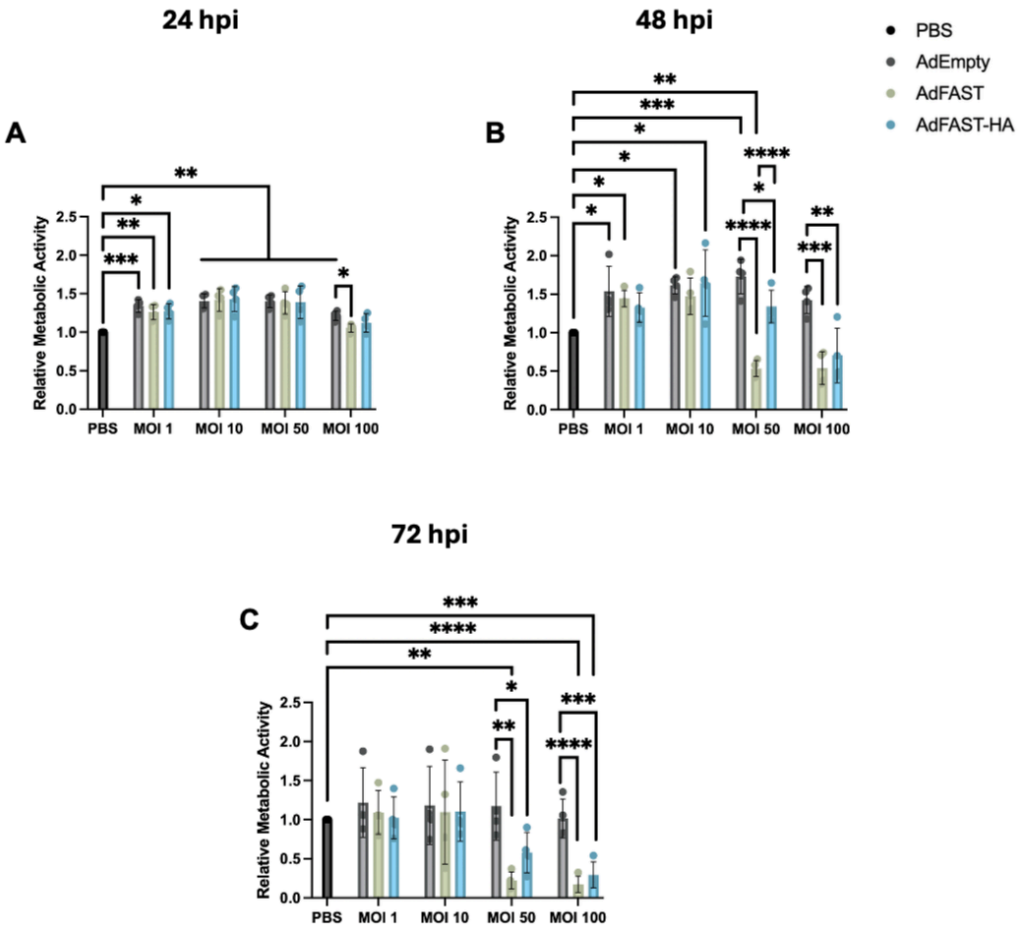

Figure 3.5 Untagged p14 FAST expressed from E1/E3-deleted HAdV induces a more pronounced decrease in metabolic activity than HA-tagged p14 FAST in A549 cells. Cells were infected at varying MOIs (1, 10, 50 and 100) with either AdEmpty, AdFAST (untagged p14 FAST) or AdFAST-HA (HA-tagged p14 FAST), with PBS used as mock control. Metabolic activity was measured 24 hpi (panel A), 48 hpi (panel B) and 72 hpi (panel C) by MTS assay. Statistical significance assessed by one-way ANOVA. Values were normalized to mock transfected cells. Data is representative of four biological replicates (n=4) with three technical replicates per infection. One asterisk (*) indicates $p<0.05$, two asterisks (**) indicate $p<0.01$, three asterisks (***) indicate $p<0.001$ and four asterisks (****) indicate $p<0.0001$.

3.3 Discussion

In Chapter 3, we assessed the fusion efficiencies and potential cytopathic effects of three different FAST proteins, p10, p14, and p15, as well as their HA-tagged counterparts. Previous work from our lab demonstrated that an HA-tagged version of p14 FAST induced syncytium formation in mice bearing A549 tumors[167]. However, despite evidence of fusion, tumor size remained largely unchanged[167]. Therefore, we sought to evaluate the fusogenic and cytopathic properties of additional FAST proteins in hopes of identifying a more effective candidate for downstream anti-cancer therapeutic applications. In addition, our lab experienced difficulty generating and propagating HAdV vectors encoding p10 and p15 FAST proteins. We hypothesized that expression of these FAST proteins may induce enhanced cytotoxicity and/or fusion during vector production, thereby impairing efficient viral propagation. Such knowledge is particularly important for the design of vectors used in oncolytic virotherapy, while also helping identify which FAST proteins are more cytopathic and may therefore present challenges during viral propagation.

We observed that untagged p14 FAST was the most efficient fast protein at inducing syncytium formation in HEK293 cells relative to other FAST protein (Figure 3.1). The increased fusogenic activity of p14 FAST was evident from qualitative analysis of fluorescence microscopy images of HEK293 cells transfected with plasmids expressing the indicated FAST proteins (Figure 3.1A), as well as from quantified data from these images demonstrating a significant increase in fusion relative to the other FAST proteins (Figure 3.1B). Previous research from the laboratory of Dr. Roy Duncan (Dalhousie University, NS, CAN) also demonstrated that p14 FAST induced considerably greater syncytium formation than p10 and p15 FAST proteins[188,189]. In particular, Salsman et al. showed that

p14 FAST mediated markedly more rapid syncytium formation than p10 and p15 following plasmid transfection, with p14-induced syncytia appearing as early as 4-6 h post-transfection, whereas p10 and p15-mediated fusion occurred substantially slower[188]. Similarly, another study by Top et al. demonstrated that the p14 FAST endodomain exhibited greater syncytiogenic enhancement activity than the corresponding endodomains derived from p10 and p15 following co-expression with their respective full-length FAST proteins[189]. The enhanced fusogenicity that we and others have observed with p14 FAST may be attributed to structural and functional differences among FAST proteins. Previous studies have shown that p10, p14 and p15 possess distinct arrangements of structural motifs including differences in their ectodomains, transmembrane domains, hydrophobic regions and endodomains[190,191]. Despite originating from the same viral family, p10, p14 and p15 FAST share no significant amino acid sequence identity to each other[188,190,191]. A possible factor contributing to the differences in fusogenic activity among the FAST proteins is the mechanism by which they mediate membrane fusion. All domains of the FAST protein contribute to the fusion process[155]. However, the ectodomain is a major determinant in the initiation of fusion events as it is primarily responsible for the initial membrane interaction and membrane destabilization steps required for cell-cell fusion[160-162]. More specifically, the ectodomain possesses a hydrophobic patch which interacts with the opposing membrane, destabilizes lipid bilayers, promotes lipid mixing and contributes to the fusion pore formation[160-162]. Given the substantial structural divergence among the FAST proteins, differences in the composition and organization of their ectodomains are possible contributors to the variability in fusogenic activity observed between p10, p14 and p15 FAST proteins. The p10 ectodomain contains a cystine loop fusion peptide that exposes

hydrophobic residues capable of destabilizing opposing lipid bilayers[160]. In contrast, p14 contains a myristoylated proline-hinged loop that is thought to facilitate membrane insertion and induce extensive lipid mixing[161,190]. p15 utilizes a polyproline type II helix-dependent fusion motif which is required to facilitate membrane interactions between neighboring cells and inducing fusion[162]. While serving similar functions, these structurally distinct fusion modules likely influence how efficiently each FAST protein destabilizes membranes and initiates fusion, thereby contributing to the differences in syncytium formation observed in this study. Additionally, differences in the processing or trafficking of p10, p14, and p15 FAST within the trans-Golgi network may also influence their delivery to the plasma membrane and contribute to the differences in fusogenic activity observed in this study.

In addition to inducing the highest level of fusion, MTS cell viability assays revealed that untagged p14 FAST also induced a pronounced decrease in metabolic activity in HEK293 and A549 cells in vitro (Figure 3.2, 3.4, 3.5). These experiments were performed to provide insight into the relative cytotoxic effects mediated by the FAST proteins and which FAST protein may be the most effective at inducing cancer cell death in downstream therapeutic application. However, an important distinction to consider is whether the observed reduction in metabolic activity is mediated directly by p14 FAST expression itself or indirectly as a consequence of the extensive syncytium formation induced by the protein. Previous studies demonstrated that the reduction in membrane integrity occurred subsequently to the formation of syncytium which then triggered apoptotic signaling cascades, DNA fragmentation, chromatin condensation and membrane instability[188]. Furthermore, reducing the extent of syncytium formation through partial

deletion of the p10 ectodomain or antibody-mediated inhibition of p14 fusion diminished these downstream effects, suggesting that the observed cellular damage was linked to syncytiogenesis rather than an intrinsic membrane-lytic activity of the FAST proteins themselves[188]. Additionally, FAST protein-mediated fusion has been reported to be a relatively non-leaky process, in which membrane integrity remains largely preserved until the later stages of syncytium formation[188]. In the context of the present study, it is important to consider that the reduced metabolic activity observed following p14 FAST expression may not be due to the direct cytotoxic effects of the protein itself. Rather, the decrease in metabolic activity could result from altered metabolic activity within multinucleated syncytia and/or from a reduction in viable cell number due to syncytium-associated cell death. From a therapeutic perspective, either outcome may be beneficial as both would be expected to reduce tumor cell fitness. Additional assays such as membrane integrity measurements, apoptosis markers, or live/dead staining could help distinguish between reduced metabolic activity and direct cell death.

When untagged p14 FAST was delivered using HAdV vectors, we similarly observed a reduction in metabolic activity in HEK293 cells (Figure 3.4). While the potent fusogenic and cytopathic properties of p14 FAST is desired for promoting tumor cell killing, these same properties may also negatively impact the viability of producer cells required for Ad amplification. Premature syncytium formation and cell death during vector production could impair efficient viral propagation and reduce overall viral yield. The reduction in metabolic activity observed following HAdV delivery of p14 FAST appeared to be time dependent. At 24 hpi, there was no observed reduction in metabolic activity despite detectable fusion as shown in Figure 3.1. This time point is relevant because the

HAdV replication cycle is typically completed within approximately 24-36 h[59,60]. However, MTS activity is only an indirect measure of cellular metabolic function and does not determine whether fused cells remain competent for viral replication. Tetrazolium reduction can be influenced by cellular glucose metabolism and can change independently of intracellular ATP levels or cell death[192]. Therefore, metabolic alterations associated with early syncytium formation could potentially maintain or transiently increase the MTS signal at 24 hpi, masking cytopathic effects that become more apparent at later time points. This distinction is important because previous work with a GALV-expressing Ad vector showed that syncytium formation can reduce total virus production under certain infection conditions, despite enhancing cytotoxicity[153]. It is therefore possible that early syncytium formation may disrupt cellular organization or interfere with processes required for viral genome replication, late protein expression, virion assembly, and/or progeny release before a measurable decrease in metabolic activity is detected. Although reductions in metabolic activity became apparent at 48 hpi and were more pronounced by 72 hpi, additional assays measuring viral genome replication, late protein expression, and/or infectious progeny production would be required to determine whether early fusion affects Ad replication and final virus yield. Taken together, these observations suggest that reduced metabolic activity alone does not fully define the impact of p14 FAST expression on Ad production. Even before metabolic activity declines, early syncytium formation may affect the ability of infected cells to support efficient virus amplification.

In contrast, experiments in A549 cells were performed to assess p14 FAST activity in a cancer cell line that better reflects the intended therapeutic application. Although the ultimate goal is to incorporate FAST proteins into CRAd vectors, the vectors used in this

experiment were E1/E3-deleted replication-defective HAdVs. This allowed us to assess the effect of p14 FAST expression on metabolic activity in the absence of viral replication. Unlike HEK293 cells, A549 cells do not provide E1A in trans and therefore do not support replication of E1-deleted HAdV vectors. Thus, in this setting, FAST protein expression depends primarily on the amount of input virus delivered rather than amplification of the vector genome. The most pronounced decrease in metabolic activity mediated by untagged p14 FAST was observed at MOIs of 50 and 100 (Figure 3.5). p14 FAST did not induce a significant reduction in metabolic activity in A549 cells infected at an MOI of 1 or 10 at any time point examined (24, 48, or 72 hpi). However, at MOIs of 50 and 100, untagged p14 FAST induced a significant decrease in metabolic activity at 48 and 72 hpi. These findings are consistent with previous work from our laboratory demonstrating that expression of p14 FAST in A549 cells by replication-defective HAdV required both higher MOIs and longer incubation periods to induce extensive syncytium formation relative to HEK293 cells[165]. Specifically, infection of A549 cells with AdFAST at an MOI of 50 resulted in a fusion index of approximately 97.5% at 72 hpi, whereas comparable levels of fusion in HEK293 cells occurred at substantially lower MOIs and earlier time points[165]. In the same study, A549 cells infected with E1/E3-deleted HAdV expressing p14 FAST at an MOI of 50 also exhibited increased lactate dehydrogenase (LDH) release into the supernatant at 72 hpi, indicating compromised membrane integrity and cell death following syncytium formation[165]. These observations support the idea that, when p14 FAST is delivered to A549 cells using a replication-defective HAdV, higher viral input is required for sufficient FAST protein accumulation to mediate extensive syncytiogenesis and downstream reductions in metabolic activity. However, increasing the MOI from 50 to 100

did not produce a proportional reduction in metabolic activity. One possible explanation is high-MOI viral interference, whereby infection of the same cell by multiple Ad particles may limit the efficient expression or processing of individual vector genomes. Thus, although a greater number of viral particles were delivered at an MOI of 100, interference among coinfecting particles may have prevented a proportional increase in p14 FAST expression and its downstream effects. However, because intracellular vector genome copy number and p14 FAST expression were not directly measured, this possibility remains speculative. Interestingly, we observed an increase in metabolic activity in cells infected with AdEmpty, AdFAST, and AdFAST-HA at 24 hpi across all MOIs, as well as at 48 and 72 hpi at MOIs of 1 and 10 (Figure 3.5). The mechanism underlying this increase is unclear. One possible explanation is that Ad transduction itself may transiently alter cellular metabolism. Previous studies have shown that wild-type HAdV infection increases glucose uptake, glycolytic activity and expression of genes involved in cell growth and proliferation during the early phase of infection[193]. The metabolic changes observed during wild-type infection have been linked in part to viral proteins such as E4ORF1, which can regulate MYC-dependent expression of metabolic genes[193]. Although the vectors used in this study were E1/E3-deleted and therefore replication-defective in A549 cells, they retain the E4 region. Thus, it is possible that early expression of E4-associated viral genes contributed to the transient increase in metabolic activity observed following infection. However, because E1/E3-deleted vectors cannot replicate in A549 cells, this effect cannot be directly equated with the metabolic reprogramming described during productive HAdV infection. At lower MOIs, FAST protein expression and syncytium formation may remain insufficient to overcome these early infection-associated increases in metabolic activity.

Interestingly, we observed a significant reduction in both fusogenic activity and cytopathic effects mediated by HA-tagged p14 FAST relative to the untagged protein. In Figure 3.1, the extent of syncytium formation induced by HA-tagged p14 FAST was significantly lower compared to the untagged version. Additionally, MTS cell viability assays revealed that untagged p14 FAST induced a significantly greater reduction in metabolic activity relative to the HA-tagged counterpart (Figures 3.2, 3.4, and 3.5). This effect was observed in both HEK293 cells (Figures 3.2 and 3.4) and A549 cells (Figure 3.5). However, HA-tagged p14 FAST was still capable of reducing metabolic activity under certain conditions. In A549 cells, the HA-tagged construct induced a significant reduction in metabolic activity relative to mock and AdEmpty infected cells at later time points (48 and 72 hpi) and at higher MOIs (50 and 100) (Figure 3.5). However, the untagged p14 FAST consistently mediated a significantly greater reduction in metabolic activity under these same conditions. These findings suggest that while the addition of the HA tag does not completely abolish p14 FAST function, it substantially impairs its fusogenic and downstream cytopathic activity. In previous studies from the lab, p14 FAST was HA-tagged to facilitate protein detection, as commercial antibodies against native FAST proteins are not available. Epitope tags such as HA are commonly used for protein detection and are generally considered to have minimal effects on protein structure and function due to their small size[194]. However, several studies have demonstrated that epitope tagging can interfere with protein folding, intracellular localization, protein-protein interactions, and overall functional activity depending on the protein context and tag positioning[187]. Proper membrane localization and structural organization are particularly important for membrane proteins as even minor alterations may disrupt membrane

insertion, topology or interactions required for biological activity[195]. The importance of maintaining proper membrane organization may be especially relevant for FAST proteins, which are exceptionally small membrane fusogens whose activity depends on precise membrane interactions mediated by their endodomain, transmembrane domain, ectodomains and hydrophobic fusion motifs. In our constructs the HA tag is positioned at the C-terminal of the FAST protein which corresponds to the endodomain. While all domains of the FAST protein play a role in the fusion process[155], previous studies have demonstrated that the endodomain functions as an syncytiogenic enhancer by promoting fusion pore expansion and mediating intracellular trafficking involved in membrane remodeling and actin dynamics required for efficient fusion[189,196]. In particular, the p14 FAST endodomain has been shown to interact with the adaptor protein Grb2 to promote actin polymerization which contributes to membrane protrusion and syncytium formation[196]. Thus, the addition of the HA tag may interfere with the ability of the FAST protein to properly interact with host cellular factors and undergo appropriate intracellular trafficking to efficiently promote membrane fusion and syncytium formation. In contrast, p10 and p15 FAST were weakly fusogenic to begin with, so the addition of an HA tag did not produce an obvious further reduction in fusion or metabolic activity under these conditions (Figure 3.1, 3.2). A recent study using the rotavirus NSP1-1 FAST protein showed that epitope tag placement can affect FAST protein activity[157]. In this study, the authors identified several rotavirus NSP1-1 proteins as functional FAST proteins and showed that epitope tagging could impair their activity. N-terminal FLAG tagging prevented human rotavirus B NSP1-1-mediated syncytium formation, while C-terminal FLAG tagging reduced syncytium size for several NSP1-1 FAST proteins. These findings

are of particular importance given that previous work from our laboratory evaluated only the HA-tagged version of p14 FAST in an A549 xenograft mouse model[167]. Although syncytium formation was observed within the tumors, the therapeutic effect remained limited, with tumor size remaining largely unchanged[167]. Based on the in vitro findings presented in this current study, it is possible that the reduced fusogenic and cytopathic activity associated with the HA-tagged construct contributed to the limited therapeutic efficacy observed in vivo. Therefore, use of the untagged p14 FAST protein may promote more extensive syncytium formation and enhanced tumor cell killing in future in vivo applications.

These findings also highlight an important technical limitation for future studies. Since HA tagging reduces p14 FAST activity, then using the untagged protein may provide a more functionally relevant therapeutic candidate. However, using the untagged protein introduces additional challenges for confirming protein expression and localization. Future studies using untagged p14 FAST would therefore require alternative detection strategies, such as obtaining antibodies against the native protein, generating new FAST-specific antibodies, or testing alternative tag placements that preserve fusogenic activity. Another alternative would be to evaluate a single FLAG epitope tag. Compared with the HA sequence, the FLAG tag is highly hydrophilic and negatively charged and may therefore have a lower tendency to engage in hydrophobic interactions with adjacent membrane or protein domains[197]. As a result, a single FLAG tag could potentially interfere less with p14 FAST conformation and fusogenic activity than the HA tag. However, this would require direct experimental comparison with untagged and HA-tagged p14 FAST. In addition, FAST expression could be assessed indirectly using a linked reporter system. This includes

IRES- or 2A self-cleaving peptide-based construct which would allow expression to be tracked without directly modifying the FAST protein sequence[198]. These strategies have been widely used to co-express multiple proteins from a single transcript, although they would not directly confirm FAST protein expression or localization.

Collectively, the findings presented in this chapter demonstrate that untagged p14 FAST was the most potent FAST protein that we evaluated in terms of both fusogenic activity and reductions in metabolic activity in vitro. Relative to p10 FAST, p15 FAST and its HA-tagged counterpart, p14 FAST consistently mediated more extensive syncytium formation and cytopathic effects in both HEK293 and A549 cells. These findings suggest that the untagged version of p14 FAST may represent the most promising candidate for incorporation into FAST-armed oncolytic Ad vectors.

Chapter 4: Investigating the efficacy of a miRNA-based system in silencing the expression of proteins expressed from HAdV

4.1 Introduction

While the cytopathic effects induced by FAST proteins could be advantageous for enhancing the therapeutic efficacy of oncolytic vectors, it can present challenges during vector production. As previously described, p14 FAST induced extensive fusion and significantly reduced metabolic activity when expressed from a plasmid or virus. This presents a challenge when attempting to grow HAdV (E1-deleted or oncolytic vectors), as both our findings and those of others indicate that HEK293 cells infected with HAdV expressing cytopathic protein often undergo cell death before sufficient viral titers can be achieved[153]. This limitation is particularly important for downstream therapeutic applications, such as in vitro dose-response experiments and in vivo tumor studies, where high-titer viral stocks are typically required. This issue is not unique to FAST proteins, but is a general challenge associated with the expression of cytotoxic transgenes from viral vectors, including non-replicating and conditionally replicating oncolytic vectors. Previous work described a miRNA-based method to silence Cas9 expression during the production of helper-dependent Ad vectors encoding CRISPR/Cas9[178]. In this system, miRNA target sequences were inserted into the Cas9 3′ UTR to reduce Cas9 mRNA levels during vector production and help prevent Cas9-mediated self-cleavage of the vector genome[178]. Additionally, miRNA-based regulation has been used to restrict Ad replication in specific tissues. Ylösmäki et al. inserted six complementary target sites for the liver-enriched miRNA miR-122 into the 3′ UTR of the Ad E1A gene[177]. This modification allowed for repressed Ad replication in normal human liver while preserving replication in tumour tissue[177]. To address the limitation regarding vector production, I sought to increase the

yield of FAST-expressing HAdV vectors by first investigating a miRNA-based strategy targeting a reporter transgene. The overall concept involves engineering HEK293 cells to express a miRNA that specifically targets a sequence present in the viral transgene transcript. During vector production, this miRNA would bind to complementary target sites in the transcript, thereby reducing transgene expression and allowing more efficient vector amplification. This system was first tested using Fluc as a reporter transgene and an HEK293 cell line which expresses a miRNA targeting Fluc.

4.2 Results

4.2.1 Generation of a HEK293 cell line with constitutive expression of a miRNA targeting firefly luciferase (Fluc)

We first generated a HEK293 cell line constitutively expressing a microRNA (miRNA) targeting the Fluc gene. To do so, cells were transfected with a plasmid encoding the miRNA sequence within the 3′ untranslated region (UTR) of an enhanced yellow fluorescent protein (eYFP) reporter. This cell line is designated as 293:eYFP-miFluc. Following transfection, cells were placed under selection with 200 µg/mL of hygromycin B to establish a stable population expressing the construct. It should be noted that 293:eYFP-miFluc represents a stable pooled cell population rather than an isolated clonal cell line. We validated the expression of the transgene by immunoblot analysis of eYFP. As the miRNA sequence is encoded within the 3′ UTR of the eYFP transcript, eYFP expression serves as a proxy for expression of the miRNA construct. Qualitative analysis revealed a strong eYFP protein signal, suggesting successful expression of the miFluc construct (Figure 4.1A). Fluorescence microscopy revealed robust eYFP expression in the selected cell population compared to parental HEK293 cells (Figure 4.1B). Together, these results

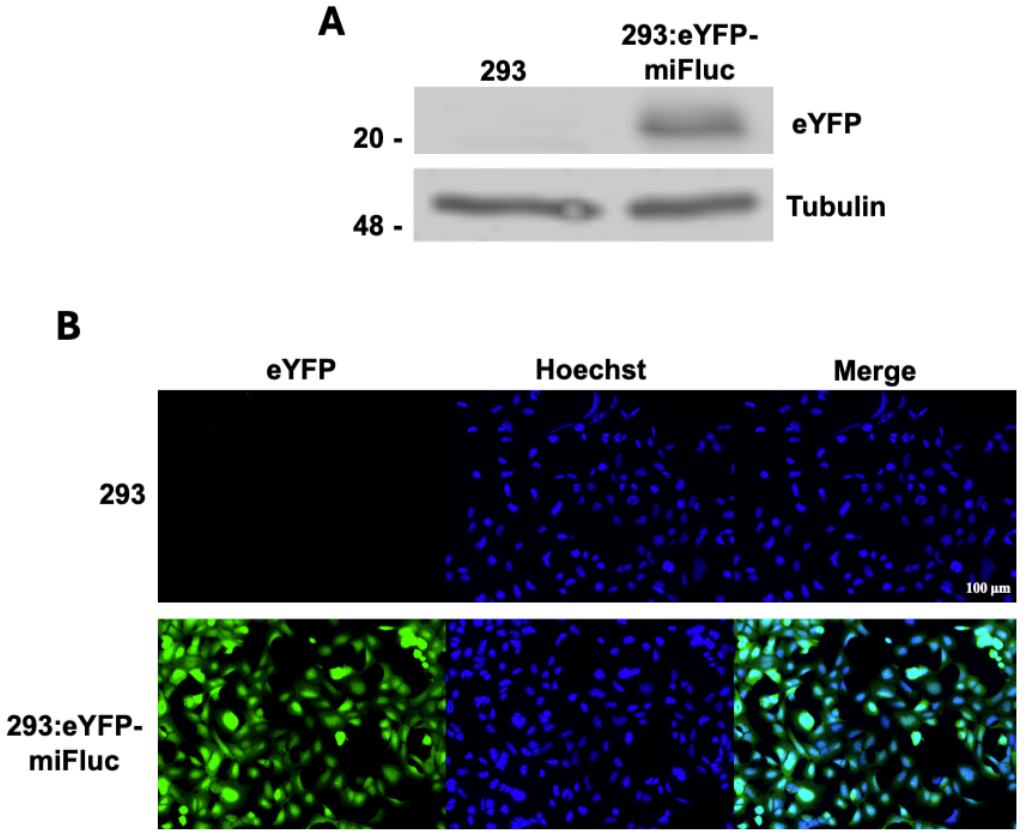

Figure 4.1 eYFP-miFluc expression in 293:eYFP-miFluc cells. A stable cell line was generated using a plasmid expressing a miRNA targeting Fluc (miFluc) which was positioned in the 3' UTR of an eYFP reporter. eYFP serves as a marker for miFluc expression. 293:eYFP-miFluc cells were optimized and maintained under selection with 200 µg/mL. A) Immunoblotting assay conducted with proteins from 293 and 293:eYFP-miFluc harvested 24 hours after seeding with a confluency of approximately 80%. B) Cells stained with Hoechst and images captured by fluorescence microscopy. Scale bar represents 100 µm.

indicate successful establishment of a stable cell line suitable for evaluating miRNA-mediated silencing.

4.2.2 The 293:eYFP-miFluc cell line effectively reduces CMV-driven Fluc expression from adenoviral vectors

Following successful generation of the cell line and confirmation of eYFP expression, we next sought to determine whether the miFluc construct was expressed and functional. To assess this, we performed a reporter-based functional assay using a HAdV vector expressing Fluc. If the miFluc construct was successfully expressed in the cell line, Fluc activity would be reduced. Schematics of viruses which were generated for this aim can be found in Figure 4.2. AdNlucFluc is a replication defective HAdV containing a CMV-Nluc expression cassette replacing the E1 region and CMV-Fluc located within the E3 region. CMV is a strong constitutive promoter derived from the immediate-early gene in cytomegalovirus and is commonly used for driving robust and sustained levels of gene expression[199]. The use of this promoter facilitates straightforward and quantitative assessment of miRNA-mediated silencing. In this construct, Nluc serves as an infection efficiency reporter, ensuring that any observed changes in Fluc activity are attributable to miFluc-mediated silencing rather than differences in infection efficiency between the cell lines. 293 and 293:eYFP-miFluc cells were infected with AdNlucFluc at an MOI of 1 or mock infected with PBS. Cells were harvested at 8 and 24 hpi and Nluc/Fluc activity was measured using a dual luciferase reporter assay. These time points were selected to determine whether miFluc-mediated silencing could reduce Fluc expression under conditions of low and high viral genome abundance. Specifically, 8 hpi represents a time point prior to DNA replication, where Fluc expression is expected to arise from relatively

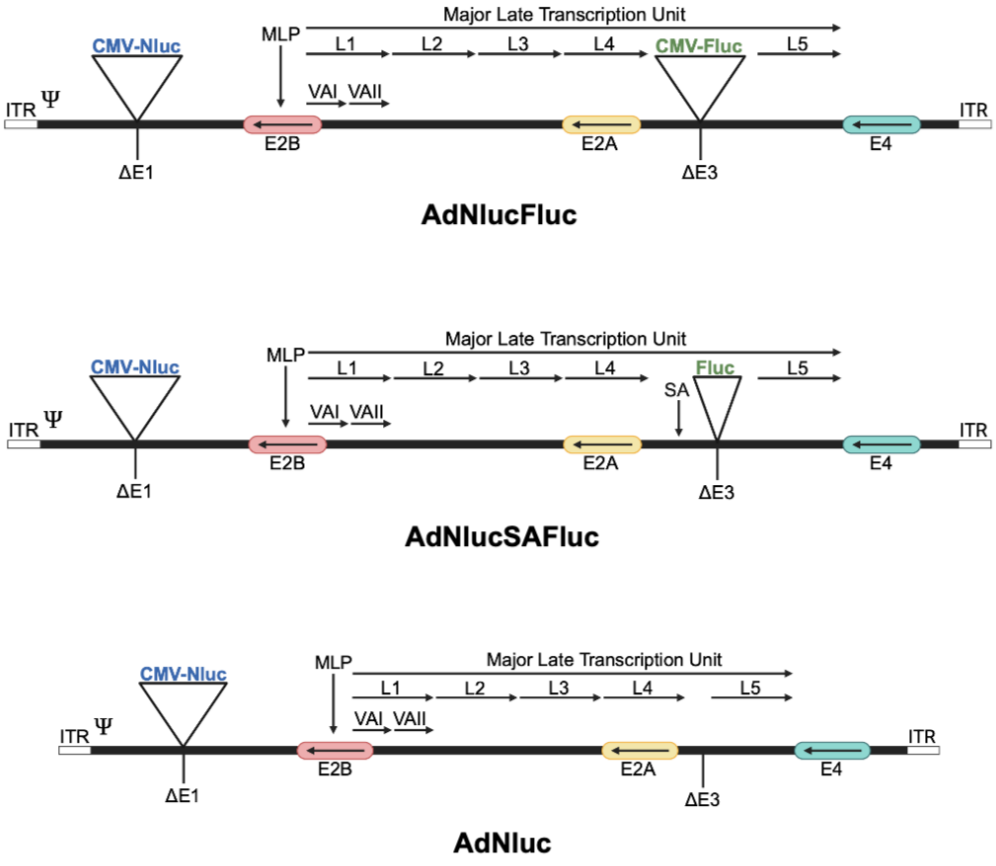

Figure 4.2 Schematic representation of adenoviral vectors used to evaluate miRNA-mediated silencing. AdNlucFluc is a E1 and E3 deleted vector which contains a CMV-Nluc expression cassette replacing the E1 region and CMV-Fluc replacing the E3 region. AdNlucSAFluc is similar to AdNlucFluc with the addition of a splice acceptor (SA) site upstream of the Fluc gene in E3, placing Fluc expression under control of the adenoviral major late promoter (MLP) rather than CMV. AdNluc is a E1 and E3 deleted vector which contains a CMV-Nluc expression cassette replacing E1 and is devoid of any transgenes in the E3 region. Schematics created with BioRender.com.

low numbers of input viral genomes. By 24 hpi, viral DNA replication should have occurred, increasing viral genome copy number and RNA transcript abundance. This allowed us to assess whether miRNA-mediated silencing remained effective when Fluc expression was more abundant and potentially more difficult to suppress[64,200]. At 8 hpi, there was no significant difference in Nluc activity, indicating that cells were successfully infected with the same amounts of virus (Figure 4.3A). We observed a significant decrease in Fluc activity in 293:eYFP-miFluc cells infected with AdNlucFluc compared to parental 293 cells, with Fluc activity decreasing approximately 3.7-fold from ~ 2.2×10^5 relative light units (RLU) in 293 cells to ~ 5.9×10^4 RLU in 293:eYFP-miFluc cells (Figure 4.3B). At 24 hpi, no significant difference in Nluc activity was observed between the two cell lines (Figure 4.3C). In contrast, Fluc activity was significantly reduced in 293:eYFP-miFluc cells compared to parental 293 cells, decreasing approximately 2.7-fold from ~ 1.7×10^6 RLU in 293 cells to ~ 6.3×10^5 RLU in 293:eYFP-miFluc cells (Figure 4.3D). Figure 4.3E depicts Fluc activity normalized to Nluc and subsequently to values from 293 cells to obtain the percentage of Fluc activity in 293:eYFP-miFluc cells relative to 293 cells. Data from both 8 hpi and 24 hpi were plotted on the same graph to enable direct comparison of knockdown efficiency across the two time points. We observed no significant difference between the knockdown of Fluc at the two time points, with Fluc activity reduced to approximately ~ 34% relative to 293 levels at 8 hpi and ~ 39% at 24 hpi. Taken together, this data suggests that the miFluc construct is expressed and functional, as it significantly reduced Fluc expression from the HAdV vector. Additionally, the knockdown capacity of the miRNA was comparable at 8 and 24 hpi, suggesting that miFluc-mediated silencing remains effective in the context of a replicating HAdV vector.

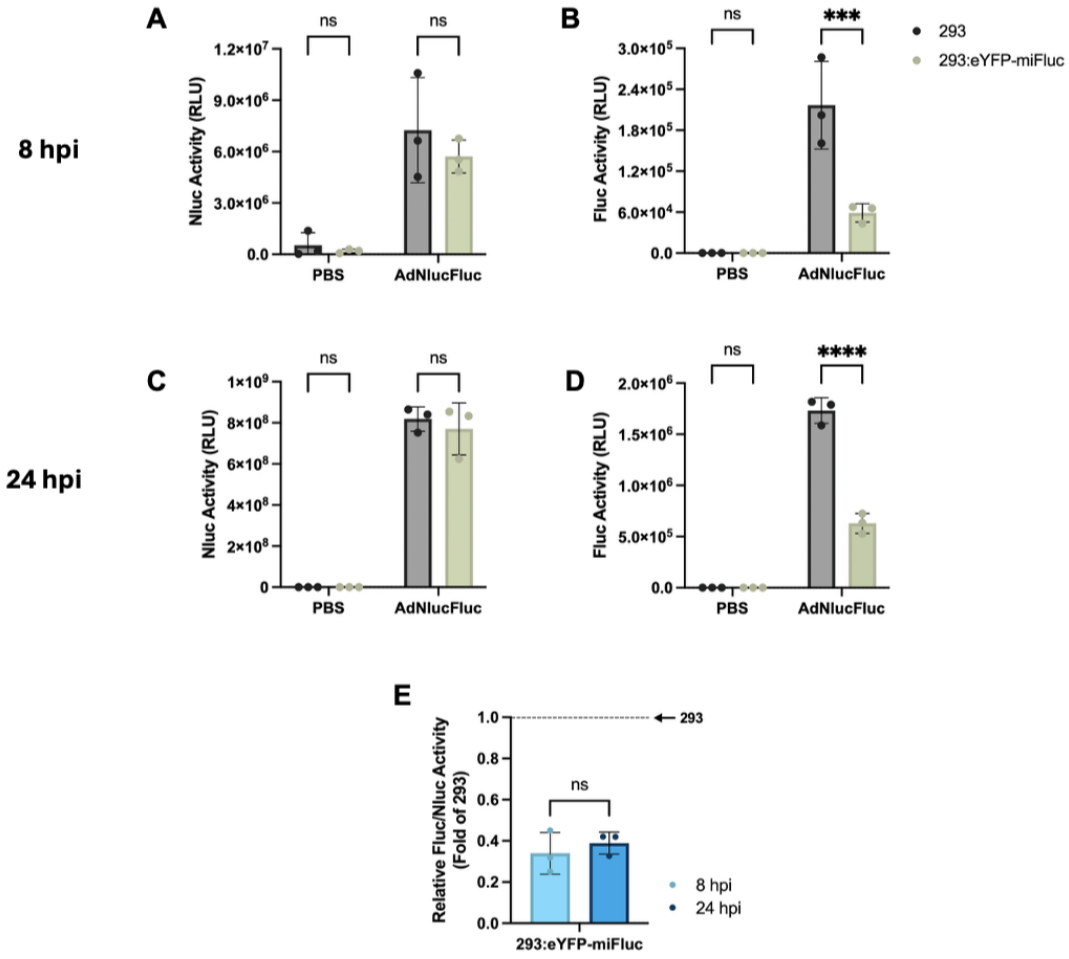

Figure 4.3 Fluc activity is significantly reduced in 293:eYFP-miFluc cells infected with AdNlucFluc. 293 and 293:eYFP-miFluc were infected with AdNlucFluc at an MOI of 1 or mock infected with PBS. Cells were harvested 8 and 24 hpi, Nluc and Fluc activity was then measured with the Nano-Glo Dual Luciferase Reporter Assay kit. Data is representative of three biological replicates (n=3) with two technical replicates per infection. Statistical significance assessed by two-way ANOVA followed by Sidak's multiple comparisons test. A) Nluc activity 8 hpi. B) Fluc activity 8 hpi. C) Nluc activity 24 hpi. D) Fluc activity 24 hpi. E) Comparison of normalized Fluc activity at 8 and 24 hpi in 293:eYFP-miFluc cells infected with AdNlucFluc. Fluc activity was normalized to Nluc activity and then to values in 293 cells. Statistical significance was assessed by unpaired t-test. Three asterisks (***) indicate $p<0.001$ and four asterisks (****) indicate $p<0.0001$.

4.2.3 The 293:eYFP-miFluc cell line effectively reduces MLP-driven transgene expression in an oncolytic-like adenoviral vector

We showed that the miRNA construct was effective at silencing Fluc expressed from a vector in which the Fluc gene was driven by the CMV promoter (Figure 4.3). While this experiment confirmed that the miFluc construct was expressed and functional, CMV-driven expression does not fully reflect the transcriptional context used for therapeutic transgene expression in armed replicating HAdV vectors. In these vectors, therapeutic genes are commonly inserted into the E3 region of the virus genome complete with a splice acceptor site upstream of the transgene[201,202]. This configuration allows transgene expression to be driven by the endogenous Ad major late promoter, thereby linking expression to viral replication. As previously mentioned, the MLP is strongly activated during late stages of infection, only after viral DNA replication has occurred[71,72]. During the late phase of infection, the MLP produces a long transcript referred to as the major late transcription unit (MLTU), which can then be spliced at the splice-acceptor site immediately upstream of the inserted transgene. Linking transgene expression to viral replication is particularly important for cytopathic transgenes, such as FAST proteins, where expression in normal cells could cause unwanted toxicity. In CRAd vectors, placing the transgene in the E3 region downstream of a splice acceptor would ensure that in normal cells, there would be little to no FAST expression. However, in cancer cells where viral replication is permitted through the previously described E1Δ24 mutation, robust transgene expression would be expected. In contrast, a CMV-driven expression cassette could result in transgene expression following vector entry in both normal and cancer cells, potentially leading to unwanted toxicity. To better model this transcriptional configuration, we

generated a replication-defective HAdV vector containing a CMV-driven Nluc expression cassette replacing the E1 region and a Fluc gene preceded by a splice acceptor site in the E3 region. This virus is designated as AdNlucSAFluc (Figure 4.2). Although this vector is not oncolytic, it models the splice acceptor-dependent E3 expression strategy used to link therapeutic transgene expression to virus replication in armed oncolytic HAdV vectors. As a control vector, we generated AdNluc, an E1/E3 deleted vector which contains a CMV-Nluc expression cassette in the E1 region and is devoid of transgenes in the E3 region (Figure 4.2). 293 and 293:eYFP-miFluc were infected with AdNlucSAFluc and AdNluc at an MOI of 1. Cells were harvested at 8 and 24 hpi and Nluc/Fluc activity was measured using a dual luciferase reporter assay. At 8 hpi, there was no significant difference in Nluc activity produced from the virus between the cell lines (Figure 4.4A). We observed a significant decrease in Fluc activity in 293:eYFP-miFluc cells infected with AdNlucSAFluc compared to parental 293 cells, with Fluc activity decreasing approximately 8.3-fold from ~ 3.5 x 10^5 RLU in 293 cells to ~ 4.2 x 10^4 RLU in 293:eYFP-miFluc cells (Figure 4.4B). At 24 hpi, Nluc activity remained consistent between the cell lines (Figure 4.4C). In contrast, Fluc activity significantly decreased in 293:eYFP-miFluc cells infected with AdNlucSAFluc, decreasing approximately 4.6-fold from ~ 5.1 × 10^7 RLU in 293 cells to ~ 1.1 × 10^7 RLU in 293:eYFP-miFluc cells (Figure 4.4D). Fluc activity in 293:eYFP-miFluc cells infected with AdNlucSAFluc at both time points was then normalised to Nluc and subsequently normalised to values from 293 cells. Data showed that there was no significant difference between the knockdown of Fluc at the two time points, with Fluc activity reduced to approximately ~ 10% relative to 293 levels at 8 hpi and ~ 14% at 24 hpi (Figure 4.4E). This suggests that miRNA-mediated silencing remained

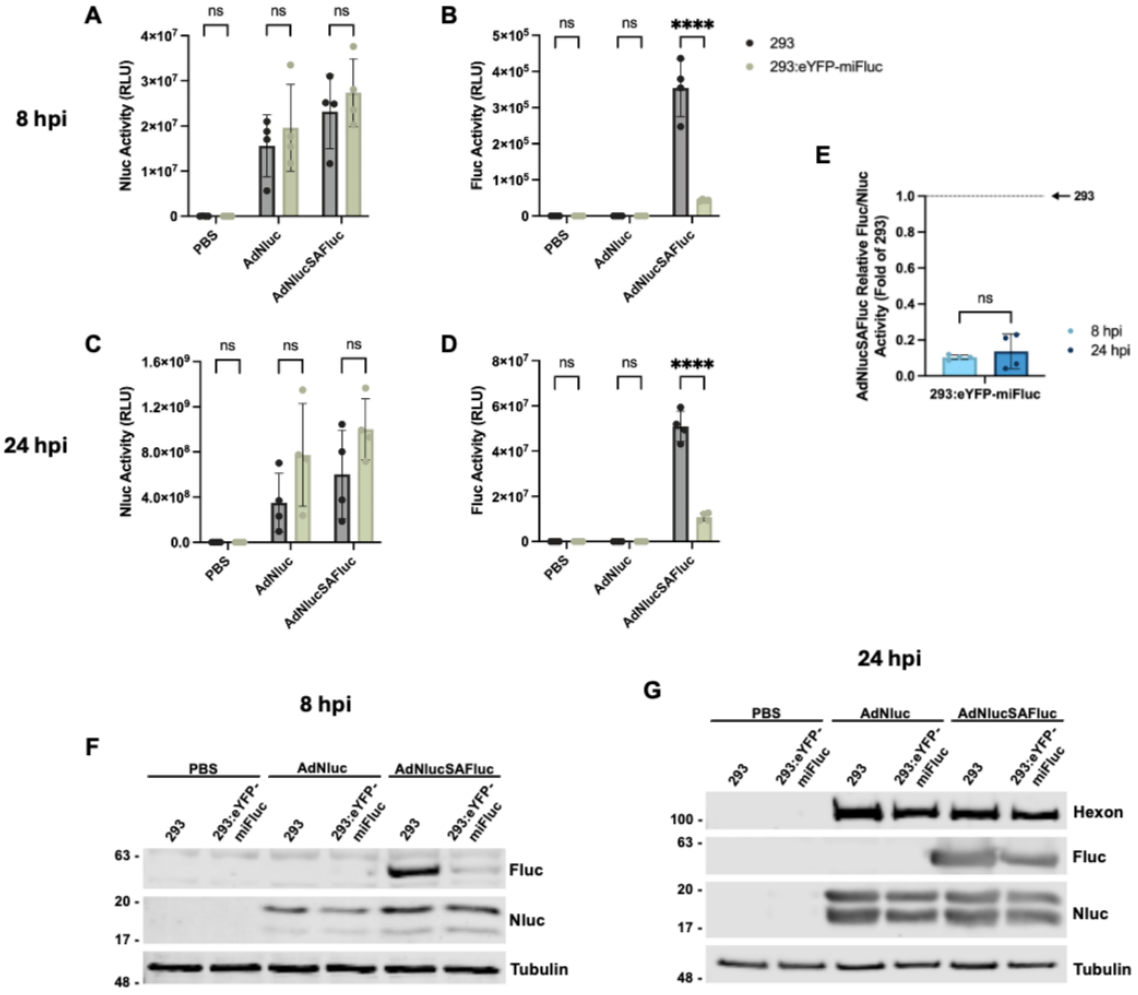

Figure 4.4 Fluc activity is significantly reduced in 293:eYFP-miFluc cells infected with AdNlucSAFluc. 293 and 293:eYFP-miFluc were infected with AdNlucSAFluc or AdNluc at an MOI of 1, or mock infected with PBS. Cells were harvested 8 and 24 hpi, Nluc and Fluc activity was then measured with the Nano-Glo Dual Luciferase Reporter Assay kit. Data is representative of four biological replicates (n=4) with two technical replicates per infection. Statistical significance assessed by two-way ANOVA followed by Sidak's multiple comparisons test. A) Nluc activity 8 hpi. B) Fluc activity 8 hpi. C) Nluc activity 24 hpi. D) Fluc activity 24 hpi. E) Comparison of normalized Fluc activity at 8 and 24 hpi in 293:eYFP-miFluc cells infected with AdNlucSAFluc. Fluc activity was normalized to Nluc activity and then to values in 293 cells. Statistical significance was assessed by unpaired t-test. F) Immunoblot from samples collected 8 hpi. G) Immunoblot from samples collected 24 hpi. Four asterisks (****) indicate $p<0.0001$.

effective even at 24 hpi, when viral DNA replication has occurred and increased viral genome copy number is expected to result in higher Fluc transcript abundance.

To further validate these finds, we conducted immunoblot assays with the samples harvested at 8 and 24 hpi. Qualitative analysis of the immunoblot of samples from 8 hpi showed a strong decrease in the Fluc protein intensity in 293:eYFP-miFluc cells infected with AdNlucSAFluc relative to 293 cells (Figure 4.4F). Nluc protein intensity remained consistent throughout cells infected with AdNlucSAFluc and AdNluc, supporting the luciferase data described in Figure 4.4A-B. Blots were also probed for hexon, an Ad capsid protein expressed at later stages of infection. As anticipated, hexon protein was not detected at 8 hpi considering this is a time point before the onset of viral DNA replication and late viral protein expression (data not shown).The immunoblot with samples from 24 hpi, showed a modest decrease in the Fluc protein intensity in 293:eYFP-miFluc cells infected with AdNlucSAFluc relative to 293 cells (Figure 4.4G). Interestingly, this decrease was less pronounced than the reduction observed in the luciferase activity assay in Figure 4.4D. Here, Nluc protein intensity also remained consistent throughout cells infected with AdNlucSAFluc and AdNluc. Probing with hexon showed consistent protein levels across all infection conditions. As previously mentioned, in the AsNlucSAFluc virus, Fluc is insterted into the E3 region of the genome which is in part transcribed as part of the major late transcription unit. This transcript is also responsible for the expression of several Ad late proteins, including hexon, penton, and fiber[73]. Therefore, we wanted to assess whether miRNA-mediated targeting of Fluc could disrupt late viral protein expression. Although Fluc expression is expected to arise from splicing of the MLTU to the splice acceptor site upstream of the Fluc sequence, it was important to determine whether this configuration

broadly affected late viral protein expression. Consistent hexon levels across conditions suggest that miFluc-mediated targeting of Fluc did not broadly disrupt late viral gene expression, at least based on hexon protein abundance. However, this does not necessarily reflect proper genome packaging and productive virion formation. Overall, this data suggests that the 293:eYFP-miFluc cell line can effectively reduce transgene expression from an HAdV with a genomic structure more closely resembling that of armed CRAd vectors, without broadly disrupting late viral protein expression.

4.2.4 AdNlucSAFluc virus production from 293:eYFP-miFluc cells is reduced at 24 hpi but recovers by 48 hpi

Data presented in Figure 4.4 shows that the miRNA system can effectively reduce transgene expression from an armed HAdV vector with a transgene in the E3 region under regulation of the MLP. Transgenes regulated by the MLP are expressed from the major late transcription unit, which also gives rise to the structural Ad proteins required for virion formation. Although the SA sequence positioned upstream of the transgene is intended to enable splicing of the transgene-containing transcript from the major late transcription unit, miRNA-mediated targeting could still potentially reduce the abundance of the common pre-spliced transcript. If this occurred, expression of Ad structural proteins could be impaired, ultimately reducing the production of infectious virions. While the data in Figure 4.3 did not show a reduction in hexon expression, this does not determine whether viral genomes are successfully packaged or whether infectious virions are produced. Therefore, it was important to assess whether miRNA-mediated silencing of Fluc negatively affects the formation of infectious virions. To assess this, viruses were first infected in either 293 or 293:eYFP-miFluc and then used to reinfect 293 cells. Nluc activity was measured after

reinfection and used as a surrogate readout of infectious virus production from the originally infected cells. This approach allowed infectious virus production to be assessed indirectly, since only infectious virions generated during the initial infection would be able to enter the second set of 293 cells and drive Nluc expression. Since Fluc is not a cytopathic protein, we would not expect Fluc knockdown to increase virus yield. Rather, we wanted to determine whether virus production was comparable between parental 293 and 293:eYFP-miFluc cells.

293 and 293:eYFP-miFluc cells were infected with AdNluc or AdNlucSAFluc. AdNluc infections were performed at an MOI of 1, whereas AdNlucSAFluc infections were performed at an MOI of 0.1 due to the lower titer of the AdNlucSAFluc stock. Since Nluc activity from each virus produced in 293:eYFP-miFluc cells was normalized to the corresponding values obtained from parental 293 cells, this difference in MOI was not expected to affect interpretation of the relative virus production from each cell line. 293 and 293:eYFP-miFluc cells were infected for 1 h, after which the inoculum was removed. Cells were then washed once with PBS, and fresh media was added. Infected cells were harvested at 24 and 48 hpi, and virus harvests from both cell lines were used to reinfect parental 293 cells. Reinfected cells were harvested at 24 hpi, after which Nluc activity was measured.

At 24 hpi, relative Nluc activity was below parental 293-derived levels for both viruses, reaching approximately 25% for AdNluc and 31% for AdNlucSAFluc (Figure 4.5). Since both viruses showed a similar reduction in recovery from the 293:eYFP-miFluc cell line at this time point, this decrease is unlikely to be specifically caused by miFluc-mediated targeting of Fluc. By 48 hpi, relative Nluc activity increased for both viruses

compared to 24 hpi. AdNluc reached approximately 72% of parental 293-derived levels, whereas AdNlucSAFluc reached approximately 124% of parental 293-derived levels (Figure 4.5). Although the difference between the two viruses was statistically significant at this time point ($p = 0.006$), both viruses showed a similar overall trend. Infectious virus recovery from 293:eYFP-miFluc cells was reduced at 24 hpi but improved by 48 hpi, approaching levels observed in parental 293 cells. Taken together, results indicate that both viruses showed a similar pattern of infectious virus recovery from 293:eYFP-miFluc cells. Since reduced recovery was also observed with AdNluc at 24 hpi, the decrease in virus production is unlikely to be specifically attributable to miFluc-mediated targeting of Fluc. Additionally, virus recovery from 293:eYFP-miFluc cells appeared to be delayed relative to parental 293 cells but improved with extended incubation, approaching parental 293-derived levels by 48 hpi.

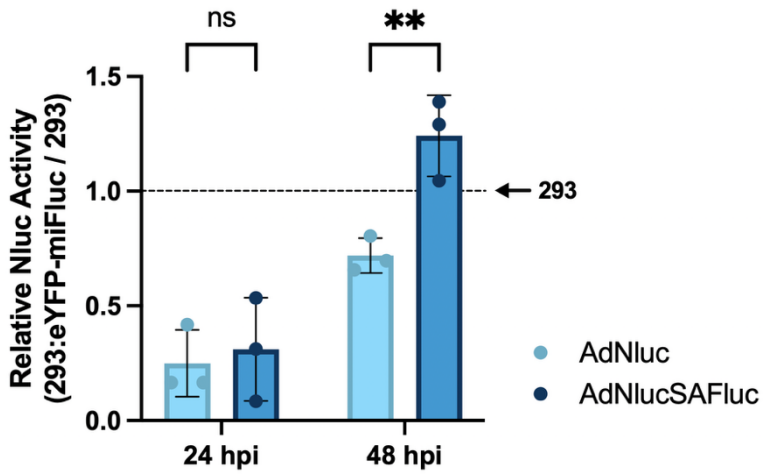

Figure 4.5 AdNlucSAFluc virus recovery from 293:eYFP-miFluc cells is reduced at 24 hpi but reaches 293-derived levels by 48 hpi. 293 and 293:eYFP-miFluc cells were infected with AdNluc at an MOI of 1 or AdNlucSAFluc at an MOI of 0.1. Cells were harvested at 24 and 48 hpi, and virus harvests were used to reinfect parental 293 cells. Reinfected 293 cells were harvested at 24 hpi, and Nluc activity was measured using a NanoLuc luciferase assay as a surrogate readout of infectious virus production. Nluc activity from viruses harvested from 293:eYFP-miFluc cells was normalized to the corresponding values obtained from parental 293 cells for each virus. Data is representative of three biological replicates (n=3) with two technical replicates per infection. Statistical significance was assessed by two-way ANOVA followed by Sidak's multiple comparisons test. Two asterisks (**) indicate $p<0.01$.

4.3 Discussion

In the previous chapter, we evaluated the efficacy of three different FAST proteins; p10, p14, and p15 FAST, as well as their HA-tagged counterparts. Results demonstrated that untagged p14 FAST mediated the greatest extent of fusion, as observed by the increased formation of syncytia and the induced reduction in metabolic activity relative to the other FAST proteins. While these properties are desirable for maximizing tumor cell killing in downstream therapeutic applications, they may be detrimental during viral production. Extensive FAST protein-mediated syncytium formation can trigger cellular stress, apoptotic signaling and membrane instability[188]. As syncytia enlarge and become increasingly dysregulated, these downstream effects may impair the cellular environment required for efficient Ad replication, assembly and/or release. Similar observations have previously been reported with Ad vectors expressing other fusogenic membrane glycoproteins. Guedan et al. demonstrated that extensive syncytium formation mediated by a replication-competent HAdV expressing the GALV fusogenic glycoprotein reduced viral production at low MOIs while simultaneously enhancing cytotoxicity[153]. Interestingly, the authors further showed that viral DNA did not efficiently spread between nuclei within syncytia, suggesting that many nuclei within fused cells were unable to contribute to productive viral replication[153]. Consistent with this, our laboratory has repeatedly observed that generating high titers of FAST-expressing viruses is challenging, often resulting in insufficient viral yields for downstream in vivo studies. This issue may become even more pronounced with the development of HAdV expressing untagged p14 FAST as the findings presented in this study demonstrated that the untagged version induces substantially greater syncytium formation and cytotoxicity relative to the HA-tagged construct. Consequently,

the enhanced fusogenic and cytopathic activity of untagged p14 FAST may further compromise producer cell viability during viral amplification and reduce overall viral yield.

To address this issue, we evaluated two strategies aimed at transiently silencing transgene expression from HAdV specifically during vector production: miRNA-mediated silencing and the LacI/LacO regulatory system. In this chapter, we focused on evaluating the efficacy of miRNA-mediated silencing at suppressing transgene expression from HAdV. Similar miRNA-mediated regulatory strategies have previously been explored in Ad vectors. In helper-dependent Ad vectors, miRNA target sites have been used to suppress Cas9 expression during vector production and prevent CRISPR/Cas9-mediated self-cleavage[178]. In oncolytic Ads, miRNA-mediated suppression of E1A has also been used to restrict Ad replication in liver cells while maintaining replication in tumour cells[177].

Firstly, we generated a HEK293 cell which stably expresses a miRNA targeting Fluc (293:eYFP-miFluc). The miRNA sequence was incorporated into the 3′ untranslated region (UTR) of an eYFP reporter gene, allowing eYFP expression to serve as an indicator of miFluc expression within the cells. As shown in Figure 4.1, strong eYFP expression was observed by both fluorescence microscopy and immunoblot analysis, confirming stable expression of eYFP and suggesting that the miRNA is likely also being expressed. Ideally, miFluc expression would have been confirmed directly, such as by RT-PCR based detection of the mature miRNA. However, the combination of strong eYFP expression and the functional knockdown of Fluc observed in subsequent experiments supports that the miFluc sequence was expressed and functional in these cells. Stable miRNA expression within producer cells would theoretically allow suppression of cytotoxic transgenes during

vector amplification while permitting transgene expression to be restored following infection of target tumor cells lacking the miRNA. Thus, this system provides a potential strategy to improve production yields of cytopathic FAST-armed HAdV vectors without permanently altering transgene function.

We showed that the miRNA construct was able to successfully reduce expression of Fluc from AdNlucFluc (Figure 4.3). Importantly, this reduction in Fluc activity occurred without any significant changes in Nluc expression at either 8 or 24 hpi, suggesting that the observed decrease in Fluc expression was not due to reduced transgene delivery or impaired viral replication, but rather resulted from sequence-specific miRNA-mediated silencing. Furthermore, comparable levels of knockdown were observed at both 8 and 24 hpi, indicating that the silencing effect was maintained over time from early to late stages of infection. However, an important consideration when utilizing miRNA-mediated silencing in Ad systems is the ability of virus-associated RNAs (VA RNAs) to interfere with cellular RNA interference activity. VA RNAs are small non-coding RNAs expressed at high levels during Ad infection and play an important role in viral replication. In particular, VA RNAs promote efficient viral growth by inhibiting protein kinase R (PKR) activation, thereby preventing global translational shutdown and supporting late viral protein synthesis[203,204]. However, VA RNAs can also interfere with cellular miRNA activity. Previous studies have demonstrated that VA RNAs can impair pri-miRNA processing through competitive interactions with key components of the miRNA biogenesis pathway, including Drosha, Exportin-5, Dicer, and Argonaute proteins[205]. Specifically, VA RNAs have been shown to bind and sequester Drosha, thereby impairing maturation of pri-miRNAs into functional mature miRNAs[76]. Consequently, Ad infection

itself may reduce the efficiency of miRNA-mediated transgene silencing. Despite these known inhibitory effects, we were still able to observe knockdown of Fluc expression in our system, suggesting that the miRNA construct retained sufficient activity to mediate transgene suppression in the context of Ad infection.

We next evaluated whether miRNA-mediated silencing could also be achieved in the context of Ad vectors which are more representative of oncolytic HAdV systems, in which transgene expression is linked to the major late promoter (Figure 4.4). Unlike the constitutively active CMV promoter used in AdNlucFluc, the MLP is activated predominantly during the late phase of Ad infection following the onset of viral DNA replication and is responsible for driving high-level expression of late viral genes[71,72]. This configuration ensures that transgene expression is largely restricted to cells in which the virus can replicate. Therefore, this structure more accurately models late viral gene expression from oncolytic CRAd vectors. A previous study reported stronger CMV-driven expression than MLP-driven expression using E1-deleted, replication-defective Ad vectors encoding luciferase or lacZ[206]. These vectors were tested in cultured rheumatoid arthritis-derived synoviocytes and in the synovium of rhesus monkeys with collagen-induced arthritis[206]. However, because those vectors were replication-defective, MLP-driven expression would not have been amplified by viral DNA replication. In contrast, the present study used HEK293 cells, which support Ad replication. We found that Fluc activity was approximately 6.3-fold higher when Fluc expression was linked to the MLP, as shown with AdNlucSAFluc (Figure 4.4), compared to when Fluc was driven by the CMV promoter, as shown with AdNlucFluc (Figure 4.3). Despite these differences in transcriptional regulation, the miFluc construct remained capable of suppressing Fluc expression from

AdNlucSAFluc at both 8 and 24 hpi (Figure 4.4). Overall, these findings demonstrate that miRNA-mediated silencing remains effective in an Ad vector configuration that more closely resembles conditionally replicating oncolytic HAdV, supporting its potential use for transiently suppressing cytotoxic transgenes during vector production.

Although the miRNA-based system effectively reduced expression of the targeted Fluc transgene, this did not determine whether the 293:eYFP-miFluc cell line could still support the production of infectious Ad particles. In Figure 4.4, hexon protein levels were maintained in the miRNA-expressing cell line, suggesting that late viral protein expression was not impaired. However, this does not necessarily indicate whether viral genomes were successfully packaged or that infectious virions capable of reinfecting cells were produced. Therefore, it was important to assess infectious virus recovery from 293:eYFP-miFluc cells. To assess this, 293 and 293:eYFP-miFluc cells were infected with AdNlucSAFluc AdNluc. Cells were harvested at 24 and 48 hpi, and the resulting virus-containing lysates were used to reinfect parental 293 cells. Since only successfully produced infectious virions would be able to reinfect 293 cells and drive Nluc expression, Nluc activity was measured as a surrogate readout of infectious virus output. At 24 hpi, infectious virus output from 293:eYFP-miFluc cells was reduced for both viruses with Nluc expression down 25% for AdNluc and 31% for AdNlucSAFluc (Figure 4.5). The similar decrease in Nluc activity observed for both AdNluc and AdNlucSAFluc suggests that this effect does not appear to be specific to miFluc-mediated targeting. By 48 hpi, infectious virus recovery from 293:eYFP-miFluc cells was improved. Notably, AdNlucSAFluc reached levels comparable to and even slightly higher than virus recovered from parental 293 cells. However, Nluc activity from AdNluc harvested from 293:eYFP-miFluc cells remained

moderately lower, reaching approximately 72% of parental 293-derived levels. The reason for this difference between the two viruses at 48 hpi is unclear. However, because Nluc activity from AdNlucSAFluc did not remain reduced at 48 hpi, these results suggest that miFluc-mediated targeting of the Fluc-containing transcript was not associated with a sustained defect in infectious virus recovery.

The reduced infectious virus recovery observed at 24 hpi may reflect delayed or less efficient virus production in the miRNA-expressing cells rather than a specific effect of miRNA targeting, since both viruses were reduced at this time point. An important consideration for the AdNlucSAFluc construct is that Fluc is position in the E3 region which is transcribed as part of the MLTU by the endogenous Ad MLP. The insertion of the SA site upstream of Fluc is expected to allow processing of a Fluc-containing mRNA from this larger transcript. However, if miFluc-mediated targeting occurs before or during transcript processing, it could potentially affect the abundance or stability of late viral RNAs (e.g. those encoding hexon, penton or fiber) before the Fluc mRNA is fully processed. This limitation can potentially explain the reduced virus recovery observed at the 24 hpi time point. While hexon protein levels from AdNlucSAFluc remained consistent in the miRNA-expressing cell line relative to parental 293 at 24 hpi (Figure 4.4), it would be beneficial to examine additional late viral proteins, such as fiber and penton. In addition, examining proteins involved in capsid assembly and genome packaging could help determine whether later stages of virion production are delayed or impaired in the miRNA-expressing cell line. These include pIIIa, pVI, pVIII, pIX, IVa2, and the core-associated proteins V, VII, and μ, could help determine whether later stages of virion assembly are delayed or impaired in the miRNA-expressing cell line. Assessing these same proteins at

48 hpi would also help determine whether delayed late protein recovers over time, potentially explaining the improved infectious virus recovery observed at this later time point. Finally, these findings should be confirmed using a true plaque assay to directly quantify infectious virus output.

Overall, these findings demonstrate that miRNA-mediated targeting can selectively reduce expression of the targeted transgene. The 293:eYFP-miFluc cell line successfully reduced Fluc activity from both CMV-driven and MLP-linked transgene cassettes without affecting activity of the untargeted Nluc reporter positioned in the E1 region. Although infectious virus recovery from 293:eYFP-miFluc cells was reduced at 24 hpi, recovery improved by 48 hpi, suggesting that virus production in the miRNA-expressing cell line may be delayed rather than substantially impaired. With further refinement of this cell line and optimization of production conditions, miRNA-mediated silencing represents a promising strategy to improve the production of Ad vectors expressing cytotoxic transgenes. Importantly, because Fluc is not cytotoxic, future experiments using FAST-armed Ad vectors will be necessary to determine whether miRNA-mediated suppression can improve viral yield when transgene expression directly compromises producer cell viability.

Chapter 5: Investigating the efficacy of a Lac repressor-based system in silencing the expression of proteins expressed from HAdV

5.1 Introduction

As described in the previous chapter, the production of HAdV expressing cytotoxic proteins is challenging, often leading to premature cell death before high titers of virus can be obtained. In chapter 4, I explored a miRNA-based system at reducing transgene expression from HAdV in order to increase viral titers. In parallel, I explored an alternative system based on the Lac repressor (LacI) and Lac operator (LacO). This system originates from the *E. coli* lac operon, where LacI binds to the LacO DNA sequence to repress transcription of the downstream genes responsible for the metabolism of lactose[179,180]. When allolactose, a metabolite of lactose, binds to LacI, it induces an allosteric conformational change that reduces its affinity for the LacO DNA sequence[179,180]. In the absence of this inducer, LacI binds with high affinity to the LacO sequence which physically obstructs RNA polymerase binding and/or transcriptional elongation, thus repressing expression of downstream genes[179,180]. A previous study had utilized the LacI/LacO system to reduce basal transgene expression from inducible promoters in HAdV by blocking transcriptional elongation[174]. This approach was primarily applied to address promoter leakiness rather than to regulate expression of cytotoxic transgenes in Ad vectors[174]. Another study demonstrated that the LacI/LacO system can repress expression of rabies virus glycoprotein transgene during Ad vector production which allowed for high titer vector recovery[173]. Building on this work, I sought to assess whether the LacI/LacO system could repress transgene expression from HAdV vectors and to compare its effectiveness with the miRNA-based silencing system described in Chapter 4.

5.2 Results

5.2.1 Generation of a HEK293 cell line with constitutive expression of the Lac repressor protein

In order to transiently silence transgene expression from HAdV, we first generated a HEK293 cell line which constitutively expresses the LacI protein. To do so, cells were transfected with a plasmid encoding an mCherry-LacI fusion protein under the control of the CMV promoter. The mCherry-LacI coding sequence was linked to a hygromycin resistance gene through an internal ribosome entry site, allowing for selection of stably transfected cells with hygromycin. To do so, cells were transfected with a plasmid encoding a fusion protein of the LacI protein with an mCherry reporter. This cell line is designated as 293:mCherry-LacI. Following transfection, cells were placed under selection with 200 µg/mL of hygromycin B to establish a stable pooled cell population expressing the construct. We then validated the expression of the transgene by immunoblot analysis of mCherry. Qualitative analysis revealed a strong protein signal of mCherry-LacI at ~ 65 kDa (Figure 5.1A). Fluorescence microscopy revealed robust mCherry expression in the selected cell population compared to parental HEK293 cells (Figure 5.1B). Together, these results confirmed the generation of a stable 293:mCherry-LacI producer cell population suitable for evaluating LacI/LacO-mediated transgene repression.

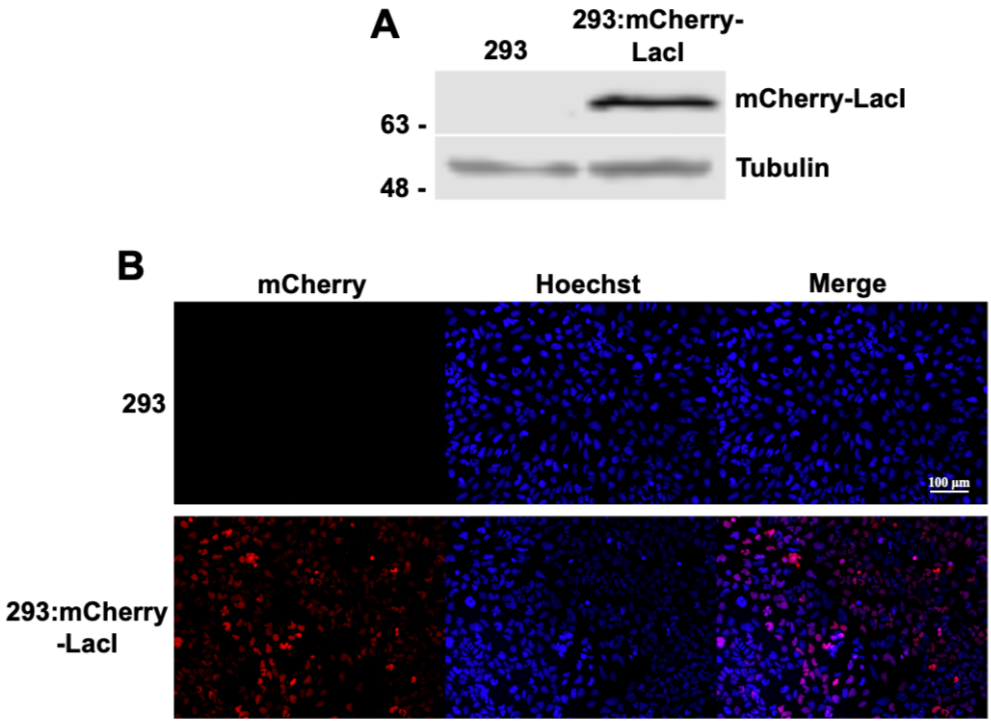

Figure 5.1 mCherry-LacI expression in 293:mCherry-LacI cells. The Lac repressor (LacI) is fused with the mCherry protein. mCherry serves as marker for LacI expression. 293:mCherry-LacI cells were selected and maintained under selection with 200 µg/mL hygromycin to support optimal transgene expression. A) Immunoblotting assay conducted with proteins from 293 and 293:mCherry-LacI harvested 24 hours after seeding with a confluency of approximately 80%. B) Cells stained with Hoechst and images captured by fluorescence microscopy. Scale bar represents 100 µm.

5.2.2 The 293:mCherry-LacI cell line effectively reduces CMV-driven transgene expression from adenoviral vectors

To initially assess the functionality of the 293:mCherry-LacI cell line at effectively reducing transgene expression, we generated viruses which encode bioluminescent protein driven by the CMV promoter with LacO sequence positioned either downstream or upstream of the transgene. Schematics of viruses which were generated for this aim can be found in Figure 5.2. AdLacONlucFluc is a replication defective HAdV which contains the Nluc gene regulated by the CMV promoter with 16 tandem repeats of the LacO sequence placed between the promoter and Nluc in the E1 region, and CMV-Fluc in the E3 region. Binding of LacI to the LacO sequences is expected to inhibit transcription of Nluc by obstructing the progression of the RNA polymerase. AdNlucLacOFluc contains the same genetic elements, however, the LacO sequences have been positioned downstream of the Nluc coding sequence. In this configuration, LacI binding may interfere with proper processing of the 3′ end of the transcript, leading to transcript instability and reduced transgene expression. AdNlucFluc has been previously described and was utilised as a control, where Nluc expression should remain consistent in both 293 and 293:mCherry-LacI cells. In these constructs, Fluc serves as an infection efficiency reporter, ensuring that any observed changes in Nluc activity are attributable to LacI-mediated silencing rather than differences in infection efficiency between the cell lines. 293 and 293:mCherry-LacI cells were infected with AdLacONlucFluc, AdNlucLacOFluc and AdNlucFluc at an MOI of 1 or mock infected with PBS. Cells were harvested at 8 and 24 hpi and Nluc/Fluc activity was measured using a dual luciferase reporter assay. At 8 hpi, Fluc activity remained unchanged between 293 and 293:mCherry-LacI cells for all viruses tested (Figure 5.3A).

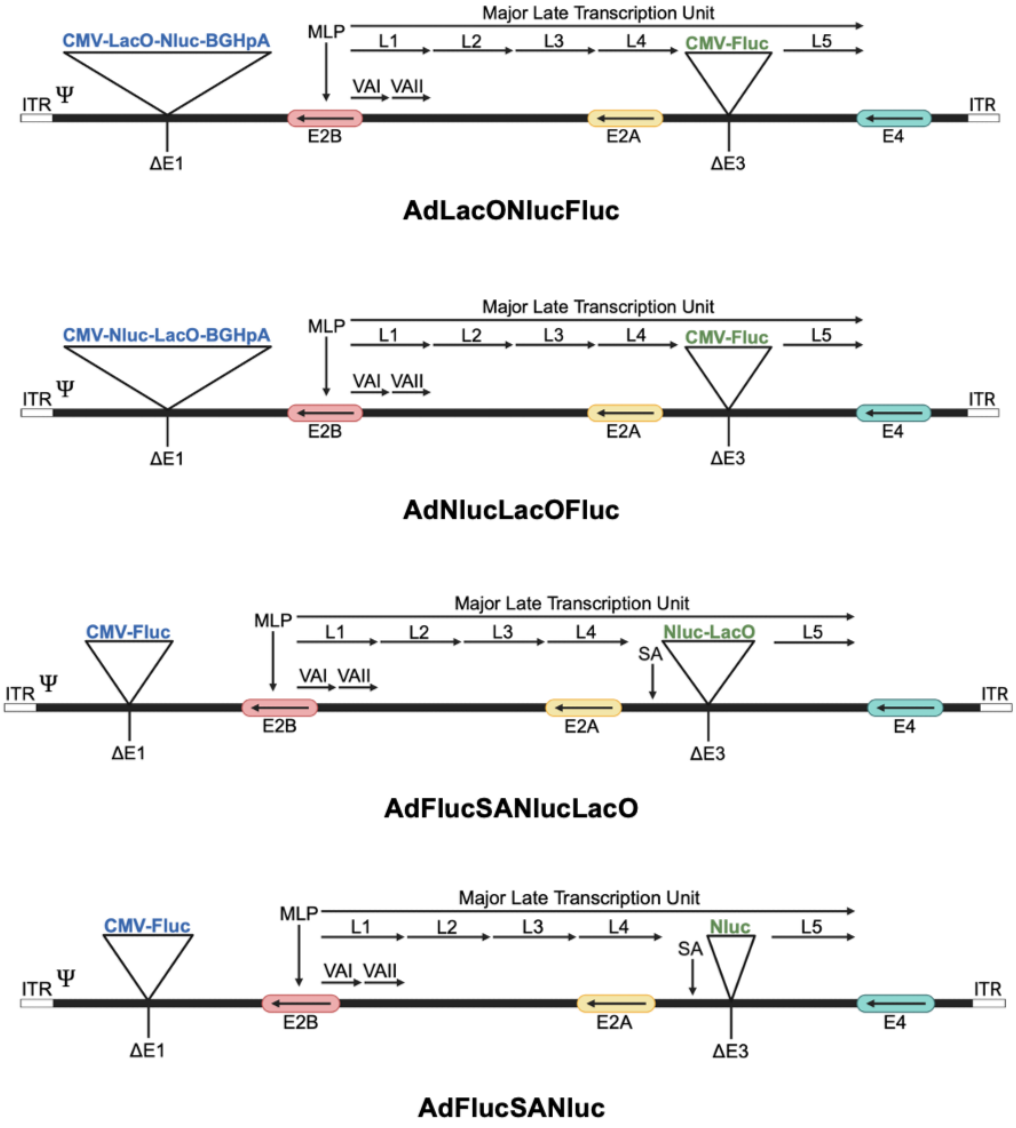

Figure 5.2 Schematic representation of adenoviral vectors used to evaluate LacI/LacO-mediated silencing. AdLacONlucFluc is a E1 and E3 deleted vector which contains a CMV–Nluc expression cassette replacing the E1 region with 16 Lac operator (LacO) repeats inserted between the promoter and coding sequence, as well as a CMV–Fluc cassette replacing the E3 region. AdNlucLacOFluc is similar to AdLacONlucFluc except that the LacO repeats are positioned downstream of the Nluc gene, between the gene and the poly(A) signal. AdFlucSANlucLacO contains a CMV-Fluc expression cassette replacing E1 and an Nluc gene followed by 16 LacO repeats replacing E3, with a splice acceptor (SA) site upstream of Nluc that places its expression under control of the adenoviral major late promoter (MLP). AdFlucSANluc is similar to AdFlucSANlucLacO but lacks the LacO sites. Schematics created with BioRender.com.

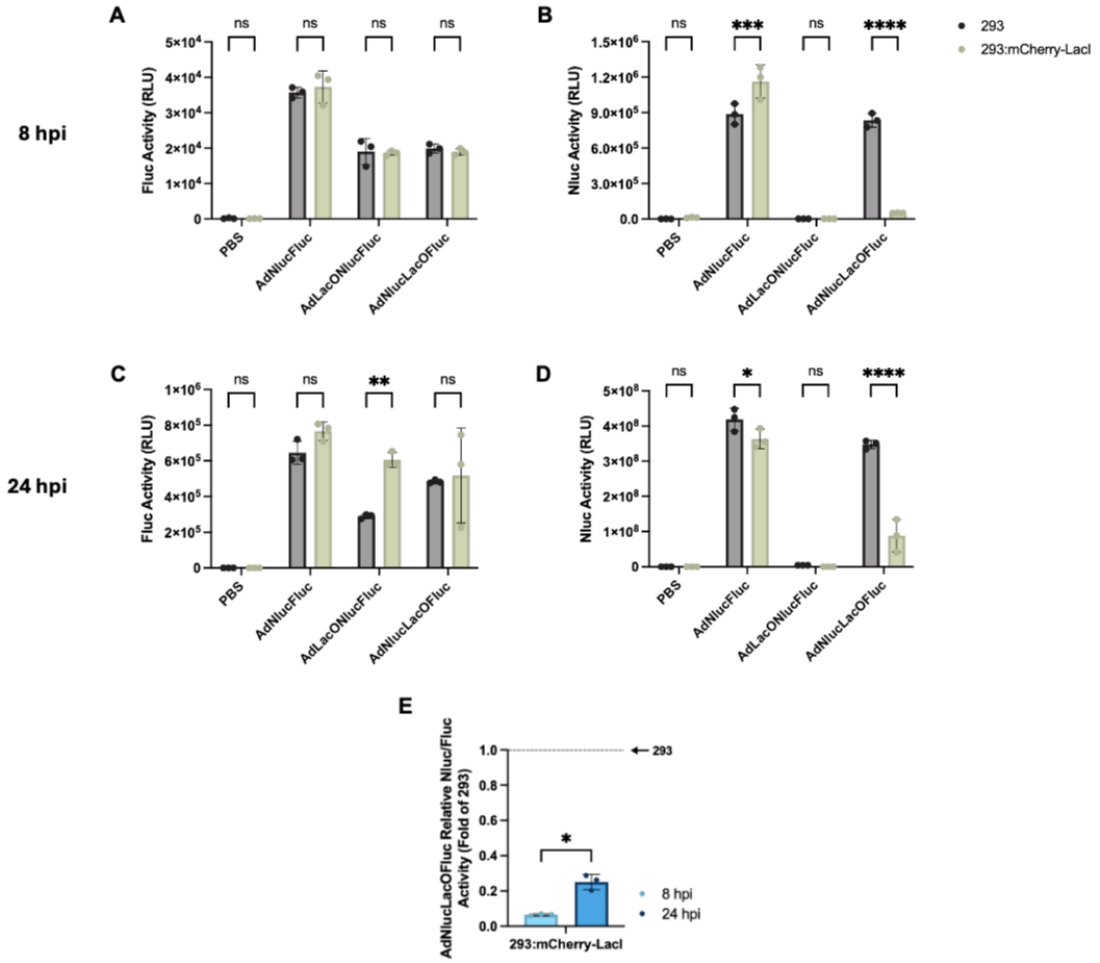

Figure 5.3 Nluc activity is significantly reduced in 293:mCherry-LacI cells infected with AdNlucLacOFluc. 293 and 293:mCherry-LacI cells were infected with AdNlucFluc, AdLacONlucFluc or AdNlucLacOFluc at an MOI of 1, or mock infected with PBS. Cells were harvested 8 and 24 hpi, Nluc and Fluc activity was then measured at 8 hpi or 24 hpi with the Nano-Glo Dual Luciferase Reporter Assay kit. Data is representative of three biological replicates (n=3) with two technical replicates per infection. Statistical significance assessed by two-way ANOVA followed by Sidak's multiple comparisons test. A) Fluc activity 8 hpi. B) Nluc activity 8 hpi. C) Fluc activity 24 hpi. D) Nluc activity 24 hpi. E) Comparison of normalized Nluc activity at 8 and 24 hpi in 293:mCherry-LacI cells infected with AdNlucLacOFluc. Nluc activity was normalized to Fluc activity and then to values in 293 cells. Statistical significance assessed by unpaired t-test. One asterisk (*) indicates $p<0.05$, two asterisks (**) indicate $p<0.01$, three asterisks (***) indicate $p<0.001$ and four asterisks (****) indicate $p<0.0001$.

In contrast, placement of the LacO sites between the Nluc gene and the poly(A) signal in AdNlucLacOFluc resulted in a significant reduction in Nluc activity in 293:mCherry-LacI cells, corresponding to an approximately 16-fold decrease relative to parental 293 cells (Figure 5.3B). When the LacO sites were positioned upstream of the Nluc gene in AdLacONlucFluc, Nluc activity was near background levels even in parental 293 cells, suggesting that this configuration impaired Nluc expression independently of LacI expression. At 24 hpi, Fluc activity again remained largely unchanged between the two cell lines, although an increase was observed in 293:mCherry-LacI cells infected with AdLacONlucFluc (Figure 5.3C). Nluc activity from AdNlucLacOFluc remained significantly reduced in 293:mCherry-LacI cells, corresponding to an approximately 4-fold decrease relative to parental 293 cells (Figure 5.3D). Similar to the 8 hpi time point, AdLacONlucFluc produced near-background levels of Nluc activity in parental 293 cells at 24 hpi. Nluc activity in 293:mCherry-LacI cells infected with AdNlucLacOFluc was normalized to Fluc activity and then expressed relative to values from parental 293 cells. This analysis showed that Nluc activity was reduced to ~ 6.5% of 293 levels at 8 hpi and ~ 25% at 24 hpi, indicating that repression was strongest at the earlier time point (Figure 5.3E). Taken together, this data highlights the effectiveness of the LacI at repressing CMV-driven transgene expression from HAdV, specifically when LacO sites are positioned downstream of the gene.

5.2.3 The 293:mCherry-LacI cell line effectively reduces MLP-driven transgene expression in an oncolytic-like adenoviral vector

The data presented in Figure 5.3 demonstrated that LacI effectively repressed CMV-driven transgene expression from an HAdV vector when the LacO sites were

positioned downstream of the transgene. Although this experiment confirmed the functionality of the cell line and viral constructs, it did not assess the system in a context representative of oncolytic Ad vectors. Therefore, new HAdV constructs were generated to more closely resemble the genomic architecture of armed oncolytic CRAd vectors, where transgenes are inserted into the E3 region. AdFlucSANlucLacO is an E1/E3-deleted HAdV vector containing the Nluc gene replacing the E3 region, in which a splice acceptor (SA) site has been positioned upstream of the Nluc gene and 16 tandem repeats of the LacO sequence are inserted downstream of the coding sequence (Figure 5.2). In addition, a CMV-driven Fluc cassette is present in the E1 region. As previously described, this places Nluc expression under the control of the Ad major late promoter, which is strongly activated at later stages of infection following the onset of viral DNA replication[71,72]. AdFlucSANluc possesses the same genetic elements with the absence of the LacO sites and was used as a control. We did not generate an HAdV construct with LacO sequences positioned upstream of the transgene, as previous data indicated that transgene expression was impaired even in parental 293 cells (Figure 5.3). 293 and 293:mCherry-LacI cells were infected with AdFlucSANlucLacO or AdFlucSANluc at an MOI of 1 or mock infected with PBS. Cells were harvested at 8 and 24 hpi and Nluc/Fluc activity was measured using a dual luciferase reporter assay.

At 8 hpi, similar levels of Fluc activity were observed between the two cell lines for all viruses tested (Figure 5.4A). In contrast, Nluc activity from AdFlucSANlucLacO was significantly reduced in 293:mCherry-LacI cells, decreasing from ~2.8×10^7 RLU in 293 cells to ~6.9×10^5 RLU in 293:mCherry-LacI cells, corresponding to an approximately 41-fold reduction (Figure 5.4B). No reduction in Nluc activity was observed for the control

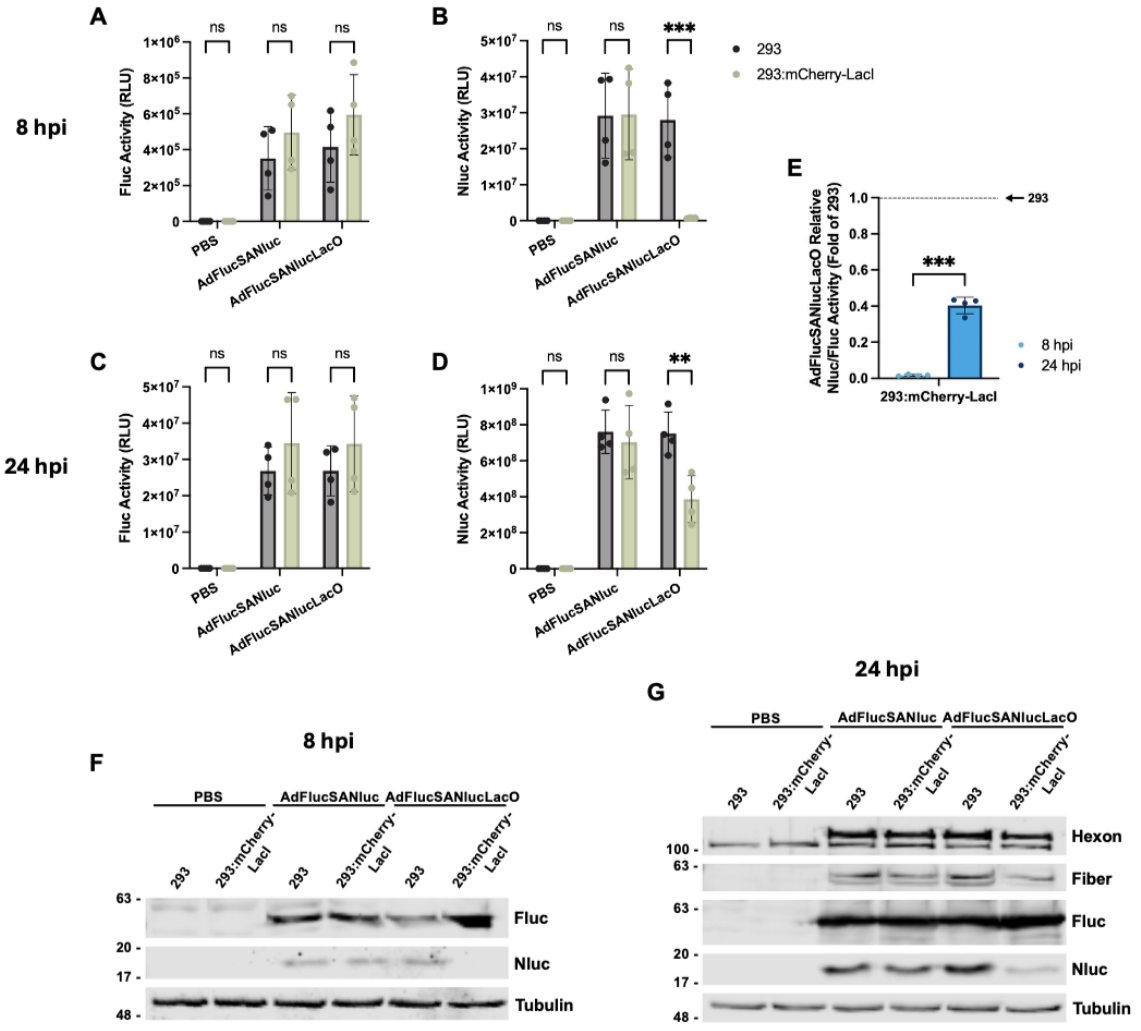

Figure 5.4 Nluc activity is significantly reduced in 293:mCherry-LacI cells infected with AdFlucSANlucLacO. 293 and 293:mCherry-LacI cells were infected with AdFlucSANluc or AdFlucSANlucLacO at an MOI of 1, or mock infected with PBS. Cells were harvested 8 and 24 hpi, Nluc and Fluc activity was then measured at 8 hpi or 24 hpi with the Nano-Glo Dual Luciferase Reporter Assay kit. Data is representative of four biological replicates (n=4) with two technical replicates per infection. Statistical significance assessed by two-way ANOVA followed by Sidak's multiple comparisons test. A) Fluc activity 8 hpi. B) Nluc activity 8 hpi. C) Fluc activity 24 hpi. D) Nluc activity 24 hpi. E) Comparison of normalized Nluc activity at 8 and 24 hpi in 293:mCherry-LacI cells infected with AdFlucSANlucLacO. Nluc activity was normalized to Fluc activity and then to values in 293 cells. Statistical significance assessed by unpaired t-test. F) Immunoblot from samples collected 8 hpi. G) Immunoblot from samples collected 24 hpi. Two asterisks (**) indicate $p<0.01$ and three asterisks (***) indicate $p<0.001$.

virus, AdFlucSANluc, suggesting that the decrease observed with AdFlucSANlucLacO was likely due to LacI binding at the LacO sites. At 24 hpi, Fluc activity remained similar between the two cell lines for both viruses tested (Figure 5.4C). Consistent with the 8 hpi data, Nluc activity from AdFlucSANlucLacO was significantly reduced in 293:mCherry-LacI cells, decreasing from ~7.5×10^8 RLU in 293 cells to ~3.9×10^8 RLU in 293:mCherry-LacI cells, corresponding to an approximately 2-fold reduction (Figure 5.4D). Nluc activity in 293:mCherry-LacI cells infected with AdFlucSANlucLacO at both time points was then normalised to Fluc and subsequently normalised to values from 293 cells. The data demonstrates a time-dependent difference in Nluc knockdown efficiency. At 8 hpi, normalized Nluc activity was reduced to ~1.8% of 293 levels, whereas by 24 hpi, it had increased to ~ 40% (Figure 5.4E). This difference suggests that LacI/LacO-mediated repression was strongest during early stages of infection, where fewer viral genome copies are present.

To further validate these finds, we conducted immunoblot assays with the samples harvested at 8 and 24 hpi. Qualitative analysis of the immunoblot of samples from 8 hpi showed a significant decrease in the Nluc protein signal from AdFlucSANlucLacO in 293:mCherry-LacI cells relative to 293, while Fluc protein levels from AdFlucSANluc remained consistent across both cell line (Figure 5.4F). At 24 hpi, Nluc protein intensity was reduced in 293:mCherry-LacI cells infected with AdFlucSANlucLacO relative to 293 cells, although the difference was less pronounced than at 8 hpi (Figure 5.4G). Fluc protein intensity from both viruses remained consistent across 293 and 293:mCherry-LacI cells. Hexon protein levels from both viruses at 24 hpi was also assessed and remained consistent across both cell lines. In contrast, fiber protein intensity appeared reduced in 293:mCherry-

LacI cells infected AdFlucSANlucLacO, relative to 293 cells. In HAdV, the fiber coding sequence is located within the L5 region of the major late transcription unit. In AdFlucSANlucLacO, insertion of the Nluc-LacO sequence within the E3 region places the LacO sites upstream of the L5 fiber coding sequence. This raises the possibility that LacI binding to the LacO sites may interfere with efficient transcription or accumulation of fiber mRNA. This is important consideration because reduced fiber expression could impair virion assembly or production. Together, data from luciferase assays and immunoblot analyses demonstrate that LacI effectively reduces MLP-driven transgene expression when LacO sites are positioned downstream of the transgene, without affecting expression from the E1 transgene expression cassette or hexon protein levels. However, the observed reduction in fiber protein intensity suggests that LacI/LacO-mediated repression may also affect downstream late gene expression in the LacO-containing virus.

5.2.4 Adenoviral vector yield is reduced in 293:mCherry-LacI cells 24 hpi

The data presented in Figure 5.4 demonstrates that the LacI/LacO system can effectively mediate knockdown of transgene expression from HAdV. In the context of FAST-expressing HAdV, the goal of this system is to suppress FAST protein expression in producer cells while still allowing efficient production of infectious viral particles. Therefore, it was important to determine whether 293:mCherry-LacI cells could support Ad vector production comparably to parental 293 cells. This was particularly important considering fiber protein intensity appeared reduced specifically in 293:mCherry-LacI cells infected with AdFlucSANlucLacO. 293 and 293:mCherry-LacI cells were infected with AdFlucSANlucLacO or AdFlucSANluc at an MOI of 3. Cells were harvested at 4 and 24 hpi and subsequently titered on 293 cells. The 4 hpi time point was used to assess residual

input virus from the inoculum prior to substantial viral replication, providing an indication of whether similar amounts of virus were present in each condition. At 4 hpi, there was no significant difference in viral titers, suggesting that infection efficiency was consistent across both 293 and 293:mCherry-LacI cells (Figure 5.5A). However, at 24 hpi, viral titers were significantly reduced for both viruses in 293:mCherry-LacI cells compared to parental 293 cells (Figure 5.5B). Viral titers at 24 hpi from 293:mCherry-LacI cells were normalized to the corresponding titers obtained from 293 cells and plotted on the same graph to determine the percentage of viral titer yield relative to 293 (Figure 5.5C). This allowed us to assess whether the observed decrease in viral titer was virus specific, resulting from LacI binding to LacO affecting viral replication and/or packaging, or instead reflected a general limitation of 293:mCherry-LacI cells in supporting Ad replication. Although the difference between the two viruses was not statistically significant, AdFlucSANlucLacO showed a trend toward lower viral titers than AdFlucSANluc when produced in 293:mCherry-LacI cells. Titers were reduced to approximately 15% and 1.7% of parental 293 levels for AdFlucSANluc and AdFlucSANlucLacO, respectively. These results suggest that although LacI efficiently reduces transgene expression from HAdV, viral yield from 293:mCherry-LacI cells is reduced compared to parental 293 cells. The reduction observed for both viruses suggests that this may partly reflect a general limitation of the 293:mCherry-LacI cell line. However, AdFlucSANlucLacO showed a greater reduction in viral titer than AdFlucSANluc. Together with the reduced fiber protein intensity observed in Figure 5.4, this raises the possibility that LacI binding to LacO sites may further impair production of the LacO-containing virus by affecting downstream late gene expression and/or virion assembly.

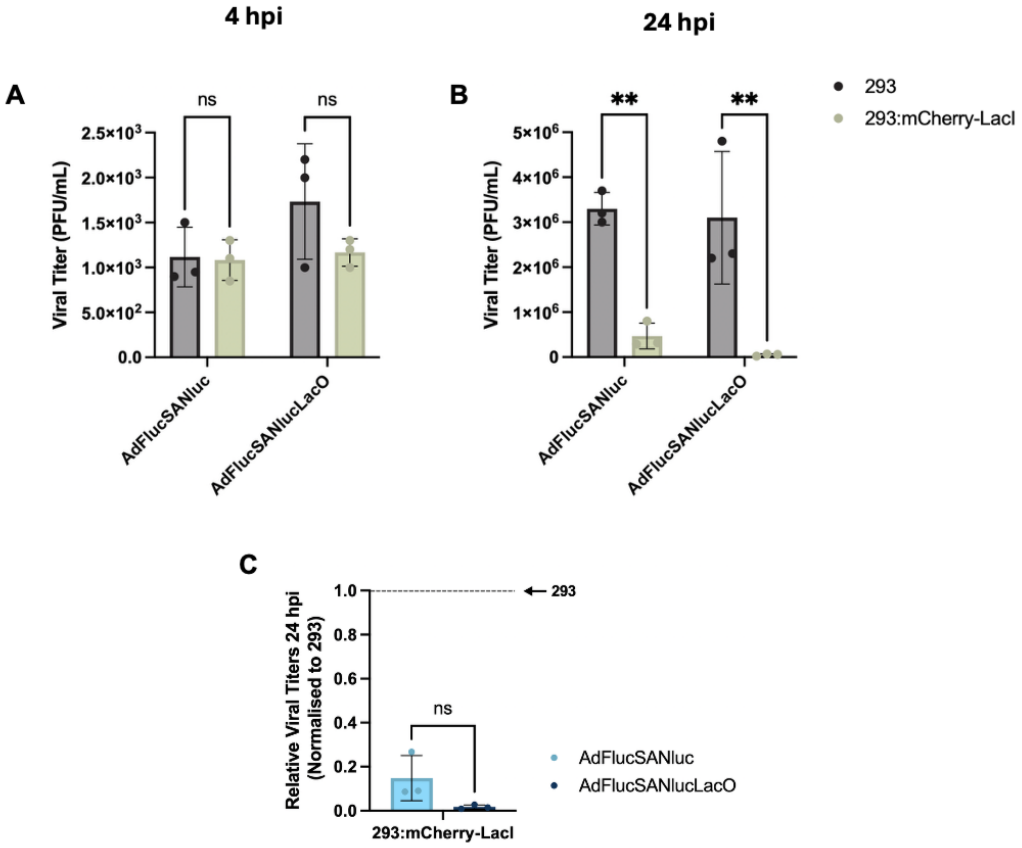

Figure 5.5 Viral titers of AdFlucSANluc and AdFlucSANlucLacO are significantly reduced 24 hpi in 293:mCherry-LacI cells compared to 293 cells. 293 and 293:mCherry-LacI were infected with AdFlucSANluc or AdFlucSANlucLacO at an MOI of 3. Cells were harvested at 4 and 24 hpi then titered on 293 cells. Data is representative of three biological replicates (n=3) with two technical replicates per infection. A) Viral titers from samples harvested at 4 hpi. Statistical significance assessed by two-way ANOVA followed by Sidak's multiple comparisons test. B) Viral titers from samples harvested at 24 hpi. Statistical significance assessed by two-way ANOVA followed by Sidak's multiple comparisons test. C) Comparison of titer reduction between AdFlucSANluc and AdFlucSANlucLacO from 293:mCherry-LacI cells 24 hpi. Titer values were normalized to those obtained from parental 293 cells. Statistical significance assessed by unpaired t-test. Two asterisks (**) indicate $p<0.01$.

5.2.5 Adenoviral yield improves 48 hpi but remains reduced in 293:mCherry-LacI cells

Given the reduced viral titers observed in 293:mCherry-LacI cells at 24 hpi, we next assessed whether extending the harvest time to 48 hpi could improve recovery of infectious virus. This was important because the reduction in fiber protein intensity observed in AdFlucSANlucLacO-infected 293:mCherry-LacI cells suggested that downstream late gene expression may be affected, which could impair infectious virion production. Therefore, the 48 hpi time point was used to determine whether the reduced viral yield reflected a persistent production defect or whether virus recovery improved with additional time. 293 and 293:mCherry-LacI cells were infected with AdFlucSANlucLacO or AdFlucSANluc at an MOI of 3. Cells were harvested 48 hpi and subsequently titered on 293 cells. We observed a significant decrease in viral titers for both viruses in 293:mCherry-LacI cells relative to parental 293 cells (Figure 5.6A). To better understand the extent of reduction in viral titers from 293:mCherry-LacI cells between the two viruses, viral titers from the LacI cell line were normalized to the corresponding titers obtained from 293 cells and plotted on the same graph (Figure 5.6B). Results showed statistical difference in the reduction of viral titer yield between AdFlucSANluc and AdFlucSANlucLacO in 293:mCherry-LacI cells, with titers reduced to approximately 60% and 40%, respectively, relative to those in 293 cells. Although viral titers increased at 48 hpi compared to 24 hpi, they remained lower than those observed in 293 cells. These findings suggest that 293:mCherry-LacI cells are capable of producing infectious Ad particles but do so less efficiently than parental 293 cells. Additionally, the lower titer recovery observed for the LacO-containing virus is consistent with the reduced fiber protein intensity observed in Figure 5.4. This supports the possibility that LacI binding to

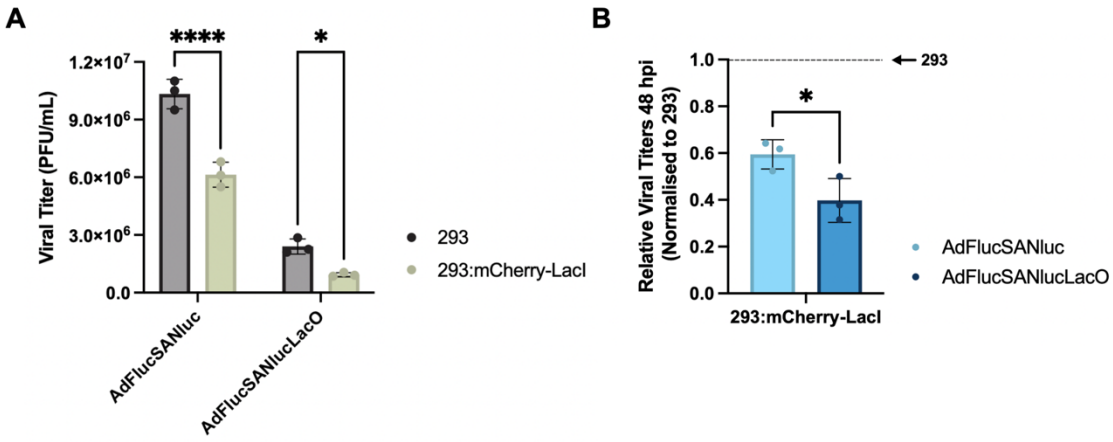

Figure 5.6 Viral titers of AdFlucSANluc and AdFlucSANlucLacO are significantly reduced 48 hpi in 293:mCherry-LacI cells compared to 293 cells. 293 and 293:mCherry-LacI were infected with AdFlucSANluc or AdFlucSANlucLacO at an MOI of 3. Cells were harvested at 48 hpi then titered on 293 cells. Data is representative of three biological replicates (n=3) with two technical replicates per infection. A) Viral titers from samples harvested at 48 hpi. Statistical significance assessed by two-way ANOVA followed by Sidak's multiple comparisons test. B) Comparison of titer reduction between AdFlucSANluc and AdFlucSANlucLacO from 293:mCherry-LacI cells 48 hpi. Titer values were normalized to those obtained from parental 293 cells. Statistical significance assessed by unpaired t-test. One asterisk (*) indicates $p<0.05$ and four asterisks (****) indicate $p<0.0001$.

the LacO sites may affect downstream late gene expression.

5.3 Discussion

In the previous chapter, we assessed the efficacy of a miRNA-based strategy for repressing transgene expression from HAdV. In parallel, we also evaluated an alternative regulatory strategy based on the LacI/LacO system to address the challenges associated with generating and propagating FAST-expressing Ad vectors. The LacI/LacO system is a naturally occurring gene regulatory system found in *E. coli* that controls the expression of genes involved in lactose metabolism[179,180]. In the absence of lactose, the LacI protein binds to the LacO sequence present in the Lac operon region and prevents transcription of downstream genes. In the presence of allolactose, a metabolite of lactose, LacI undergoes a conformational change that reduces its affinity for the LacO sequence, thereby allowing transcription to proceed[179,180]. Because of its well-characterized and reversible regulatory properties, the LacI/LacO system has been widely adapted as a tool in eukaryotic systems. Early work by Hu and Davidson demonstrated that the LacI/LacO system could function in mammalian cells, with LacI repressing expression of a transfected MSV-CAT reporter when LacO sequences were inserted near the promoter region[207]. Beyond regulating gene expression, LacI/LacO has been used to label and visualize DNA in living cells, where fluorescent LacI fusion proteins bind tandem LacO repeats to mark specific chromosomal loci[208,209]. This strategy has enabled live-cell analysis of chromosome dynamics, chromatin organization, and gene activity in mammalian cells and yeast[208,210]. Previous studies have used the LacI/LacO system in the context of Ad vector production, where LacI-mediated repression improved the rescue and propagation of vectors expressing cytotoxic

transgenes[173,174]. Therefore, we investigated whether this system could be applied to transiently repress FAST transgene expression during Ad vector production.

We first generated a HEK293 cell line which stably expresses a fusion protein of the LacI and an mCherry reporter (293:mCherry-LacI) (Figure 5.1). In this construct, mCherry served as an expression marker for LacI. We observed strong mCherry expression from this cell line as observed by both fluorescence microscopy and immunoblot analysis, confirming stable expression of the LacI. In principle, stable LacI expression in producer cells would allow repression of LacO-containing transgenes during viral amplification, while permitting transgene expression to be restored following infection of target cells that do not express LacI. Therefore, this system may provide a strategy to improve the production of Ad vectors encoding highly fusogenic or cytotoxic transgenes, such as FAST proteins.

To assess the efficacy of this system, we examined the silencing of Nluc via the LacI protein. The viruses generated for this aim possessed 16 repeats of the LacO sequence positioned either between the CMV promoter and the Nluc gene (AdLacONlucFlluc) or placed downstream of the Nluc gene, before the polyA signal (AdNlucLacOFluc). This design allowed us to compare whether LacI-mediated repression was more effective when LacO sequences were placed upstream of the coding sequence, where they may interfere with transcriptional initiation/elongation or downstream of the transgene, where they may interfere with transcript processing or stability. In the latter configuration, polymerase stalling or premature dissociation could reduce the production of properly cleaved and polyadenylated transcripts, resulting in unstable or incompletely processed RNA and reduced Nluc expression. Effective silencing of Nluc expression was observed when LacO

sites were positioned downstream of the transgene (Figure 5.3). Interestingly, when the LacO sites were positioned between the promoter and the transgene, Nluc activity was not detected even in parental 293 cells. Previous work by Matthews et al. demonstrated that insertion of a LacO sequence immediately downstream of the transcription start site allowed LacI-mediated repression of rabies virus glycoprotein expression and enabled efficient rescue of recombinant Ads that could not be generated in parental 293 cells[173]. In that study, however, only a single LacO sequence was inserted downstream of the transcription start site, whereas our construct contained 16 tandem LacO repeats positioned upstream of the Nluc coding sequence. The use of 16 LacO repeats was intended to maximize the number of available LacI-binding sites and thereby increase the likelihood of efficient repression. We initially hypothesized that insertion of the 16 LacO repeats upstream of the transgene may have disrupted the Nluc open reading frame, resulting in expression of a non-functional protein. Each LacO repeat contains an ATG sequence, which could potentially act as an upstream start codon and interfere with initiation at the correct Nluc start site. However, sequencing of the viral genome confirmed that the Nluc gene remained in frame despite the presence of upstream ATG sequences within the LacO repeats (data not shown). Although the Nluc gene remained within the open reading frame, the presence of the upstream LacO repeats may still interfere with Nluc translation. Previous studies have shown that repetitive sequences in the 5'UTR can promote the formation of secondary structures in the mRNA which interfere with ribosome preinitiation complex assembly or ribosome scanning, ultimately impairing translation[211,212]. In addition, previous studies have shown that upstream AUG sites within the 5′ UTR can reduce translation of the main open reading frame by limiting the number of ribosomes that

reach the intended start codon[213]. In this context, translation of Nluc would primarily depend on ribosomes bypassing upstream AUGs through leaky scanning or reinitiation at the downstream Nluc start codon[213]. Despite these limitations, Nluc expression was successfully repressed when the LacO repeats were positioned downstream of the transgene, before the polyadenylation signal. Therefore, we moved forward with this configuration to further assess its potential as a LacI-mediated regulatory strategy for suppressing transgene expression during Ad vector production. Interestingly, repression of Nluc expression was stronger at 8 hpi than at 24 hpi, with Nluc activity reduced approximately 16-fold and 4-fold, respectively. This difference in knockdown suggests that the effectiveness of the LacI/LacO system may decrease as infection progresses. This is an important consideration for future vector design, as incomplete repression at later stages of infection may still allow expression of highly fusogenic or cytotoxic transgenes during production. Nevertheless, the ability of the downstream LacO configuration to substantially reduce Nluc expression supports the potential use of this system as a strategy to transiently repress transgene expression during Ad vector amplification.

Similar to the miRNA-mediated strategy, we assessed the effectiveness of the LacI at repressing transgene expression from an oncolytic-like vector where Nluc expression is under regulation by the MLP (Figure 5.4). Consistent with our previous findings, positioning the LacO sites downstream of the transgene resulted in a significant reduction in Nluc expression at both 8 and 24 hpi. Repression was more pronounced at 8 hpi than at 24 hpi, with Nluc activity reduced by approximately 41-fold and 2-fold, respectively. An important consideration is that as Ad replication progresses, viral genome copy number increases, thereby increasing the number of LacO-containing DNA templates requiring

LacI binding. This may exceed the repressive capacity of the available LacI protein and could explain why repression was reduced at 24 hpi compared to 8 hpi. Despite this limitation, these findings demonstrate that downstream LacO placement can mediate transgene repression in the context of MLP-regulated expression, supporting its potential utility for transiently suppressing cytotoxic transgenes from oncolytic HAdV.

While we determined that the 293:mCherry-LacI cell line can effectively repress transgene expression from HAdV, this does not directly address whether the system improves vector yield. The ultimate goal of developing this regulatory strategy is to increase viral production by suppressing cytotoxic transgenes that would otherwise be expressed in producer cells and impair viral amplification. Therefore, the next step was to compare viral yields generated from parental 293 cells and 293:mCherry-LacI cells. In the present study, however, the target transgene was a bioluminescent reporter, which is not expected to be cytotoxic. As a result, comparable viral yields would be expected between the two cell lines, as repression of Nluc should not substantially improve producer cell viability or viral propagation. However, results indicated that viral yields were significantly reduced in 293:mCherry-LacI cells at 24 hpi for both AdFlucSANlucLacO and the control virus AdFlucSANluc, which lacks LacO sites (Figure 5.5). This suggests that the reduced viral yield is not solely due to LacI binding to LacO sequences or repression of the target transgene but may also reflect a broader limitation of the 293:mCherry-LacI cell line in supporting Ad production. Although this cell line was generated from a pooled population of transformed cells, it still represents a selected subset of the parental 293 cell population and may therefore differ from parental 293 cells in ways that affect Ad amplification. These differences could include altered metabolism, viral permissiveness, growth kinetics, or

cellular stress associated with stable transgene expression. In addition, the 293:mCherry-LacI cell line was maintained under hygromycin B selection, which may impose additional selective pressure and could potentially affect growth rate, metabolic activity, or viral amplification capacity.

In addition to the general reduction in viral yield observed for both viruses, AdFlucSANlucLacO showed lower recovery than control virus lacking LacO sites. At 24 hpi, AdFlucSANlucLacO titers were reduced to approximately 1.7% of those obtained from parental 293 cells, whereas AdFlucSANluc titers were reduced to approximately 15% (Figure 5.5). Although recovery improved at 48 hpi, AdFlucSANlucLacO remained lower than the non-LacO control, with titers reaching approximately 40% and 60% of parental 293 levels, respectively (Figure 5.6). This lower recovery of the LacO-containing virus is consistent with the reduced fiber protein intensity observed in Figure 5.4. In the AdFlucSANlucLacO construct, the E3 region is replaced with an SA-Nluc-LacO expression cassette, placing the LacO sites upstream of the fiber coding sequence. Therefore, while LacI binding to the LacO sites successfully reduced Nluc activity, LacI occupancy at the LacO sites may also impede RNA polymerase progression past this region. This could reduce production or accumulation of the full major late transcript and downstream late mRNAs. Reduced fiber expression could impair the recovery of infectious virions, as fiber forms the capsid projections involved in receptor binding and efficient infection[214]. Fiber-deficient Ads have been shown to retain the ability to assemble and form virions, but these particles exhibit severely reduced infectivity[215]. It is also possible that LacI binding to the viral genome may affect DNA replication[216]. If LacI remains tightly bound to the LacO sites during infection, it could potentially interfere with progression of

the viral DNA polymerase across the genome, thereby reducing viral genome replication and limiting the production of infectious virus. This could be tested by performing qPCR to measure viral genome accumulation over time in infected cells. Overall, reduced viral yield from the LacO-containing virus could reflect impaired viral DNA replication, reduced downstream late gene expression, defective virion assembly, or a combination of these effects.

Another important consideration is whether LacI remains associated with LacO-containing viral genomes during virion assembly or genome packaging. Although LacI binding is desirable during vector production because it can repress transgene expression in producer cells, persistent association of LacI with packaged viral genomes could be problematic after infection of target cells. For FAST-expressing vectors, the goal is to suppress FAST expression only during production, while allowing FAST expression to be restored in cancer cells. If LacI-bound genomes are packaged into virions, LacI could potentially remain bound after infection of target cells and continue to repress downstream viral gene expression, including the therapeutic FAST transgene. This could ultimately reduce the effectiveness of the vector, even if infectious particles are successfully produced. To assess if LacI remains associated with packaged viral genomes, purified virions could be examined by immunoblot. Detection of LacI in purified AdFlucSANlucLacO particles would suggest that LacI remains associated with the LacO-containing viral genome during virion assembly or packaging. Additionally, IPTG could be used to test whether LacI binding functionally contributes to reduced transgene expression or virus recovery. IPTG is a non-metabolizable lactose analog that mimics allolactose, the natural inducer of the LacI/LacO system, by binding to LacI and inducing a conformational change that reduces

its affinity for LacO[217]. Previous studies have shown that IPTG can relieve LacI/LacO-mediated repression in Ad vector systems. Matthews et al. used a 293-derived LacI-expressing cell line to repress rabies virus glycoprotein expression from LacO-containing Ad vectors, with repression at least partly relieved by IPTG[173]. Similarly, Edholm et al. inserted LacO sites downstream of an ASF/SF2 transgene in an Ad vector and showed that IPTG restored expression from the LacO-containing virus in 293-LacI cells[174]. In the context of this study, IPTG could therefore be used to determine whether reduced Nluc expression, reduced fiber protein intensity, and/or reduced recovery of AdFlucSANlucLacO is directly related to LacI binding. If IPTG restores these readouts, this would support the possibility that persistent LacI/LacO interaction contributes to the reduced performance of the LacO-containing virus.

Collectively, the findings presented in this chapter demonstrate that the LacI/LacO system can repress transgene expression from HAdV when LacO sequences are positioned downstream of the transgene. This repression was observed in both CMV-driven and MLP-regulated expression contexts, suggesting that this strategy can function in Ad vectors that more closely resemble conditionally replicating oncolytic HAdV. These findings are relevant to the broader goal of improving the production of FAST-expressing HAdV vectors, as transient repression of highly fusogenic or cytotoxic transgenes during amplification may help preserve producer cell viability and improve viral propagation. However, the reduced viral yields observed in 293:mCherry-LacI cells indicate that this system requires further optimization before it can be used to improve vector production. In addition, the lower recovery of the LacO-containing virus, together with the reduced fiber protein intensity observed by immunoblotting, suggests that LacI binding to LacO sites

within the viral genome may also interfere with downstream late gene expression, viral DNA replication, genome packaging, or virion assembly. Overall, while the LacI/LacO system shows promise as a regulatory strategy for repressing transgene expression during Ad vector production, further refinement will be required to determine whether it can effectively improve yields of highly cytotoxic FAST-armed oncolytic Ads.

Chapter 6: Conclusions and Future Directions

Oncolytic Ads represent a promising anti-cancer therapeutic. However, as with all oncolytic viruses their efficacy is often limited by poor spread following intratumoral injection[49]. To address this limitation, this work explored FAST proteins as fusogenic transgenes with the potential to enhance tumour cell killing by comparing the fusion profiles and effects on metabolic activity of p10, p14, and p15 FAST. However, the same fusogenic and cytopathic properties that make FAST proteins ideal therapeutic transgenes can also impair viral production by inducing premature fusion and cell death in producer cells. Therefore, this work aimed to identify a potent FAST protein candidate for oncolytic Ad therapy and to evaluate regulatory strategies capable of suppressing transgene expression during vector production.

In Chapter 3, we demonstrated that untagged p14 FAST was the most fusogenic and cytopathic FAST protein tested, inducing the greatest levels of syncytium formation and reductions in metabolic activity in both HEK293 and A549 cells. Importantly, the addition of an HA tag substantially reduced the activity of p14 FAST, suggesting that untagged p14 FAST-expressing vectors may produce improved therapeutic outcomes in future in vivo studies. In Chapters 4 and 5, we evaluated two regulatory systems designed to transiently repress transgene expression during Ad production. Both miRNA-mediated silencing and the LacI/LacO system were capable of reducing reporter transgene expression from HAdV, including in vector configurations that more closely resemble oncolytic Ad systems. However, both systems would require further optimization to improve vector recovery. Together, these findings support the use of producer cell-specific

regulatory strategies to improve the production of Ad vectors encoding highly fusogenic or cytotoxic transgenes.

Luciferase assay results showed that both miRNA-mediated silencing and the LacI/LacO system reduced reporter transgene expression from HAdV vectors. However, the two systems differed in their effects on vector recovery. In the miRNA system, Fluc expression was reduced at both 8 and 24 hpi without affecting expression of the untargeted Nluc reporter, indicating selective silencing of the targeted transcript (Figure 4.4). Infectious virus recovery from the 293:eYFP-miFluc cell line was reduced at 24 hpi but improved by 48 hpi, suggesting that virus production in this cell line may be delayed but not permanently impaired under the conditions tested (Figure 4.5). In contrast, LacI/LacO-mediated repression reduced reporter expression (Figure 5.4), but infectious virus recovery remained reduced even at 48 hpi, suggesting a more sustained effect on vector production (Figure 5.6). Additionally, the ability of the two systems to reduce transgene expression at 24 hpi differed. In the miRNA system, transgene repression was maintained from 8 to 24 hpi. In contrast, LacI/LacO-mediated repression was reduced by 24 hpi, suggesting that this system was less able to maintain transgene suppression at later stages of infection. This reduced LacI/LacO-mediated repression at later time points may reflect saturation of available LacI protein as viral genome replication increases the number of LacO-containing templates. This limitation is an important consideration because cytotoxic transgene repression would likely need to be sustained throughout vector amplification to prevent premature producer-cell toxicity. Notably, virus recovery was assessed differently for the two systems. For the miRNA system, Nluc activity following reinfection was used as a surrogate readout of infectious virus output, whereas infectious titers were measured

directly for the LacI/LacO system. Future studies should compare virus recovery from both strategies using the same experimental design to more accurately evaluate and compare their effects on HAdV vector production.

Future work should also focus on optimizing both regulatory producer cell systems and determining why vector recovery was reduced under certain conditions. For the miRNA-based system, infectious virus recovery from 293:eYFP-miFluc cells was reduced at 24 hpi but improved substantially by 48 hpi, suggesting that virus production in this cell line may be delayed rather than severely impaired. Further analysis of late viral protein expression, genome packaging, and virion assembly at both 24 and 48 hpi would help confirm whether virus production is delayed in this cell line. In addition, alternative miRNA target site placement could be explored to further optimize transgene silencing while minimizing the possibility that miRNA-mediated targeting affects the processing or stability of late viral transcripts. For the LacI/LacO system, transgene repression was less effective at 24 hpi. Therefore, future work could involve screening additional LacI-expressing producer cell lines and optimizing LacI expression levels to determine whether stronger LacI expression improves repression at later stages of infection. In addition, vector yield was reduced at both 24 and 48 hpi. Future LacO designs should aim to repress the cytotoxic transgene without interfering with transcription of downstream Ad late genes.

The work presented in this study provides foundational insight into which FAST protein may be most beneficial for incorporation into HAdV, as well as the ability of the regulatory systems to suppress transgene expression. However, future work should evaluate whether these regulatory systems can specifically repress FAST protein expression during Ad production. Although reporter genes such as Fluc and Nluc provided

useful models for assessing regulatory activity, the ultimate goal of this work is to suppress the expression of fusogenic FAST proteins during vector production in order to generate higher viral titers for downstream therapeutic applications. We have generated and recovered FAST-expressing HAdV vectors containing regulatory elements. These include vectors containing miRNA target sites within the 3′ UTR of the FAST transgene, as well as vectors containing LacO regulatory elements positioned downstream of the FAST-coding sequence. However, their functionality remains to be evaluated. These vectors should be used to assess whether FAST expression and syncytium formation are reduced in the corresponding regulatory producer cell lines. Once an optimized regulatory system is identified, the next major step will be to determine whether it enables the production of high-titer untagged p14 FAST-expressing oncolytic HAdV vectors. This will be particularly important because the results presented in this thesis suggest that untagged p14 FAST has substantially greater fusogenic and cytopathic activity than the HA-tagged version. Therefore, successful production of high-titer vectors expressing untagged p14 FAST could allow this more potent fusogen to be evaluated in relevant cancer models.

Future work could also expand beyond the FAST proteins evaluated in this thesis. Although this study focused on p10, p14, and p15 FAST, additional FAST proteins have recently been identified. Rotavirus NSP1-1 proteins from species B, G, and I were shown to induce syncytium formation in primate-derived cells[157]. Putative FAST-like proteins have also been identified in viruses of the family Pistolviridae, although these remain largely sequence-based predictions and require functional validation[158]. In addition to testing newly identified FAST proteins, future studies could evaluate engineered FAST variants. For example, previous work has shown that by combining the p14 ectodomain

with the p15 endodomain, fusion activity greatly increased[155]. Therefore, comparing p14 FAST with newly identified or engineered FAST proteins may help identify candidates with stronger fusion activity and improved potential for incorporation into oncolytic CRAds vectors.

Ultimately, by using these silencing mechanisms, future studies should evaluate the therapeutic efficacy of untagged p14 FAST-armed oncolytic CRAds in vivo. Previous studies using HA-tagged p14 FAST demonstrated syncytium formation within tumors but limited effects on tumor size[167]. Given the reduced activity of HA-tagged p14 FAST observed in this thesis, it will be important to determine whether untagged p14 FAST can promote more extensive tumor cell fusion and enhance tumor cell killing in animal models. Overall, the findings presented in this thesis provide a strong foundation for the development of improved FAST-expressing oncolytic CRAd vectors and supports the continued optimization of regulated expression systems to overcome current barriers in vector production. With further refinement, these strategies may improve the production and feasibility of oncolytic CRAds encoding cytotoxic or otherwise challenging transgenes, supporting their long-term development as a more versatile therapeutic platform for cancer treatment.

References

1. Bray F, Laversanne M, Sung H, et al. Global cancer statistics 2022: GLOBOCAN estimates of incidence and mortality worldwide for 36 cancers in 185 countries. CA Cancer J Clin. 2024;74(3):229-263. doi:10.3322/caac.21834
2. Canadian Cancer Statistics Advisory Committee in collaboration with the Canadian Cancer Society, Statistics Canada and the Public Health Agency of Canada. Canadian Cancer Statistics 2025. Toronto, ON: Canadian Cancer Society; 2025. Accessed 2026 Apr. 15, http://cancer.ca/Canadian-Cancer-Statistics-2025-EN
3. Brenner DR, Gillis J, Demers AA, et al. Projected estimates of cancer in Canada in 2026. CMAJ. Apr 12 2026;198(14):E526-E534. doi:10.1503/cmaj.252152
4. Hanahan D. Hallmarks of cancer-Then and now, and beyond. Cell. Apr 16 2026;189(8):2254-2277. doi:10.1016/j.cell.2025.12.049
5. Quail DF, Joyce JA. Cancer ecosystems: A dynamic interplay across scales. Cell. Apr 16 2026;189(8):2441-2463. doi:10.1016/j.cell.2026.03.003
6. Marine JC, Bartok O, Sagie S, et al. Mapping intratumor heterogeneity across layers for advancing immunotherapy. Cell. Apr 16 2026;189(8):2416-2440. doi:10.1016/j.cell.2026.03.025
7. Subudhi S, Lee S, Jain RK. Targeting angiogenesis: Lessons from 25 years of normalizing tumor vasculature. Cell. Apr 16 2026;189(8):2379-2415. doi:10.1016/j.cell.2026.03.016
8. Abbas Z, Rehman S. An Overview of Cancer Treatment Modalities. In: Shahzad HN, ed. Neoplasm. IntechOpen; 2018:chap 6.
9. Yap TA, Manning HC, Sapra P, Mills GB, O'Connor MJ. Targeting genomic instability in cancer. Cell. Apr 16 2026;189(8):2278-2306. doi:10.1016/j.cell.2026.03.035
10. Zafar A, Khatoon S, Khan MJ, Abu J, Naeem A. Advancements and limitations in traditional anti-cancer therapies: a comprehensive review of surgery, chemotherapy, radiation therapy, and hormonal therapy. Discov Oncol. Apr 24 2025;16(1):607. doi:10.1007/s12672-025-02198-8
11. van den Boogaard WMC, Komninos DSJ, Vermeij WP. Chemotherapy Side-Effects: Not All DNA Damage Is Equal. Cancers (Basel). Jan 26 2022;14(3)doi:10.3390/cancers14030627
12. Dagogo-Jack I, Shaw AT. Tumour heterogeneity and resistance to cancer therapies. Nat Rev Clin Oncol. Feb 2018;15(2):81-94. doi:10.1038/nrclinonc.2017.166
13. Mellman I, Coukos G, Dranoff G. Cancer immunotherapy comes of age. Nature. Dec 21 2011;480(7378):480-9. doi:10.1038/nature10673
14. Sahu M, Suryawanshi H. Immunotherapy: The future of cancer treatment. J Oral Maxillofac Pathol. 2021;25(2):371. doi:10.4103/0973-029X.325257
15. Sharma P, Hu-Lieskovan S, Wargo JA, Ribas A. Primary, Adaptive, and Acquired Resistance to Cancer Immunotherapy. Cell. Feb 09 2017;168(4):707-723. doi:10.1016/j.cell.2017.01.017
16. Kaufman HL, Kohlhapp FJ, Zloza A. Oncolytic viruses: a new class of immunotherapy drugs. Nat Rev Drug Discov. Sep 2015;14(9):642-62. doi:10.1038/nrd4663

17. Bommareddy PK, Zloza A, Rabkin SD, Kaufman HL. Oncolytic virus immunotherapy induces immunogenic cell death and overcomes STING deficiency in melanoma. Oncoimmunology. 2019;8(7):1591875. doi:10.1080/2162402X.2019.1591875
18. Russell SJ, Peng KW, Bell JC. Oncolytic virotherapy. Nat Biotechnol. Jul 10 2012;30(7):658-70. doi:10.1038/nbt.2287
19. Keller BA, Bell JC. Oncolytic viruses-immunotherapeutics on the rise. J Mol Med (Berl). Sep 2016;94(9):979-91. doi:10.1007/s00109-016-1453-9
20. Lemos de Matos A, Franco LS, McFadden G. Oncolytic Viruses and the Immune System: The Dynamic Duo. Mol Ther Methods Clin Dev. Jun 12 2020;17:349-358. doi:10.1016/j.omtm.2020.01.001
21. Breitbach CJ, De Silva NS, Falls TJ, et al. Targeting tumor vasculature with an oncolytic virus. Mol Ther. May 2011;19(5):886-94. doi:10.1038/mt.2011.26
22. Lichty BD, Breitbach CJ, Stojdl DF, Bell JC. Going viral with cancer immunotherapy. Nat Rev Cancer. Aug 2014;14(8):559-67. doi:10.1038/nrc3770
23. Dock G. THE INFLUENCE OF COMPLICATING DISEASES UPON LEUKAEMIA. The American Journal of the Medical Sciences. 1904;127(4)
24. Kelly E, Russell SJ. History of oncolytic viruses: genesis to genetic engineering. Mol Ther. Apr 2007;15(4):651-9. doi:10.1038/sj.mt.6300108
25. Zhang S, Rabkin SD. The discovery and development of oncolytic viruses: are they the future of cancer immunotherapy? Expert Opin Drug Discov. Apr 2021;16(4):391-410. doi:10.1080/17460441.2021.1850689
26. Yun CO, Hong J, Yoon AR. Current clinical landscape of oncolytic viruses as novel cancer immunotherapeutic and recent preclinical advancements. Front Immunol. 2022;13:953410. doi:10.3389/fimmu.2022.953410
27. Lin D, Shen Y, Liang T. Oncolytic virotherapy: basic principles, recent advances and future directions. Signal Transduct Target Ther. Apr 11 2023;8(1):156. doi:10.1038/s41392-023-01407-6
28. Liang M. Oncorine, the World First Oncolytic Virus Medicine and its Update in China. Curr Cancer Drug Targets. 2018;18(2):171-176. doi:10.2174/1568009618666171129221503
29. Zhang QN, Li Y, Zhao Q, et al. Recombinant human adenovirus type 5 (Oncorine) reverses resistance to immune checkpoint inhibitor in a patient with recurrent non-small cell lung cancer: A case report. Thorac Cancer. May 2021;12(10):1617-1619. doi:10.1111/1759-7714.13947
30. Rehman H, Silk AW, Kane MP, Kaufman HL. Into the clinic: Talimogene laherparepvec (T-VEC), a first-in-class intratumoral oncolytic viral therapy. J Immunother Cancer. 2016;4:53. doi:10.1186/s40425-016-0158-5
31. Greig SL. Talimogene Laherparepvec: First Global Approval. Drugs. Jan 2016;76(1):147-54. doi:10.1007/s40265-015-0522-7
32. Todo T, Ito H, Ino Y, et al. Intratumoral oncolytic herpes virus G47Δ for residual or recurrent glioblastoma: a phase 2 trial. Nat Med. Aug 2022;28(8):1630-1639. doi:10.1038/s41591-022-01897-x
33. Stojdl DF, Lichty B, Knowles S, et al. Exploiting tumor-specific defects in the interferon pathway with a previously unknown oncolytic virus. Nat Med. Jul 2000;6(7):821-5. doi:10.1038/77558

34. Alemany R, Balagué C, Curiel DT. Replicative adenoviruses for cancer therapy. Nat Biotechnol. Jul 2000;18(7):723-7. doi:10.1038/77283
35. Meyers DE, Wang AA, Thirukkumaran CM, Morris DG. Current Immunotherapeutic Strategies to Enhance Oncolytic Virotherapy. Front Oncol. 2017;7:114. doi:10.3389/fonc.2017.00114
36. Patel MR, Kratzke RA. Oncolytic virus therapy for cancer: the first wave of translational clinical trials. Transl Res. Apr 2013;161(4):355-64. doi:10.1016/j.trsl.2012.12.010
37. Maroun J, Muñoz-Alía M, Ammayappan A, Schulze A, Peng KW, Russell S. Designing and building oncolytic viruses. Future Virol. Apr 2017;12(4):193-213. doi:10.2217/fvl-2016-0129
38. Xiao D, Zhang H, Liu Y, Li Y, Li G, Ning Y. Oncolytic viruses: advanced strategies in cancer therapy. Signal Transduct Target Ther. Feb 05 2026;11(1):45. doi:10.1038/s41392-025-02343-3
39. Muthukutty P, Yoo SY. Oncolytic Virus Engineering and Utilizations: Cancer Immunotherapy Perspective. Viruses. Jul 28 2023;15(8)doi:10.3390/v15081645
40. Sampath P, Thorne SH. Arming viruses in multi-mechanistic oncolytic viral therapy: current research and future developments, with emphasis on poxviruses. Oncolytic Virother. 2014;3:1-9. doi:10.2147/OV.S36703
41. Minchinton AI, Tannock IF. Drug penetration in solid tumours. Nat Rev Cancer. Aug 2006;6(8):583-92. doi:10.1038/nrc1893
42. Jain RK. Transport of molecules, particles, and cells in solid tumors. Annu Rev Biomed Eng. 1999;1:241-63. doi:10.1146/annurev.bioeng.1.1.241
43. Jain RK. Normalizing tumor microenvironment to treat cancer: bench to bedside to biomarkers. J Clin Oncol. Jun 10 2013;31(17):2205-18. doi:10.1200/JCO.2012.46.3653
44. Matsunaga W, Gotoh A. Adenovirus as a Vector and Oncolytic Virus. Curr Issues Mol Biol. Jun 02 2023;45(6):4826-4840. doi:10.3390/cimb45060307
45. Wold WS, Toth K. Adenovirus vectors for gene therapy, vaccination and cancer gene therapy. Curr Gene Ther. Dec 2013;13(6):421-33. doi:10.2174/1566523213666131125095046
46. Sandig V, Brand K, Herwig S, Lukas J, Bartek J, Strauss M. Adenovirally transferred p16INK4/CDKN2 and p53 genes cooperate to induce apoptotic tumor cell death. Nat Med. Mar 1997;3(3):313-9. doi:10.1038/nm0397-313
47. Antrobus RD, Coughlan L, Berthoud TK, et al. Clinical assessment of a novel recombinant simian adenovirus ChAdOx1 as a vectored vaccine expressing conserved Influenza A antigens. Mol Ther. Mar 2014;22(3):668-674. doi:10.1038/mt.2013.284
48. Wang Y, Hu JK, Krol A, Li YP, Li CY, Yuan F. Systemic dissemination of viral vectors during intratumoral injection. Mol Cancer Ther. Nov 2003;2(11):1233-42.
49. Sauthoff H, Hu J, Maca C, et al. Intratumoral spread of wild-type adenovirus is limited after local injection of human xenograft tumors: virus persists and spreads systemically at late time points. Hum Gene Ther. Mar 20 2003;14(5):425-33. doi:10.1089/104303403321467199

50. Watanabe M, Nishikawaji Y, Kawakami H, Kosai KI. Adenovirus Biology, Recombinant Adenovirus, and Adenovirus Usage in Gene Therapy. Viruses. Dec 14 2021;13(12)doi:10.3390/v13122502
51. ROWE WP, HUEBNER RJ, GILMORE LK, PARROTT RH, WARD TG. Isolation of a cytopathogenic agent from human adenoids undergoing spontaneous degeneration in tissue culture. Proc Soc Exp Biol Med. Dec 1953;84(3):570-3. doi:10.3181/00379727-84-20714
52. HILLEMAN MR, WERNER JH. Recovery of new agent from patients with acute respiratory illness. Proc Soc Exp Biol Med. Jan 1954;85(1):183-8. doi:10.3181/00379727-85-20825
53. Lion T. Adenovirus infections in immunocompetent and immunocompromised patients. Clin Microbiol Rev. Jul 2014;27(3):441-62. doi:10.1128/CMR.00116-13
54. Ison MG. Adenovirus infections in transplant recipients. Clin Infect Dis. Aug 01 2006;43(3):331-9. doi:10.1086/505498
55. Shieh WJ. Human adenovirus infections in pediatric population - An update on clinico-pathologic correlation. Biomed J. Feb 2022;45(1):38-49. doi:10.1016/j.bj.2021.08.009
56. Lynch JP, Kajon AE. Adenovirus: Epidemiology, Global Spread of Novel Serotypes, and Advances in Treatment and Prevention. Semin Respir Crit Care Med. Aug 2016;37(4):586-602. doi:10.1055/s-0036-1584923
57. Schmitz H, Wigand R, Heinrich W. Worldwide epidemiology of human adenovirus infections. Am J Epidemiol. Apr 1983;117(4):455-66. doi:10.1093/oxfordjournals.aje.a113563
58. Kulanayake S, Tikoo SK. Adenovirus Core Proteins: Structure and Function. Viruses. Feb 28 2021;13(3)doi:10.3390/v13030388
59. Saha B, Wong CM, Parks RJ. The adenovirus genome contributes to the structural stability of the virion. Viruses. Sep 24 2014;6(9):3563-83. doi:10.3390/v6093563
60. Russell WC. Adenoviruses: update on structure and function. J Gen Virol. Jan 2009;90(Pt 1):1-20. doi:10.1099/vir.0.003087-0
61. Rux JJ, Burnett RM. Adenovirus structure. Hum Gene Ther. Dec 2004;15(12):1167-76. doi:10.1089/hum.2004.15.1167
62. Russell WC, Laver WG, Sanderson PJ. Internal components of adenovirus. Nature. Sep 14 1968;219(5159):1127-30. doi:10.1038/2191127a0
63. Chatterjee PK, Vayda ME, Flint SJ. Identification of proteins and protein domains that contact DNA within adenovirus nucleoprotein cores by ultraviolet light crosslinking of oligonucleotides 32P-labelled in vivo. J Mol Biol. Mar 05 1986;188(1):23-37. doi:10.1016/0022-2836(86)90477-8
64. Jennings MR, Parks RJ. Human Adenovirus Gene Expression and Replication Is Regulated through Dynamic Changes in Nucleoprotein Structure throughout Infection. Viruses. Jan 05 2023;15(1)doi:10.3390/v15010161
65. Flint J. Organization of the adenoviral genome. In: Seth P, ed. Adenoviruses: Basic Biology to Gene Therapy R.G. Landes Company; 1999:17-30.
66. Davison AJ, Benkő M, Harrach B. Genetic content and evolution of adenoviruses. J Gen Virol. Nov 2003;84(Pt 11):2895-2908. doi:10.1099/vir.0.19497-0

67. Singhal G, Leo E, Setty SK, Pommier Y, Thimmapaya B. Adenovirus E1A oncogene induces rereplication of cellular DNA and alters DNA replication dynamics. J Virol. Aug 2013;87(15):8767-78. doi:10.1128/JVI.00879-13
68. Hidalgo P, Ip WH, Dobner T, Gonzalez RA. The biology of the adenovirus E1B 55K protein. FEBS Lett. Dec 2019;593(24):3504-3517. doi:10.1002/1873-3468.13694
69. Horwitz MS. Function of adenovirus E3 proteins and their interactions with immunoregulatory cell proteins. J Gene Med. Feb 2004;6 Suppl 1:S172-83. doi:10.1002/jgm.495
70. Weitzman MD. Functions of the adenovirus E4 proteins and their impact on viral vectors. Front Biosci. May 01 2005;10:1106-17. doi:10.2741/1604
71. Thomas GP, Mathews MB. DNA replication and the early to late transition in adenovirus infection. Cell. Nov 1980;22(2 Pt 2):523-33. doi:10.1016/0092-8674(80)90362-1
72. Larsson S, Svensson C, Akusjärvi G. Control of adenovirus major late gene expression at multiple levels. J Mol Biol. May 20 1992;225(2):287-98. doi:10.1016/0022-2836(92)90922-7
73. Akusjärvi G, Persson H. Controls of RNA splicing and termination in the major late adenovirus transcription unit. Nature. Jul 30 1981;292(5822):420-6. doi:10.1038/292420a0
74. Smith AC, Poulin KL, Parks RJ. DNA genome size affects the stability of the adenovirus virion. J Virol. Feb 2009;83(4):2025-8. doi:10.1128/JVI.01644-08
75. Christensen JB, Byrd SA, Walker AK, Strahler JR, Andrews PC, Imperiale MJ. Presence of the adenovirus IVa2 protein at a single vertex of the mature virion. J Virol. Sep 2008;82(18):9086-93. doi:10.1128/JVI.01024-08
76. Kim JH, Lee CH, Lee SW. Adenovirus VA RNAs impair maturation of primary microRNA. J Gene Med. Dec 2023;25(12):e3564. doi:10.1002/jgm.3564
77. O'Malley RP, Mariano TM, Siekierka J, Mathews MB. A mechanism for the control of protein synthesis by adenovirus VA RNAI. Cell. Feb 14 1986;44(3):391-400. doi:10.1016/0092-8674(86)90460-5
78. Bergelson JM, Cunningham JA, Droguett G, et al. Isolation of a common receptor for Coxsackie B viruses and adenoviruses 2 and 5. Science. Feb 28 1997;275(5304):1320-3. doi:10.1126/science.275.5304.1320
79. Wickham TJ, Filardo EJ, Cheresh DA, Nemerow GR. Integrin alpha v beta 5 selectively promotes adenovirus mediated cell membrane permeabilization. J Cell Biol. Oct 1994;127(1):257-64. doi:10.1083/jcb.127.1.257
80. Nemerow GR, Pache L, Reddy V, Stewart PL. Insights into adenovirus host cell interactions from structural studies. Virology. Feb 20 2009;384(2):380-8. doi:10.1016/j.virol.2008.10.016
81. Wiethoff CM, Wodrich H, Gerace L, Nemerow GR. Adenovirus protein VI mediates membrane disruption following capsid disassembly. J Virol. Feb 2005;79(4):1992-2000. doi:10.1128/JVI.79.4.1992-2000.2005
82. Bremner KH, Scherer J, Yi J, Vershinin M, Gross SP, Vallee RB. Adenovirus transport via direct interaction of cytoplasmic dynein with the viral capsid hexon subunit. Cell Host Microbe. Dec 17 2009;6(6):523-35. doi:10.1016/j.chom.2009.11.006

83. Kelkar SA, Pfister KK, Crystal RG, Leopold PL. Cytoplasmic dynein mediates adenovirus binding to microtubules. J Virol. Sep 2004;78(18):10122-32. doi:10.1128/JVI.78.18.10122-10132.2004
84. Greber UF, Suomalainen M, Stidwill RP, Boucke K, Ebersold MW, Helenius A. The role of the nuclear pore complex in adenovirus DNA entry. EMBO J. Oct 01 1997;16(19):5998-6007. doi:10.1093/emboj/16.19.5998
85. Hidalgo P, Anzures L, Hernández-Mendoza A, et al. Morphological, Biochemical, and Functional Study of Viral Replication Compartments Isolated from Adenovirus-Infected Cells. J Virol. Jan 13 2016;90(7):3411-27. doi:10.1128/JVI.00033-16
86. Tollefson AE, Ryerse JS, Scaria A, Hermiston TW, Wold WS. The E3-11.6-kDa adenovirus death protein (ADP) is required for efficient cell death: characterization of cells infected with adp mutants. Virology. Jun 01 1996;220(1):152-62. doi:10.1006/viro.1996.0295
87. Ginn SL, Mandwie M, Alexander IE, Edelstein M, Abedi MR. Gene therapy clinical trials worldwide to 2023-an update. J Gene Med. Aug 2024;26(8):e3721. doi:10.1002/jgm.3721
88. Kossila M, Jauhiainen S, Laukkanen MO, et al. Improvement in adenoviral gene transfer efficiency after preincubation at +37 degrees C in vitro and in vivo. Mol Ther. Jan 2002;5(1):87-93. doi:10.1006/mthe.2001.0516
89. Crystal RG. Adenovirus: the first effective in vivo gene delivery vector. Hum Gene Ther. Jan 2014;25(1):3-11. doi:10.1089/hum.2013.2527
90. Bett AJ, Prevec L, Graham FL. Packaging capacity and stability of human adenovirus type 5 vectors. J Virol. Oct 1993;67(10):5911-21. doi:10.1128/JVI.67.10.5911-5921.1993
91. Bett AJ, Haddara W, Prevec L, Graham FL. An efficient and flexible system for construction of adenovirus vectors with insertions or deletions in early regions 1 and 3. Proc Natl Acad Sci U S A. Sep 13 1994;91(19):8802-6. doi:10.1073/pnas.91.19.8802
92. Graham FL, Smiley J, Russell WC, Nairn R. Characteristics of a human cell line transformed by DNA from human adenovirus type 5. J Gen Virol. Jul 1977;36(1):59-74. doi:10.1099/0022-1317-36-1-59
93. Zhang SW, Xiao SW, Liu CQ, et al. [Treatment of head and neck squamous cell carcinoma by recombinant adenovirus-p53 combined with radiotherapy: a phase II clinical trial of 42 cases]. Zhonghua Yi Xue Za Zhi. Dec 10 2003;83(23):2023-8.
94. Boorjian SA, Alemozaffar M, Konety BR, et al. Intravesical nadofaragene firadenovec gene therapy for BCG-unresponsive non-muscle-invasive bladder cancer: a single-arm, open-label, repeat-dose clinical trial. Lancet Oncol. Jan 2021;22(1):107-117. doi:10.1016/S1470-2045(20)30540-4
95. Zhang C, Zhou D. Adenoviral vector-based strategies against infectious disease and cancer. Hum Vaccin Immunother. Aug 02 2016;12(8):2064-2074. doi:10.1080/21645515.2016.1165908
96. Tatsis N, Ertl HC. Adenoviruses as vaccine vectors. Mol Ther. Oct 2004;10(4):616-29. doi:10.1016/j.ymthe.2004.07.013

97. Chavda VP, Bezbaruah R, Valu D, et al. Adenoviral Vector-Based Vaccine Platform for COVID-19: Current Status. Vaccines (Basel). Feb 13 2023;11(2)doi:10.3390/vaccines11020432
98. Macedo N, Miller DM, Haq R, Kaufman HL. Clinical landscape of oncolytic virus research in 2020. J Immunother Cancer. Oct 2020;8(2)doi:10.1136/jitc-2020-001486
99. Mathis JM, Stoff-Khalili MA, Curiel DT. Oncolytic adenoviruses - selective retargeting to tumor cells. Oncogene. Nov 21 2005;24(52):7775-91. doi:10.1038/sj.onc.1209044
100. Ding M, Cao X, Xu HN, et al. Prostate cancer-specific and potent antitumor effect of a DD3-controlled oncolytic virus harboring the PTEN gene. PLoS One. 2012;7(4):e35153. doi:10.1371/journal.pone.0035153
101. Rodriguez R, Schuur ER, Lim HY, Henderson GA, Simons JW, Henderson DR. Prostate attenuated replication competent adenovirus (ARCA) CN706: a selective cytotoxic for prostate-specific antigen-positive prostate cancer cells. Cancer Res. Jul 01 1997;57(13):2559-63.
102. Oh E, Hong J, Kwon OJ, Yun CO. A hypoxia- and telomerase-responsive oncolytic adenovirus expressing secretable trimeric TRAIL triggers tumour-specific apoptosis and promotes viral dispersion in TRAIL-resistant glioblastoma. Sci Rep. Jan 23 2018;8(1):1420. doi:10.1038/s41598-018-19300-6
103. Heise C, Hermiston T, Johnson L, et al. An adenovirus E1A mutant that demonstrates potent and selective systemic anti-tumoral efficacy. Nat Med. Oct 2000;6(10):1134-9. doi:10.1038/80474
104. Bandara LR, La Thangue NB. Adenovirus E1a prevents the retinoblastoma gene product from complexing with a cellular transcription factor. Nature. Jun 06 1991;351(6326):494-7. doi:10.1038/351494a0
105. Nemajerova A, Talos F, Moll UM, Petrenko O. Rb function is required for E1A-induced S-phase checkpoint activation. Cell Death Differ. Sep 2008;15(9):1440-9. doi:10.1038/cdd.2008.66
106. Jiang H, Alemany R, Gomez-Manzano C, et al. Downmodulation of E1A protein expression as a novel strategy to design cancer-selective adenoviruses. Neoplasia. Aug 2005;7(8):723-9. doi:10.1593/neo.04793
107. Fueyo J, Gomez-Manzano C, Alemany R, et al. A mutant oncolytic adenovirus targeting the Rb pathway produces anti-glioma effect in vivo. Oncogene. Jan 06 2000;19(1):2-12. doi:10.1038/sj.onc.1203251
108. Nevins JR. The Rb/E2F pathway and cancer. Hum Mol Genet. Apr 2001;10(7):699-703. doi:10.1093/hmg/10.7.699
109. Bischoff JR, Kirn DH, Williams A, et al. An adenovirus mutant that replicates selectively in p53-deficient human tumor cells. Science. Oct 18 1996;274(5286):373-6. doi:10.1126/science.274.5286.373
110. Dix BR, Edwards SJ, Braithwaite AW. Does the antitumor adenovirus ONYX-015/dl1520 selectively target cells defective in the p53 pathway? J Virol. Jun 2001;75(12):5443-7. doi:10.1128/JVI.75.12.5443-5447.2001
111. O'Shea CC, Johnson L, Bagus B, et al. Late viral RNA export, rather than p53 inactivation, determines ONYX-015 tumor selectivity. Cancer Cell. Dec 2004;6(6):611-23. doi:10.1016/j.ccr.2004.11.012

112. Nemunaitis J, Khuri F, Ganly I, et al. Phase II trial of intratumoral administration of ONYX-015, a replication-selective adenovirus, in patients with refractory head and neck cancer. J Clin Oncol. Jan 15 2001;19(2):289-98. doi:10.1200/JCO.2001.19.2.289
113. Aghi M, Martuza RL. Oncolytic viral therapies - the clinical experience. Oncogene. Nov 21 2005;24(52):7802-16. doi:10.1038/sj.onc.1209037
114. Kawashima T, Kagawa S, Kobayashi N, et al. Telomerase-specific replication-selective virotherapy for human cancer. Clin Cancer Res. Jan 01 2004;10(1 Pt 1):285-92. doi:10.1158/1078-0432.ccr-1075-3
115. Sarkar S, Khan S, Eads J, et al. Phase II study of telomelysin (OBP-301) in combination with pembrolizumab in gastroesophageal (GEA) adenocarcinoma. Journal for ImmunoTherapy of Cancer. 2023;11doi:10.1136/jitc-2023-SITC2023.0586
116. Fueyo J, Alemany R, Gomez-Manzano C, et al. Preclinical characterization of the antiglioma activity of a tropism-enhanced adenovirus targeted to the retinoblastoma pathway. J Natl Cancer Inst. May 07 2003;95(9):652-60. doi:10.1093/jnci/95.9.652
117. Lang FF, Conrad C, Gomez-Manzano C, et al. Phase I Study of DNX-2401 (Delta-24-RGD) Oncolytic Adenovirus: Replication and Immunotherapeutic Effects in Recurrent Malignant Glioma. J Clin Oncol. May 10 2018;36(14):1419-1427. doi:10.1200/JCO.2017.75.8219
118. Rojas JJ, Cascallo M, Guedan S, et al. A modified E2F-1 promoter improves the efficacy to toxicity ratio of oncolytic adenoviruses. Gene Ther. Dec 2009;16(12):1441-51. doi:10.1038/gt.2009.103
119. Nokisalmi P, Pesonen S, Escutenaire S, et al. Oncolytic adenovirus ICOVIR-7 in patients with advanced and refractory solid tumors. Clin Cancer Res. Jun 01 2010;16(11):3035-43. doi:10.1158/1078-0432.CCR-09-3167
120. Pesonen S, Kangasniemi L, Hemminki A. Oncolytic adenoviruses for the treatment of human cancer: focus on translational and clinical data. Mol Pharm. Feb 07 2011;8(1):12-28. doi:10.1021/mp100219n
121. Raja J, Ludwig JM, Gettinger SN, Schalper KA, Kim HS. Oncolytic virus immunotherapy: future prospects for oncology. J Immunother Cancer. Dec 04 2018;6(1):140. doi:10.1186/s40425-018-0458-z
122. Stylianopoulos T, Martin JD, Chauhan VP, et al. Causes, consequences, and remedies for growth-induced solid stress in murine and human tumors. Proc Natl Acad Sci U S A. Sep 18 2012;109(38):15101-8. doi:10.1073/pnas.1213353109
123. Smith E, Breznik J, Lichty BD. Strategies to enhance viral penetration of solid tumors. Hum Gene Ther. Sep 2011;22(9):1053-60. doi:10.1089/hum.2010.227
124. Cuevas Y, Hernández-Alcoceba R, Aragones J, et al. Specific oncolytic effect of a new hypoxia-inducible factor-dependent replicative adenovirus on von Hippel-Lindau-defective renal cell carcinomas. Cancer Res. Oct 15 2003;63(20):6877-84.
125. Post DE, Devi NS, Li Z, et al. Cancer therapy with a replicating oncolytic adenovirus targeting the hypoxic microenvironment of tumors. Clin Cancer Res. Dec 15 2004;10(24):8603-12. doi:10.1158/1078-0432.CCR-04-1432
126. Lang FF, Bruner JM, Fuller GN, et al. Phase I trial of adenovirus-mediated p53 gene therapy for recurrent glioma: biological and clinical results. J Clin Oncol. Jul 01 2003;21(13):2508-18. doi:10.1200/JCO.2003.21.13.2508

127. Medina-Echeverz J, Aranda F, Berraondo P. Myeloid-derived cells are key targets of tumor immunotherapy. Oncoimmunology. 2014;3:e28398. doi:10.4161/onci.28398
128. Whiteside TL. Regulatory T cell subsets in human cancer: are they regulating for or against tumor progression? Cancer Immunol Immunother. Jan 2014;63(1):67-72. doi:10.1007/s00262-013-1490-y
129. Loskog A. Immunostimulatory Gene Therapy Using Oncolytic Viruses as Vehicles. Viruses. Nov 06 2015;7(11):5780-91. doi:10.3390/v7112899
130. Choi IK, Yun CO. Recent developments in oncolytic adenovirus-based immunotherapeutic agents for use against metastatic cancers. Cancer Gene Ther. Feb 2013;20(2):70-6. doi:10.1038/cgt.2012.95
131. Cody JJ, Douglas JT. Armed replicating adenoviruses for cancer virotherapy. Cancer Gene Ther. Jun 2009;16(6):473-88. doi:10.1038/cgt.2009.3
132. Ramesh N, Ge Y, Ennist DL, et al. CG0070, a conditionally replicating granulocyte macrophage colony-stimulating factor--armed oncolytic adenovirus for the treatment of bladder cancer. Clin Cancer Res. Jan 01 2006;12(1):305-13. doi:10.1158/1078-0432.CCR-05-1059
133. Havunen R, Kalliokoski R, Siurala M, et al. Cytokine-Coding Oncolytic Adenovirus TILT-123 Is Safe, Selective, and Effective as a Single Agent and in Combination with Immune Checkpoint Inhibitor Anti-PD-1. Cells. Jan 27 2021;10(2)doi:10.3390/cells10020246
134. Bazan-Peregrino M, Garcia-Carbonero R, Laquente B, et al. VCN-01 disrupts pancreatic cancer stroma and exerts antitumor effects. J Immunother Cancer. Nov 2021;9(11)doi:10.1136/jitc-2021-003254
135. Jin F, Kretschmer PJ, Hermiston TW. Identification of novel insertion sites in the Ad5 genome that utilize the Ad splicing machinery for therapeutic gene expression. Mol Ther. Dec 2005;12(6):1052-63. doi:10.1016/j.ymthe.2005.07.696
136. Carette JE, Graat HC, Schagen FH, Abou El Hassan MA, Gerritsen WR, van Beusechem VW. Replication-dependent transgene expression from a conditionally replicating adenovirus via alternative splicing to a heterologous splice-acceptor site. J Gene Med. Aug 2005;7(8):1053-62. doi:10.1002/jgm.754
137. Kim JH, Lee YS, Kim H, Huang JH, Yoon AR, Yun CO. Relaxin expression from tumor-targeting adenoviruses and its intratumoral spread, apoptosis induction, and efficacy. J Natl Cancer Inst. Oct 18 2006;98(20):1482-93. doi:10.1093/jnci/djj397
138. Ganesh S, Gonzalez Edick M, Idamakanti N, et al. Relaxin-expressing, fiber chimeric oncolytic adenovirus prolongs survival of tumor-bearing mice. Cancer Res. May 01 2007;67(9):4399-407. doi:10.1158/0008-5472.CAN-06-4260
139. Guedan S, Rojas JJ, Gros A, Mercade E, Cascallo M, Alemany R. Hyaluronidase expression by an oncolytic adenovirus enhances its intratumoral spread and suppresses tumor growth. Mol Ther. Jul 2010;18(7):1275-83. doi:10.1038/mt.2010.79
140. Choi IK, Lee YS, Yoo JY, et al. Effect of decorin on overcoming the extracellular matrix barrier for oncolytic virotherapy. Gene Ther. Feb 2010;17(2):190-201. doi:10.1038/gt.2009.142
141. Del Papa J, Parks RJ. Adenoviral Vectors Armed with Cell Fusion-Inducing Proteins as Anti-Cancer Agents. Viruses. Jan 19 2017;9(1)doi:10.3390/v9010013

142. Krabbe T, Altomonte J. Fusogenic Viruses in Oncolytic Immunotherapy. Cancers (Basel). Jun 26 2018;10(7)doi:10.3390/cancers10070216
143. Harrison SC. Mechanism of membrane fusion by viral envelope proteins. Adv Virus Res. 2005;64:231-61. doi:10.1016/S0065-3527(05)64007-9
144. Bateman AR, Harrington KJ, Kottke T, et al. Viral fusogenic membrane glycoproteins kill solid tumor cells by nonapoptotic mechanisms that promote cross presentation of tumor antigens by dendritic cells. Cancer Res. Nov 15 2002;62(22):6566-78.
145. Hoffmann D, Bayer W, Grunwald T, Wildner O. Intratumoral expression of respiratory syncytial virus fusion protein in combination with cytokines encoded by adenoviral vectors as in situ tumor vaccine for colorectal cancer. Mol Cancer Ther. Jul 2007;6(7):1942-50. doi:10.1158/1535-7163.MCT-06-0790
146. Li H, Haviv YS, Derdeyn CA, et al. Human immunodeficiency virus type 1-mediated syncytium formation is compatible with adenovirus replication and facilitates efficient dispersion of viral gene products and de novo-synthesized virus particles. Hum Gene Ther. Dec 10 2001;12(18):2155-65. doi:10.1089/10430340152710504
147. Bateman A, Bullough F, Murphy S, et al. Fusogenic membrane glycoproteins as a novel class of genes for the local and immune-mediated control of tumor growth. Cancer Res. Mar 15 2000;60(6):1492-7.
148. Errington F, Jones J, Merrick A, et al. Fusogenic membrane glycoprotein-mediated tumour cell fusion activates human dendritic cells for enhanced IL-12 production and T-cell priming. Gene Ther. Jan 2006;13(2):138-49. doi:10.1038/sj.gt.3302609
149. Fu X, Tao L, Jin A, Vile R, Brenner MK, Zhang X. Expression of a fusogenic membrane glycoprotein by an oncolytic herpes simplex virus potentiates the viral antitumor effect. Mol Ther. Jun 2003;7(6):748-54. doi:10.1016/s1525-0016(03)00092-3
150. Ayala-Breton C, Russell LO, Russell SJ, Peng KW. Faster replication and higher expression levels of viral glycoproteins give the vesicular stomatitis virus/measles virus hybrid VSV-FH a growth advantage over measles virus. J Virol. Aug 2014;88(15):8332-9. doi:10.1128/JVI.03823-13
151. Ebert O, Shinozaki K, Kournioti C, Park MS, García-Sastre A, Woo SL. Syncytia induction enhances the oncolytic potential of vesicular stomatitis virus in virotherapy for cancer. Cancer Res. May 01 2004;64(9):3265-70. doi:10.1158/0008-5472.can-03-3753
152. Dewar RL, Natarajan V, Vasudevachari MB, Salzman NP. Synthesis and processing of human immunodeficiency virus type 1 envelope proteins encoded by a recombinant human adenovirus. J Virol. Jan 1989;63(1):129-36. doi:10.1128/JVI.63.1.129-136.1989
153. Guedan S, Gros A, Cascallo M, Vile R, Mercade E, Alemany R. Syncytia formation affects the yield and cytotoxicity of an adenovirus expressing a fusogenic glycoprotein at a late stage of replication. Gene Ther. Sep 2008;15(17):1240-5. doi:10.1038/gt.2008.94
154. Shmulevitz M, Duncan R. A new class of fusion-associated small transmembrane (FAST) proteins encoded by the non-enveloped fusogenic reoviruses. EMBO J. Mar 01 2000;19(5):902-12. doi:10.1093/emboj/19.5.902

155. Ciechonska M, Duncan R. Reovirus FAST proteins: virus-encoded cellular fusogens. Trends Microbiol. Dec 2014;22(12):715-24. doi:10.1016/j.tim.2014.08.005
156. Duncan R. Fusogenic Reoviruses and Their Fusion-Associated Small Transmembrane (FAST) Proteins. Annu Rev Virol. Sep 29 2019;6(1):341-363. doi:10.1146/annurev-virology-092818-015523
157. Sartalamacchia K, Veletanlic V, Diller JR, Ogden KM. Multiple rotavirus species encode fusion-associated small transmembrane (FAST) proteins with cell type-specific activity. J Virol. Dec 23 2025;99(12):e0158725. doi:10.1128/jvi.01587-25
158. Amono R, Markussen T, Evensen Ø, Mikalsen AB. Putative Fusion-Associated Small Transmembrane (FAST) Proteins Encoded by Viruses of Pistolviridae, Order Ghabrivirales, Indentified from In Silico Analyses. Viruses. Feb 01 2026;18(2)doi:10.3390/v18020193
159. Sartalamacchia K, Porter MS, Veletanlic V, Ogden KM. Avian deltacoronaviruses encode fusion-associated small transmembrane proteins that can induce syncytia formation. Virology. Dec 2024;600:110258. doi:10.1016/j.virol.2024.110258
160. Shmulevitz M, Epand RF, Epand RM, Duncan R. Structural and functional properties of an unusual internal fusion peptide in a nonenveloped virus membrane fusion protein. J Virol. Mar 2004;78(6):2808-18. doi:10.1128/jvi.78.6.2808-2818.2004
161. Corcoran JA, Syvitski R, Top D, et al. Myristoylation, a protruding loop, and structural plasticity are essential features of a nonenveloped virus fusion peptide motif. J Biol Chem. Dec 03 2004;279(49):51386-94. doi:10.1074/jbc.M406990200
162. Top D, Read JA, Dawe SJ, Syvitski RT, Duncan R. Cell-cell membrane fusion induced by p15 fusion-associated small transmembrane (FAST) protein requires a novel fusion peptide motif containing a myristoylated polyproline type II helix. J Biol Chem. Jan 27 2012;287(5):3403-14. doi:10.1074/jbc.M111.305268
163. Brown CW, Stephenson KB, Hanson S, et al. The p14 FAST protein of reptilian reovirus increases vesicular stomatitis virus neuropathogenesis. J Virol. Jan 2009;83(2):552-61. doi:10.1128/JVI.01921-08
164. Le Boeuf F, Gebremeskel S, McMullen N, et al. Reovirus FAST Protein Enhances Vesicular Stomatitis Virus Oncolytic Virotherapy in Primary and Metastatic Tumor Models. Mol Ther Oncolytics. Sep 15 2017;6:80-89. doi:10.1016/j.omto.2017.08.001
165. Wong CM, Poulin KL, Tong G, et al. Adenovirus-Mediated Expression of the p14 Fusion-Associated Small Transmembrane Protein Promotes Cancer Cell Fusion and Apoptosis In Vitro but Does Not Provide Therapeutic Efficacy in a Xenograft Mouse Model of Cancer. PLoS One. 2016;11(3):e0151516. doi:10.1371/journal.pone.0151516
166. Wong CM, Nash LA, Del Papa J, et al. Expression of the fusogenic p14 FAST protein from a replication-defective adenovirus vector does not provide a therapeutic benefit in an immunocompetent mouse model of cancer. Cancer Gene Ther. Oct 2016;23(10):355-364. doi:10.1038/cgt.2016.41
167. Del Papa J, Petryk J, Bell JC, Parks RJ. An Oncolytic Adenovirus Vector Expressing p14 FAST Protein Induces Widespread Syncytium Formation and Reduces Tumor

Growth Rate. Mol Ther Oncolytics. Sep 27 2019;14:107-120. doi:10.1016/j.omto.2019.05.001
168. Su CQ, Wang XH, Chen J, et al. Antitumor activity of an hTERT promoter-regulated tumor-selective oncolytic adenovirus in human hepatocellular carcinoma. World J Gastroenterol. Dec 21 2006;12(47):7613-20. doi:10.3748/wjg.v12.i47.7613
169. Montaño-Samaniego M, Bravo-Estupiñan DM, Méndez-Guerrero O, Alarcón-Hernández E, Ibáñez-Hernández M. Strategies for Targeting Gene Therapy in Cancer Cells With Tumor-Specific Promoters. Front Oncol. 2020;10:605380. doi:10.3389/fonc.2020.605380
170. Massie B, Couture F, Lamoureux L, et al. Inducible overexpression of a toxic protein by an adenovirus vector with a tetracycline-regulatable expression cassette. J Virol. Mar 1998;72(3):2289-96. doi:10.1128/JVI.72.3.2289-2296.1998
171. Brade AM, Szmitko P, Ngo D, Liu FF, Klamut HJ. Heat-directed tumor cell fusion. Hum Gene Ther. Mar 20 2003;14(5):447-61. doi:10.1089/104303403321467216
172. Geisler A, Fechner H. MicroRNA-regulated viral vectors for gene therapy. World J Exp Med. May 20 2016;6(2):37-54. doi:10.5493/wjem.v6.i2.37
173. Matthews DA, Cummings D, Evelegh C, Graham FL, Prevec L. Development and use of a 293 cell line expressing lac repressor for the rescue of recombinant adenoviruses expressing high levels of rabies virus glycoprotein. J Gen Virol. Feb 1999;80 (Pt 2):345-353. doi:10.1099/0022-1317-80-2-345
174. Edholm D, Molin M, Bajak E, Akusjärvi G. Adenovirus vector designed for expression of toxic proteins. J Virol. Oct 2001;75(20):9579-84. doi:10.1128/JVI.75.20.9579-9584.2001
175. Wilson RC, Doudna JA. Molecular mechanisms of RNA interference. Annu Rev Biophys. 2013;42:217-39. doi:10.1146/annurev-biophys-083012-130404
176. O'Brien J, Hayder H, Zayed Y, Peng C. Overview of MicroRNA Biogenesis, Mechanisms of Actions, and Circulation. Front Endocrinol (Lausanne). 2018;9:402. doi:10.3389/fendo.2018.00402
177. Ylösmäki E, Lavilla-Alonso S, Jäämaa S, et al. MicroRNA-mediated suppression of oncolytic adenovirus replication in human liver. PLoS One. 2013;8(1):e54506. doi:10.1371/journal.pone.0054506
178. Palmer DJ, Turner DL, Ng P. Production of CRISPR/Cas9-Mediated Self-Cleaving Helper-Dependent Adenoviruses. Mol Ther Methods Clin Dev. Jun 14 2019;13:432-439. doi:10.1016/j.omtm.2019.04.003
179. Riggs AD, Bourgeois S, Newby RF, Cohn M. DNA binding of the lac repressor. J Mol Biol. Jul 14 1968;34(2):365-8. doi:10.1016/0022-2836(68)90261-1
180. Jobe A, Bourgeois S. lac Repressor-operator interaction. VI. The natural inducer of the lac operon. J Mol Biol. Aug 28 1972;69(3):397-408. doi:10.1016/0022-2836(72)90253-7
181. Graham FL. Growth of 293 cells in suspension culture. J Gen Virol. Mar 1987;68 (Pt 3):937-40. doi:10.1099/0022-1317-68-3-937
182. Giard DJ, Aaronson SA, Todaro GJ, et al. In vitro cultivation of human tumors: establishment of cell lines derived from a series of solid tumors. J Natl Cancer Inst. Nov 1973;51(5):1417-23. doi:10.1093/jnci/51.5.1417

183. Chartier C, Degryse E, Gantzer M, Dieterle A, Pavirani A, Mehtali M. Efficient generation of recombinant adenovirus vectors by homologous recombination in Escherichia coli. J Virol. Jul 1996;70(7):4805-10. doi:10.1128/JVI.70.7.4805-4810.1996
184. Sadler JR, Tecklenburg M, Betz JL. Plasmids containing many tandem copies of a synthetic lactose operator. Gene. Feb 1980;8(3):279-300. doi:10.1016/0378-1119(80)90005-0
185. Ross PJ, Parks RJ. Construction and characterization of adenovirus vectors. Cold Spring Harb Protoc. May 2009;2009(5):pdb.prot5011. doi:10.1101/pdb.prot5011
186. Cohen M, Lichten M. C-Terminal HA Tags Compromise Function and Exacerbate Phenotypes of. G3 (Bethesda). Aug 05 2020;10(8):2811-2818. doi:10.1534/g3.120.401324
187. Zordan RE, Beliveau BJ, Trow JA, Craig NL, Cormack BP. Avoiding the ends: internal epitope tagging of proteins using transposon Tn7. Genetics. May 2015;200(1):47-58. doi:10.1534/genetics.114.169482
188. Salsman J, Top D, Boutilier J, Duncan R. Extensive syncytium formation mediated by the reovirus FAST proteins triggers apoptosis-induced membrane instability. J Virol. Jul 2005;79(13):8090-100. doi:10.1128/JVI.79.13.8090-8100.2005
189. Top D, Barry C, Racine T, Ellis CL, Duncan R. Enhanced fusion pore expansion mediated by the trans-acting Endodomain of the reovirus FAST proteins. PLoS Pathog. Mar 2009;5(3):e1000331. doi:10.1371/journal.ppat.1000331
190. Corcoran JA, Duncan R. Reptilian reovirus utilizes a small type III protein with an external myristylated amino terminus to mediate cell-cell fusion. J Virol. Apr 2004;78(8):4342-51. doi:10.1128/jvi.78.8.4342-4351.2004
191. Dawe S, Duncan R. The S4 genome segment of baboon reovirus is bicistronic and encodes a novel fusion-associated small transmembrane protein. J Virol. Mar 2002;76(5):2131-40. doi:10.1128/jvi.76.5.2131-2140.2002
192. Xie L, Dai Z, Pang C, Lin D, Zheng M. Cellular glucose metabolism is essential for the reduction of cell-impermeable water-soluble tetrazolium (WST) dyes. Int J Biol Sci. 2018;14(11):1535-1544. doi:10.7150/ijbs.25629
193. Prusinkiewicz MA, Mymryk JS. Metabolic Reprogramming of the Host Cell by Human Adenovirus Infection. Viruses. Feb 08 2019;11(2)doi:10.3390/v11020141
194. Brizzard B. Epitope tagging. Biotechniques. Apr 2008;44(5):693-5. doi:10.2144/000112841
195. Brown M, Stafford LJ, Onisk D, et al. Snorkel: an epitope tagging system for measuring the surface expression of membrane proteins. PLoS One. 2013;8(9):e73255. doi:10.1371/journal.pone.0073255
196. Yang Y, Margam NN. Structural Insights into Membrane Fusion Mediated by Convergent Small Fusogens. Cells. Jan 15 2021;10(1)doi:10.3390/cells10010160
197. Young CL, Britton ZT, Robinson AS. Recombinant protein expression and purification: a comprehensive review of affinity tags and microbial applications. Biotechnol J. May 2012;7(5):620-34. doi:10.1002/biot.201100155
198. Goedhart J, van Weeren L, Adjobo-Hermans MJ, Elzenaar I, Hink MA, Gadella TW. Quantitative co-expression of proteins at the single cell level--application to a multimeric FRET sensor. PLoS One. 2011;6(11):e27321. doi:10.1371/journal.pone.0027321

199. Radhakrishnan P, Basma H, Klinkebiel D, Christman J, Cheng PW. Cell type-specific activation of the cytomegalovirus promoter by dimethylsulfoxide and 5-aza-2'-deoxycytidine. Int J Biochem Cell Biol. 2008;40(9):1944-55. doi:10.1016/j.biocel.2008.02.014
200. Komatsu T, Haruki H, Nagata K. Cellular and viral chromatin proteins are positive factors in the regulation of adenovirus gene expression. Nucleic Acids Res. Feb 2011;39(3):889-901. doi:10.1093/nar/gkq783
201. Clarkin RG, Del Papa J, Poulin KL, Parks RJ. The genome position of a therapeutic transgene strongly influences the level of expression in an armed oncolytic human adenovirus vector. Virology. Sep 2021;561:87-97. doi:10.1016/j.virol.2021.06.005
202. Farrera-Sal M, de Sostoa J, Nuñez-Manchón E, et al. Arming Oncolytic Adenoviruses: Effect of Insertion Site and Splice Acceptor on Transgene Expression and Viral Fitness. Int J Mol Sci. Jul 21 2020;21(14)doi:10.3390/ijms21145158
203. Punga T, Darweesh M, Akusjärvi G. Synthesis, Structure, and Function of Human Adenovirus Small Non-Coding RNAs. Viruses. Oct 19 2020;12(10)doi:10.3390/v12101182
204. Thimmappaya B, Weinberger C, Schneider RJ, Shenk T. Adenovirus VAI RNA is required for efficient translation of viral mRNAs at late times after infection. Cell. Dec 1982;31(3 Pt 2):543-51. doi:10.1016/0092-8674(82)90310-5
205. Carnero E, Sutherland JD, Fortes P. Adenovirus and miRNAs. Biochim Biophys Acta. 2011;1809(11-12):660-7. doi:10.1016/j.bbagrm.2011.05.004
206. Goossens PH, Schouten GJ, Heemskerk B, et al. The effect of promoter strength in adenoviral vectors in hyperplastic synovium. Clin Exp Rheumatol. 2000;18(5):547-52.
207. Hu MC, Davidson N. The inducible lac operator-repressor system is functional in mammalian cells. Cell. Feb 27 1987;48(4):555-66. doi:10.1016/0092-8674(87)90234-0
208. Robinett CC, Straight A, Li G, et al. In vivo localization of DNA sequences and visualization of large-scale chromatin organization using lac operator/repressor recognition. J Cell Biol. Dec 1996;135(6 Pt 2):1685-700. doi:10.1083/jcb.135.6.1685
209. Belmont AS, Straight AF. In vivo visualization of chromosomes using lac operator-repressor binding. Trends Cell Biol. Mar 1998;8(3):121-4. doi:10.1016/s0962-8924(97)01211-7
210. Tsukamoto T, Hashiguchi N, Janicki SM, Tumbar T, Belmont AS, Spector DL. Visualization of gene activity in living cells. Nat Cell Biol. Dec 2000;2(12):871-8. doi:10.1038/35046510
211. Pelletier J, Sonenberg N. Insertion mutagenesis to increase secondary structure within the 5' noncoding region of a eukaryotic mRNA reduces translational efficiency. Cell. Mar 1985;40(3):515-26. doi:10.1016/0092-8674(85)90200-4
212. Leppek K, Das R, Barna M. Functional 5' UTR mRNA structures in eukaryotic translation regulation and how to find them. Nat Rev Mol Cell Biol. Mar 2018;19(3):158-174. doi:10.1038/nrm.2017.103

213. Wang XQ, Rothnagel JA. 5'-untranslated regions with multiple upstream AUG codons can support low-level translation via leaky scanning and reinitiation. Nucleic Acids Res. 2004;32(4):1382-91. doi:10.1093/nar/gkh305
214. Wu E, Pache L, Von Seggern DJ, et al. Flexibility of the adenovirus fiber is required for efficient receptor interaction. J Virol. Jul 2003;77(13):7225-35. doi:10.1128/jvi.77.13.7225-7235.2003
215. Legrand V, Spehner D, Schlesinger Y, Settelen N, Pavirani A, Mehtali M. Fiberless recombinant adenoviruses: virus maturation and infectivity in the absence of fiber. J Virol. Feb 1999;73(2):907-19. doi:10.1128/JVI.73.2.907-919.1999
216. Payne BT, van Knippenberg IC, Bell H, Filipe SR, Sherratt DJ, McGlynn P. Replication fork blockage by transcription factor-DNA complexes in Escherichia coli. Nucleic Acids Res. 2006;34(18):5194-202. doi:10.1093/nar/gkl682
217. Marbach A, Bettenbrock K. lac operon induction in Escherichia coli: Systematic comparison of IPTG and TMG induction and influence of the transacetylase LacA. J Biotechnol. Jan 2012;157(1):82-8. doi:10.1016/j.jbiotec.2011.10.009

Contributions of Collaborators

Plasmids used in this study were generated by me, Dr. Robin Parks, or previous students in the Parks lab. Dr. Parks provided editorial comments on this work and guidance throughout my studies. Kathy Poulin provided technical assistance for experimental set-up. FAST protein cDNAs used in this study were obtained from Dr. Roy Duncan (Dalhousie University, NS, CAN) or Dr. John Bell (Ottawa Hospital Research Institute, ON, CAN). AI-assisted tools were used sparingly for grammatical editing and sentence structure refinement.

George Akl

EDUCATION

Master of Science in Microbiology & Immunology 2024-2026
University of Ottawa, Ottawa, Ontario
- Supervised by Dr. Robin J. Parks, PhD
- Project: Exploring novel methods to express cytotoxic proteins from oncolytic adenoviral vectors

Honours Bachelor of Science in Biomedical Science 2020-2024
Minor in Psychology
University of Ottawa, Ottawa, Ontario
- Graduated with Summa Cum Laude distinction

HONORS & AWARDS

- Poster Award - TOH Department of Medicine Research Day 2025
- Poster Award - OHRI Research Day 2024
- University of Ottawa Graduate Merit Scholarship ($4,000) 2024
- Gold Medal Award - OHRI Summer Student Seminar Program 2024
- Honours BSc Summa Cum Laude Distinction 2024
- University of Ottawa BSc Dean's Honour List 2020-2024
- University of Ottawa BSc Merit Scholarships ($6,000) 2020-2024
- University of Ottawa BSc Admission Scholarship ($2,000) 2020

PROFESSIONAL EXPERIENCE

Summer Student Researcher 2024
Ottawa Hospital Research Institute – Parks Lab, Ottawa, Ontario

Bilingual Patient Services Clerk 2021-2024
ByWard Family Health Team, Ottawa, Ontario

Store Supervisor 2018-2021
Boathouse, Ottawa, Ontario

LEADERSHIP & VOLUNTEER EXPERIENCE

The Ottawa Lebanese Festival Volunteer 2018-Present
Saint Elias Centre, Ottawa, Ontario

Canine Enrichment Volunteer 2023-2024
Ottawa Humane Society, Ottawa, Ontario

Lab Assistant 2019
University of Ottawa CMM Lab, Ottawa, Ontario

Nursing Assistant 2019
Montfort Hospital, Ottawa, Ontario

COMMITTEES

uOttawa Faculty of Medicine Council Member 2026-Present

uOttawa Biochemistry, Microbiology & Immunology Graduate Student Association VP Internal 2026-Present

uOttawa Biochemistry, Microbiology & Immunology Cyclical Review Student Delegate 2025-Present

uOttawa Biochemistry, Microbiology & Immunology Graduate Student Association OHRI Representative 2025-2026

Ottawa Hospital Research Institute Regenerative Medicine Program Trainee Committee 2024-Present

CERTIFICATIONS & PROFESSIONAL DEVELOPMENT

- Tri-Council Policy Statement: Ethical Conduct for Research Involving Humans Course on Research Ethics (TCPS 2: CORE) 2024
- Health Canada Division 5 – Drugs for Clinical Trials Involving Human Subjects 2024
- CIHR Integrating Sex and Gender in Biomedical Research Training 2024
- Canada Good Clinical Practices (GCP) 2024

SEMINAR & POSTER PRESENTATIONS

2026 TOH Department of Medicine Research Day
Seminar: "Arming of oncolytic adenovirus vectors with the fusion associated small transmembrane (FAST) proteins to enhance anti-cancer therapeutic efficacy" (Akl, G. M., and Parks, R. J.)

2026 University of Ottawa Biochemistry, Microbiology and Immunology Poster/Seminar Day
Poster: "Arming of oncolytic adenovirus vectors with the fusion associated small transmembrane (FAST) proteins to enhance anti-cancer therapeutic efficacy" (Akl, G., and Parks, R. J.)

2025 Ottawa Hospital Research Institute Research Day
Poster: "Arming of oncolytic adenovirus vectors with the fusion associated small transmembrane (FAST) proteins to enhance anti-cancer therapeutic efficacy" (Akl, G. M., Poulin, K. L. and Parks, R. J.)

2025 TOH Department of Medicine Research Day
Poster: "Arming of oncolytic adenovirus vectors with the fusion associated small transmembrane (FAST) proteins to enhance anti-cancer therapeutic efficacy" (Akl, G. M., Poulin, K. L. and Parks, R. J.)

2025 University of Ottawa Biochemistry, Microbiology and Immunology Symposium
Poster: "Arming of oncolytic adenovirus vectors with the fusion associated small transmembrane (FAST) proteins to enhance anti-cancer therapeutic efficacy" (Akl, G. M., Poulin, K. L. and Parks, R. J.)

2025 CSMB-PRinCE Joint Conference: Protein Homeostasis
Poster: "Arming of oncolytic adenovirus vectors with the fusion associated small transmembrane (FAST) proteins to enhance anti-cancer therapeutic efficacy" (Akl, G. M., Poulin, K. L. and Parks, R. J.)

2025 University of Ottawa Biochemistry, Microbiology and Immunology Poster/Seminar Day
Seminar: "Exploring Novel Methods to Express Cytotoxic Proteins from Oncolytic Adenoviral Vectors" (Akl, G., and Parks, R. J.)

2024 Ottawa Hospital Research Institute Research Day
Poster: "Exploring novel methods to express toxic proteins from oncolytic adenoviral vectors" (Akl, G., and Parks, R. J.)

2024 Ottawa Hospital Research Institute Summer Student Seminar Series
Seminar: "Development of oncolytic adenoviral vectors for use in cancer gene therapy" (Akl, G., and Parks, R. J.)

CONFERENCE ATTENDANCE

- 2026 The Ottawa Hospital Department of Medicine Research Day 2026
- 2025 Ottawa Hospital Research Institute Research Day 2025
- 7th Ottawa International Conference on Neuromuscular Disease & Biology 2025
- 2025 The Ottawa Hospital Department of Medicine Research Day 2025
- 2025 CSMB-PRinCE Joint Conference: Protein Homeostasis 2025
- 2024 Ottawa Hospital Research Institute Research Day 2024
- Cold Spring Harbor Laboratory Cell & Membrane Fusion Meeting (Virtual Attendance) 2024

Ad Hoc REVIEWER

- International Journal of Molecular Sciences 2025
- ACS Omega 2024